Remote Sensing of Environment 232 (2019) 111280

Contents lists available at ScienceDirect

Remote Sensing of Environment

journal homepage: www.elsevier.com/locate/rse

Airborne and spaceborne remote sensing for archaeological and cultural heritage applications: A review of the century (1907–2017)

Lei Luo[a,b], Xinyuan Wang[a,b,*], Huadong Guo[a,b], Rosa Lasaponara[c], Xin Zong[d], Nicola Masini[e], Guizhou Wang[a], Pilong Shi[a], Houcine Khatteli[f], Fulong Chen[a,b], Shahina Tariq[g], Jie Shao[h], Nabil Bachagha[a,i], Ruixia Yang[a,b], Ya Yao[a,i]

[a] Key Laboratory of Digital Earth Science, Institute of Remote Sensing and Digital Earth (RADI), Chinese Academy of Sciences (CAS), Beijing 100094, China
[b] International Centre on Space Technologies for Natural and Cultural Heritage (HIST) under the Auspices of UNESCO, Beijing 100094, China
[c] Institute of Methodologies for Environmental Analysis (IMAA), CNR, C.da Santa Loja, 85050 Tito Scalo, Italy
[d] Department of Natural Resources, Faculty of Geo-Information Science and Earth Observation (ITC), University of Twente, Enschede 7514 AE, Netherlands
[e] Institute of Archeological Heritage—Monuments and Sites (IBAM), CNR, C.da Santa Loja, 85050 Tito Scalo, Italy
[f] Institut des Regions Arides (IRA)-Medenine, Medenine 4119, Tunisia
[g] COMSATS University Islamabad (CUI), Islamabad 45550, Pakistan
[h] IRIT, CNRS, Université de Toulouse, Toulouse 31062, France
[i] University of Chinese Academy of Sciences, Beijing 100049, China

ARTICLE INFO

Keywords:
Archaeological
Cultural heritage
Remote sensing
Airborne
Spaceborne
Photography
Spectral
SAR
LiDAR
Site
Marks
DTM
UAVs

ABSTRACT

Archaeological and cultural heritage (ACH), one of the core carriers of cultural diversity on our planet, has a direct bearing on the sustainable development of mankind. Documenting and protecting ACH is the common responsibility and duty of all humanity. It is governed by UNESCO along with the scientific communities that foster and encourage the use of advanced non-invasive techniques and methods for promoting scientific research into ACH and conservation of ACH sites. The use of remote sensing, a non-destructive tool, is increasingly popular by specialists around the world as it allows fast prospecting and mapping at multiple scales, rapid analysis of multisource datasets, and dynamic monitoring of ACH sites and their surrounding environments. The cost of using remote sensing is lower or even zero in practical applications. In this review, in order to discuss the advantages of airborne and spaceborne remote sensing (ASRS), the principles that make passive (photography, multispectral and hyperspectral) and active (synthetic aperture radar (SAR) and light detection and ranging radar (LiDAR)) imaging techniques suitable for ACH applications are first summarized and pointed out; a review of ASRS and the methodologies used over the past century is then presented together with relevant highlights from well-known research projects. Selected case studies from Mediterranean regions to East Asia illustrate how ASRS can be used effectively to investigate and understand archaeological features at multiple -scales and to monitor and assess the conservation status of cultural heritage sites in the context of sustainable development. An in-depth discussion on the limitations of ASRS and associated remaining challenges is presented along with conclusions and a look at future trends.

1. Introduction

The conservation of archaeological and cultural heritage (ACH) is a strategic priority, not only so that cultural property and evidence from the past can be safeguarded and passed on to future generations (Lasaponara et al., 2018) but also because these are valuable assets whose exploitation supports the UN's 2030 Sustainable Development Goals (SDGs) (UN, 2015; Cuca and Hadjimitsis, 2017; Stott et al., 2018; Xiao et al., 2018). ACH is one of the fields in which remote sensing from elevated points was first used - the use of kites was followed by hot-air balloons, aircrafts and helicopters, shuttles, rockets, space stations and finally satellites (Fig. 1). Using each of these platforms, archaeologists and specialists have recognized the great value of multi-platform remote sensing in gaining a view from above in order to better identify and understand ACH sites and their wider environments (Aminzadeh and Samani, 2006; Luo et al., 2017b; Tapete, 2018).

* Corresponding author at: Key Laboratory of Digital Earth Science, Institute of Remote Sensing and Digital Earth (RADI), Chinese Academy of Sciences (CAS), Beijing 100094, China.
E-mail address: wangxy@radi.ac.cn (X. Wang).

https://doi.org/10.1016/j.rse.2019.111280
Received 31 March 2019; Received in revised form 17 June 2019; Accepted 22 June 2019
Available online 11 July 2019

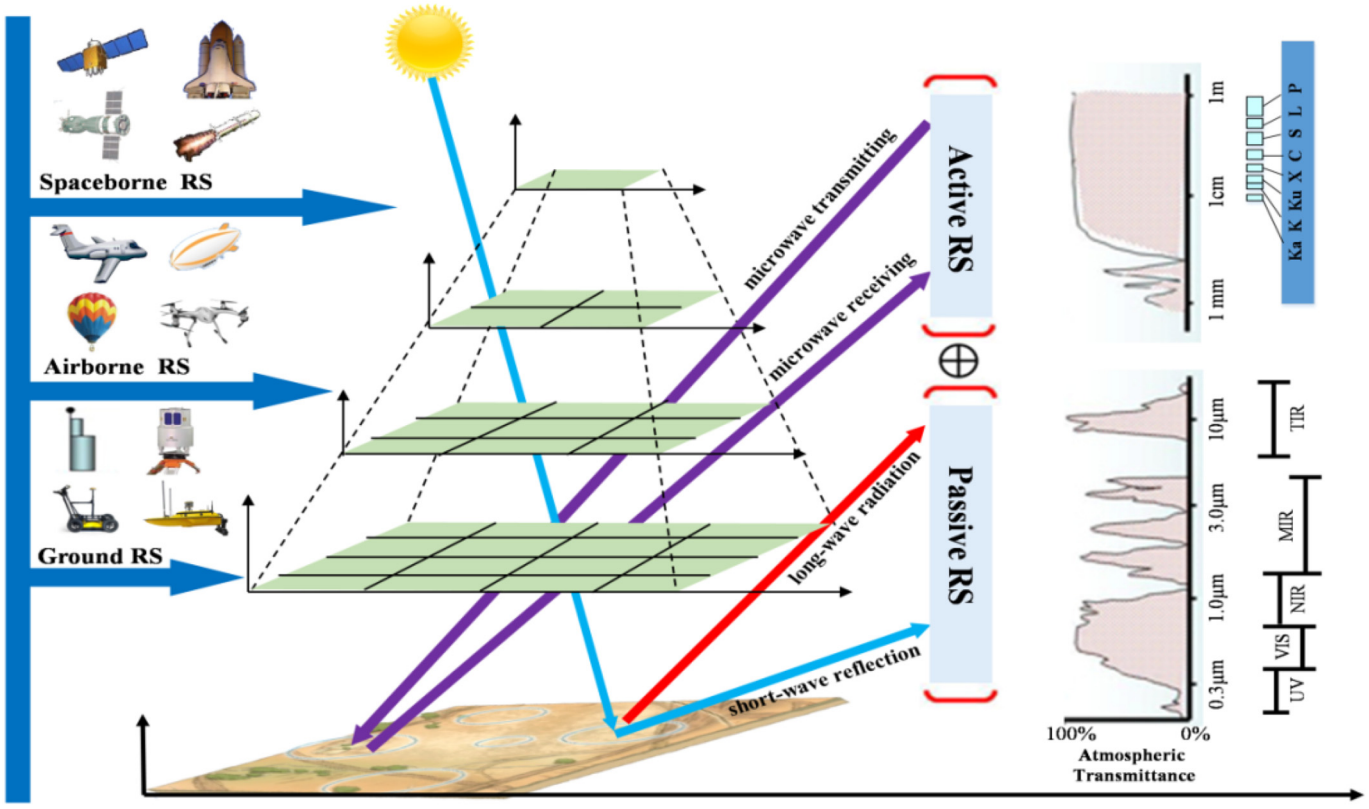

Fig. 1. The schematic diagram of remote sensing (RS) for ACH applications.

In the field of ACH, remote sensing is a general name given to all techniques that use non-direct contact devices to observe targets of interest on the Earth's (sub-) surface either from the surface of the ground or from above it (Wang and Guo, 2015). This definition includes geophysical methods (e.g. ground penetrating radar, electrical resistivity tomography, and electromagnetic methods) and acoustic methods (e.g. sound navigation and ranging), even though some scholars and specialists refer to these as ground-based or underwater remote sensing (Ballard, 2007; Deng et al., 2010; Ødegård et al., 2018). In this review, we focus on airborne and spaceborne remote sensing (ASRS) techniques, which are the most widely used tools for ACH purposes (Lambers, 2018; Luo et al., 2017b). By taking advantage of the fast imaging, large-spatial coverage, high spatial and spectral resolution and signal sensitivity to anomalies linked to exposed and subsurface features that ASRS provides, ASRS can be successfully adopted for use in ACH applications (Rowlands and Sarris, 2007).

In the past twenty years, ASRS has witnessed many novel applications and faced several new challenges which have possibly not been mentioned in existing reviews (Bewley, 2003; Crutchley, 2009; Scollar et al., 1990). Many recent reviews (Agapiou and Lysandrou, 2015; Ceraudo, 2004; Chen et al., 2017c; Deng et al., 2010; Giardino, 2011; Lasaponara and Masini, 2013; Luo et al., 2018a; Masini and Lasaponara, 2013; Opitz and Herrmann, 2018; Tapete, 2018; Tapete and Cigna, 2017b; Verhoeven, 2017) and book chapters (Alexakis et al., 2012; Harrower and Comer, 2013; Lasaponara and Masini, 2012b; Leisz, 2013; Masini and Lasaponara, 2013; Parcak, 2009; Wiseman and El-Baz, 2007) that point out the basic principles and practices that make different ASRS techniques suitable for ACH and lead to successful results have been published. However, most of these focus on a single imaging technique, single platform and sensor or single application field within a given period of time; a collective review has not been carried out and an in-depth discussion on methodologies, trends and challenges is lacking.

Although ASRS techniques have already played crucial roles in the exploration and understanding of the archaeological landscape and of cultural heritage, it is still important to review key concepts, principles and methods (Aqdus et al., 2012; McCoy and Ladefoged, 2009; Parcak, 2009; Rowlands and Sarris, 2007; Verhoeven, 2017). In addition to the generic cases that Deng et al. (2010) and Agapiou and Lysandrou (2015) discussed, the distinctive merits that characterize ASRS and which may have been pivotal to its success in ACH applications need to be closely examined. The advantages that have sustained the influence of ASRS are worth dissecting in detail as this may provide an important reference point for the future development of Remote Sensing Archaeology and Digital Heritage (Wang and Guo, 2015). In this context, we have taken the liberty of conducting a collective review of ASRS in ACH applications over the period 1907–2017.

2. A brief history of ASRS for ACH applications

More than a century has passed since airborne remote sensing was first used in ACH around 1900. Since 1839, when photography was born, photographers had sought to carry cameras aloft to obtain a view of the Earth's surface from above. In 1906, a British general used a hot-air military balloon to take both vertical and oblique photographs of the Stonehenge site (Capper, 1907; Deng et al., 2010). After the 1900s, most photographs taken from above the Earth's surface were taken from airplanes (Agapiou et al., 2016a; Crawford, 1923; Ceraudo, 2004; Leisz, 2013). After 1959, images of our planet were also taken from spaceborne platforms (Giardino, 2011; Lasaponara and Masini, 2011; Luo et al., 2017a; McCauley et al., 1982). One of the earliest published scientific contributions on airborne remote sensing applied to ACH came out of the intersection of using aerial photographs to survey an area as part of map production in support of military purposes (Beazeley, 1919; Leisz, 2013). In the short period of about 60 years since the launch of the first spaceborne platform - the spy CORONA satellite - in 1959, satellite remote sensing technology has made many breakthroughs in terms of spatial, radiometric, spectral and temporal

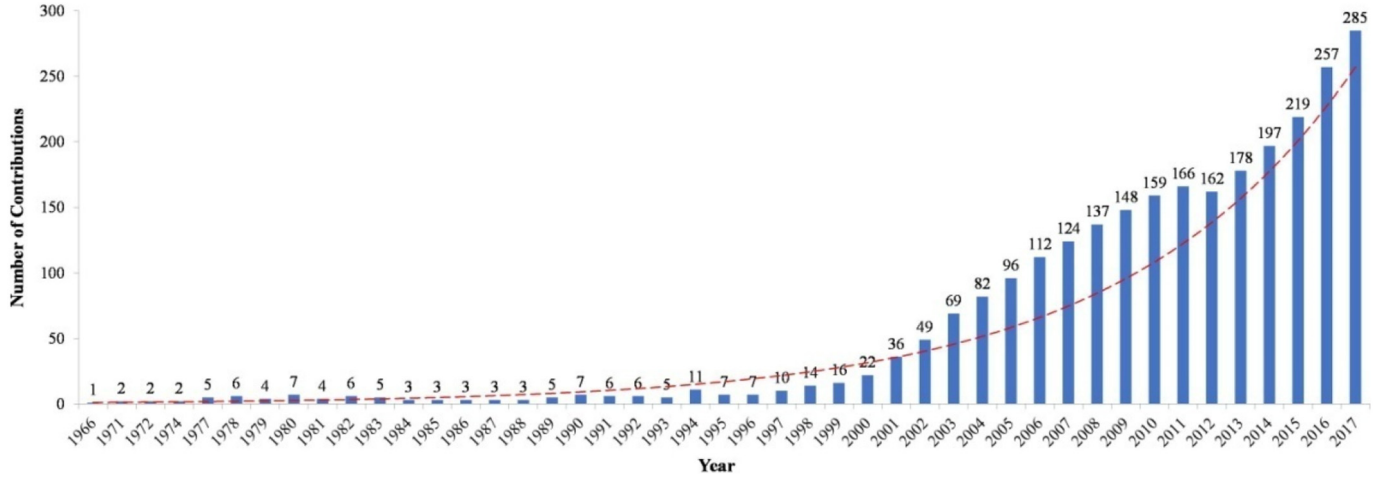

Fig. 2. 50-year (1967–2017) literature count for articles introducing ASRS for ACH applications, extracted from the database Scopus (last access 15 October 2018).

resolution. This has allowed the beginning of data mining from big remote sensing data, which has led to more new discoveries (Giardino, 2011; Luo et al., 2017b). Accompanied by the development of different imaging technologies, the use of satellite data as a novel tool to uncover remains left by ancient human occupation and to study past landscapes has become more and more popular since the 1970s, when the data started to become available for civil purposes (Agapiou et al., 2015a; Agapiou et al., 2016b, 2016c; Beck et al., 2007; Bewley et al., 2005; Brivio et al., 2000; Donoghue and Shennan, 1988; Giardino, 2011; Gumerman and Lyons, 1971; Luo et al., 2014b; Noviello et al., 2013; Tang et al., 2016; Tapete and Cigna, 2017b; Tapete et al., 2013).

Based on the imaging technique used, the existing ASRS tools used in ACH can be categorized into four main types: photography (Agapiou et al., 2016a; Beck et al., 2007; Casana and Cothren, 2008; Connah, 1978; Evers and Masters, 2018; Fowler and Fowler, 2005; Goossens et al., 2006; Gumerman and Lyons, 1971; Liritzis et al., 1983; Parcak, 2007; Philip et al., 2002; Ur, 2003), multispectral and hyperspectral imaging (Agapiou et al., 2014a; Agapiou et al., 2012; Agapiou et al., 2013b; Alexakis et al., 2009; Aqdus et al., 2012; De Laet et al., 2007; De Laet et al., 2015; Doneus et al., 2014; Lasaponara et al., 2016; Lasaponara and Masini, 2007; Le Tourneau, 1998; McLeester et al., 2018; Tan et al., 2005; Winterbottom and Dawson, 2005), synthetic aperture radar (SAR) (Balz et al., 2016; Chen et al., 2017a; Cigna et al., 2014; Holcomb, 1996; Lasaponara et al., 2017a; Moore et al., 2007; Rutishauser et al., 2017; Stewart et al., 2014; Stewart et al., 2018; Tapete et al., 2016) and light detection and ranging (LiDAR) (Chase et al., 2012; Chase et al., 2011; Devereux et al., 2005; Doneus et al., 2008; Evans et al., 2013; Hesse, 2010; Lasaponara et al., 2010; Trier and Pilø, 2012; Von Schwerin et al., 2016a).

Platforms used for viewing the Earth's surface have moved from the atmosphere to outer space over the past century. While satellite remote sensing has flourished, airborne remote sensing has continued to be the workhorse for ACH applications at local scales and has seen just as many technological innovations as satellite remote sensing in recent years (Lambers, 2018). Conversely, although historical photographs taken from airborne and spaceborne platforms continue to be used by archaeologists, multispectral and hyperspectral imaging systems, as well as LiDAR and SAR, have also begun to be used (Harrower and Comer, 2013). In this paper, for ease of presentation, the four main types of ASRS techniques mentioned above have been classified into passive (photography and spectral imaging) and active (SAR and LiDAR). Whereas passive remote sensing systems capture naturally occurring radiation such as emitted thermal energy or reflected solar radiation (Verhoeven, 2017), active systems produce their own radiation (Fig. 1).

3. Literature overview of ASRS for ACH applications

During the last century, a large number of peer-reviewed contributions on the use of ASRS in ACH have been published, thus showing that Earth-observation technologies have triggered improvements and the development of new tools. It should be noted that only a dozen contributions were published in the period 1907–1967, due to the influence of the two World Wars. To obtain an overview of the growing use of ASRS in the field, we searched a widely used electronic database, namely *Scopus* (http://www.scopus.com/) for the period 1 January 1967 to 31 December 2017. Using 11 independent filters, a total of 2651 publication records were retrieved from the literature database *Scopus*. The filters used were: “remote sensing”, “aerial”, “satellite”, “airborne”, “spaceborne”, “CORONA”, “photography”, “multispectral”, “hyperspectral”, “LiDAR” and “SAR”. In the returned results, the terms “archaeological”, “archaeology” or “cultural heritage” were mentioned at least once in the title, abstract or keywords, these filtered records were then combined into a new set and the duplicates removed using Endnote. A bibliometric analysis based on the retrieved literature data was conducted in order to reveal the spatiotemporal patterns in ASRS development over the past half centuries.

We began with a multi-year trend analysis to track the development of ASRS applications in ACH. All the retrieved publication records were aggregated by year to show the year-on-year growth (Fig. 2). Fig. 2 shows a two-stage feature: a period of stagnation from 1967 to 1997 and a period of linear increase from 1997 to 2017. This indicates the high degree of importance and the acceptance that ASRS technologies have gained in the fields of archaeology and cultural heritage science over the last 20 years. These bibliometric statistics are similar to results found in earlier studies (Agapiou and Lysandrou, 2015). The differences between the results of these two studies might be caused by the different search filters that were used for searching the databases.

The 2651 publications found were narrowed down to a set of journal papers in the English language; the categories “Conference Paper”, “Book Chapter”, “Special Report”, “Manual” and “Erratum” were excluded. Next, a journal ranking analysis was conducted to show the orientation of ASRS in ACH applications. By doing this, we reduced the dataset down to a list of 1571 articles published in 363 mostly international peer-reviewed journals. Total 661 and 143 articles were attributed to the top-ranking 10 journals (covered by SCIE or SSCI) in categories of *Archaeology* and *Remote Sensing*, respectively (Fig. 3). These top journals focus mostly on archaeological science subjects, particularly on geoarchaeology and cultural heritage.

Although here we carried out a comprehensive bibliometric analysis, it still has insurmountable shortcomings in the absence of ‘grey literature’ (Vlachidis et al., 2010) which the most common type is

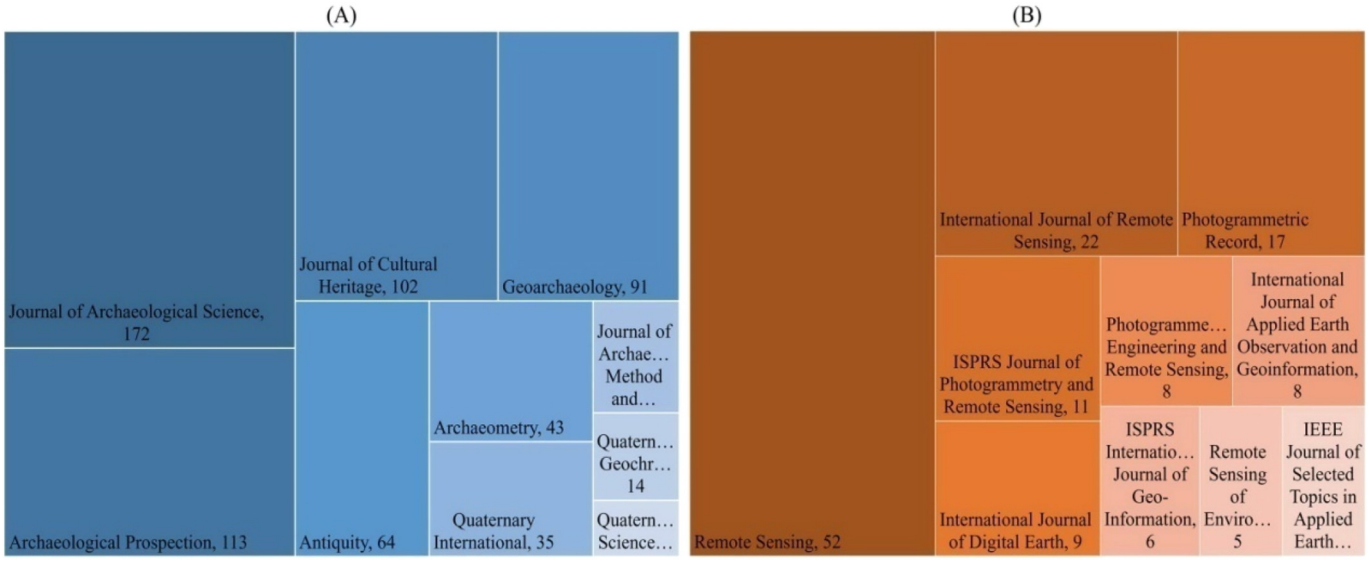

Fig. 3. Ranking treemaps of the top 10 journals by number of publications in categories of archaeology (A) and remote sensing (B).

unpublished or informal published materials (e.g. Dissertations, Reports, Conference Abstracts, Notes and Manuals). In these materials the use of remote sensing in ACH applications is also included (Gibbs and Colley, 2012). Grey literature is a kind of important and valuable information recourse, especially for local and regional researches in ACH. This means that those carrying out systematic reviews need to search for trials in both the published (Agapiou and Lysandrou, 2015) and grey literature in order to help minimize the effects of publication bias in review (Cooper and Green, 2016; Richards, 1997). Just as the other disciplines, it is turned into a major and challenging issue that how to collect and use grey literature (Conn et al., 2003) are also exits in ACH studies.

On the other hand, it should be discussed openly the fact that only the English-written papers were taken into consideration, missing thus other studies published in other languages in our bibliometric analysis. Actually, remote sensing archaeologists or specialists all over the world usually contribute their work to archaeological or remote sensing journals, often of local range and publishing in native language (Aliphat Fernandez, 1996; Doneus, 2009; Guo, 1997; Wang and Guo, 2015), are not freely accessible. The non-English papers may be difficult to discover, access, and evaluate, but this can be addressed through the formulation of sound search strategies (Gibbs and Colley, 2012). They contain author's original ideas and a large number of meaningful background information of local archaeology. Thus, the role and impact of the non-English papers should be investigated in the meta-analyses of ASRS-based ACH studies in the future.

4. Passive remote sensing in ACH applications

4.1. Photography

4.1.1. Background

The use of photography in ACH applications has become increasingly more common over the past 110 years. Photography provides the ability to discover archaeological sites prior to destruction due to intense human activities or natural erosion processes. The theoretical foundation for aerial photography archaeology, the principle behind archaeological remote sensing, was first established by Crawford in the early 1920s (Deng et al., 2010). Traces of ancient human transformations of the landscape create subtle features, namely surface anomalies that are only visible when viewed from above (Crawford, 1923; Lasaponara and Masini, 2012c). The image characteristics of these features strongly depend on local geographic environmental conditions such as the vegetation cover and phenology, pedology, soil types and topography. This results in spatial and temporal variation in the pixels' brightness and contrast values in aerial photographs. Crawford was the first specialist to systematically propose and use three interpretation proxies - crop, soil and shadow marks - for prospecting and mapping archaeological sites (Crawford, 1923; Leisz, 2013; Verhoeven, 2017) using aerial photographs. Subsequently, specialists gradually began to use these and other related proxies (e.g. snow, frost, flood and damp marks) to detect, identify and map ACH sites not only from aerial photographs but also from the satellite photographs (Agapiou et al., 2014a; Lasaponara and Masini, 2012c).

4.1.2. Photograrchaeology: photography of archaeological sites

The majority of historic photographs have been acquired with imaging sensors that are sensitive to the visible part of the electromagnetic spectrum between 400 nm and 700 nm. Photography often allows the detection of buried archaeological remains through small changes in relief or discoloration of overlying soils or crops, and allows large areas to be surveyed within short time-scales. Crop marks are dependent on buried features either enhancing or reducing the growth of overlying vegetation by increasing or reducing moisture availability. Soil marks occur where past activity has led to variations in the color and character of the topsoil and are usually only evident when fields have just been ploughed. Shadow marks can be seen where variations in micro-topographic relief are made visible by shadowing at low sun angle (Luo et al., 2018b). Sometimes, archaeological features are detectable by photography only under optimal conditions and circumstances. Historic vertical aerial photographic data have been widely used by archaeologists because they retain archaeolandscapes and cultural heritage sites that have been damaged or have disappeared (Beazeley, 1919; St Joseph, 1945). Throughout the 20th century, photography archaeology (Bewley, 2003; Cox, 1992; Denbow, 1979; Hanson and Oltean, 2013; St Joseph, 1961; Verhoeven and Sevara, 2016) began to develop rapidly both in the West and East, especially as economic development in developing countries led to sharp tensions between economic growth and the preservation of ACH sites (Cowley and Stichelbaut, 2012; Deng et al., 2010; Leisz, 2013; Nie and Yang, 2009). This led to great importance being attached to photography archaeology. This review mainly focuses on ACH applications that used historic airborne and spaceborne photographic data.

4.1.3. Airborne and spaceborne photography

Aerial photography, also called airborne photography, can be

divided into two categories: vertical and oblique. The first aerial images for archaeological purposes were taken above the Stonehenge site from a military balloon (Capper, 1907; Deng et al., 2010) at the beginning of 20th century. Shortly afterwards, during World War I, black-and-white aerial photographs taken for military reconnaissance from airplanes covered many archaeological ruins and cultural heritage sites in Europe for the first time (Cowley and Stichelbaut, 2012; Lambers, 2018; Stichelbaut, 2011). During World War II, aerial photography was further developed, and the vertical and oblique photography technologies were greatly improved; color photography and color infrared photography were also invented (Thomas, 1945). The use of infrared and later multispectral photography in aerial archaeology in the 1970s increased the visible range so that differences in soil moisture and crop growth could be used more effectively (Estes, 1966; Rigaud and Herse, 1986; Verhoeven, 2008; Verhoeven, 2012). However, inherent conceptual issues such as survey bias (Lambers, 2018; Verhoeven and Sevara, 2016; Verhoeven, 2017) could not be resolved through technological innovation.

During the period of the Cold War, several spy satellite photography systems were designed and launched; of particular note are the USA's Keyhole (KH) Program and the former Soviet Union's ZENIT Program. The KH Program started with CORONA (KH-1 to KH-4B) in 1959, followed by ARGON (KH-5), LANYARD (KH-6), GAMBIT (KH-7, KH-8) and HEXAGON (KH-9) (Lasaponara et al., 2018). The spatial resolution of CORONA spy photographs taken during the Cold War could reach up to 0.6 m. Such data are valuable in areas where the archaeolandscape has changed dramatically as a result of human activity such as agricultural production and urbanization (Conesa et al., 2015; De Meyer, 2004; Fowler, 2011; Fowler and Fowler, 2005; Kennedy, 1998; Lasaponara et al., 2018). CORONA was officially classified as top secret until 1992. Then, in 1995, the photos taken by the CORONA satellites were declassified. Spaceborne spy photography data (ZENIT, COSMOS, and Kometa KVR-1000) from the former Soviet Union and subsequent Russian space programs have been available since 1961 and have a high resolution of up to 2 m. Even though those photographs have been used by several researchers (Comer, 2012; Comfort and Ergeç, 2001; Fowler, 1996; Hadjimitsis et al., 2013b), their application is still limited due to their high cost or inaccessibility.

4.1.4. Airborne and spaceborne photography in ACH applications

The holistic study of archaeological sites or ruins was the initial purpose of aerial archaeology. It provided a view from above that could be used to uncover archaeological earthworks that are invisible to the observer on the ground. Beazeley (1919) discovered a number of unknown archaeological sites based on the use of military air photos in Mesopotamia. In addition, aerial photographs can be used to support landscape archaeology by allowing the analysis of the relationship between sites and their surrounding environments (Lu et al., 2017; St Joseph, 1945; St Joseph, 1961). After the Second World War, aerial photography provided a further boost to archaeology as the use of aerial reconnaissance during the war meant that photographs of places that otherwise would not have been surveyed had been obtained (Bradford and Williams-Hunt, 1946; Leisz, 2013; Thomas, 1945). The use of historic aerial photographs in recording archaeological sites worldwide has continued to the present day (Lu et al., 2017; Stichelbaut, 2005; Stichelbaut, 2006; Stichelbaut, 2011; Stott et al., 2018).

Since their declassification, the potential of spy satellite photographs for researchers in archaeology (Fowler, 1996; Kennedy, 1998) and other fields (such as glaciology and forestry (Bindschadler and Vornberger, 1998; Kim et al., 2006; Nita et al., 2018) has gradually been recognized. These photographs have been considered an invaluable resource for archaeological investigations by many archaeologists. These studies concentrated on archaeological investigation and (re-) discovery in the Near East and Middle East (Agapiou et al., 2016a; Alizadeh and Ur, 2007; Altaweel, 2005; Beck et al., 2007; Bitelli and Girelli, 2009; Casana, 2013; Casana, 2015; Casana and Cothren, 2008; Casana et al., 2014; Casana and Laugier, 2017; Challis et al., 2004; Conesa et al., 2015; Elfadaly et al., 2017; Fowler, 2004; Fowler, 2011; Fowler and Fowler, 2005; Gheyle et al., 2004; Lasaponara et al., 2017b; Parcak, 2007; Philip et al., 2002; Ur, 2003; Wilkinson et al., 2006). Kennedy (1998) carried out the first applications of CORONA images for virtual investigation of the Euphrates valley in Turkey. Ur (2003) exploited CORONA spy photography to investigate archaeological sites and road traces in northern Syria and thereby discovered an ancient road system. While the CORONA satellite photos have been the most used by archaeologists, there are also other examples of photographs taken from space. For instance, Fowler (1996) exploited Russian declassified KVR-1000 imagery to identify archaeological features in the surrounding of Stonehenge using crop and soil marks.

Numerous ACH applications were conducted using historic aerial and spy satellite photographs, or by integrating them with other remote sensing data (Agapiou et al., 2016a; Altaweel, 2005; Coluzzi et al., 2010; Hritz, 2013; Masini and Lasaponara, 2017; Watanabe et al., 2017). This extensive use necessitated an improvement in data-processing, mainly in overcoming the complex issues related to metrical or quantitative use (Lasaponara et al., 2018). These issues arose due to the severe distortions affecting data acquisition that prevent visual or even automatic archaeolandscape analysis procedures being carried out (Casana and Cothren, 2008; Casana et al., 2012; Rayne and Donoghue, 2018). Thus, one of the key problems is how to rectify these raw aerial and satellite photographs, especially in mountainous areas. In order to overcome the distortions, several photogrammetric and geometric approaches were proposed, along with the use of well-distributed and reliable ground control points (GCPs) (Bitelli and Girelli, 2009; Casana and Cothren, 2008; Nita et al., 2018). Doneus (2001) and Goossens et al. (2006) proposed similar ground control point methods to reduce geometric distortion in aerial photographs and CORONA images, respectively. For inaccessible areas of interest or regions of conflict, GCPs were generally collected from other sources, including rectified historical aerial photographs and CORONA images, modern satellite imagery, Google Earth and DEM products (Casana and Cothren, 2013; Rayne and Donoghue, 2018). Casana and Cothren (2008) reduced the geometric distortion in CORONA sub-images by selecting GCPs from SPOT imagery and SRTM data. Subsequently, Casana et al. (2012) developed a low time-consumption method for efficient orthorectification of full CORONA scenes using an automated scale-invariant feature transform (SIFT) algorithm and Google Maps reference data. Nita et al. (2018) developed an accurate and fast method for orthorectifying high-resolution CORONA photographs of mountain areas, and rectified scanned CORONA photography based on Structure from Motion (SfM) technology.

Due to the gradual changes in land use and land cover that have occurred over the past century, most ACH applications have favored using historical aerial and spy satellite photographs. Many archaeological features and old landscapes have been preserved in these dust-laden data (Stichelbaut, 2006). For instance, Fig. 4A and B shows rectified aerial and CORONA images of the Beijing Old City (BOC) in 1945 and 1967, respectively, showing a scene that is very different from today's metropolis (Fig. 4C). Fig. 4B shows the walls of BOC have demolished completely in 1967, due to the increasing urban sprawl of Beijing from 1950s to 1970s. The moats of BOC stood for nearly 550 years, but in the period of 1960s–1980s, were partially filled or covered to allow for constructing the Ring Road and Beijing Subway (Fig. 4C). In 1945, the urban and built-up area of Beijing only was about 100 km^2. Meanwhile, it has spread rapidly outward, and has grown to about 300 km^2 in 1967, reaching an area up to 2600 km^2 in 2015 (Huang et al., 2017). The rapid urban sprawl places BOC at great risk and irreversible landscape transformation means that valuable information about how imperial city planned and interacted with environment is lost. The BOC's old system of walls, gates and moats has reconstructed (Fig. 4D) by using old photographs.

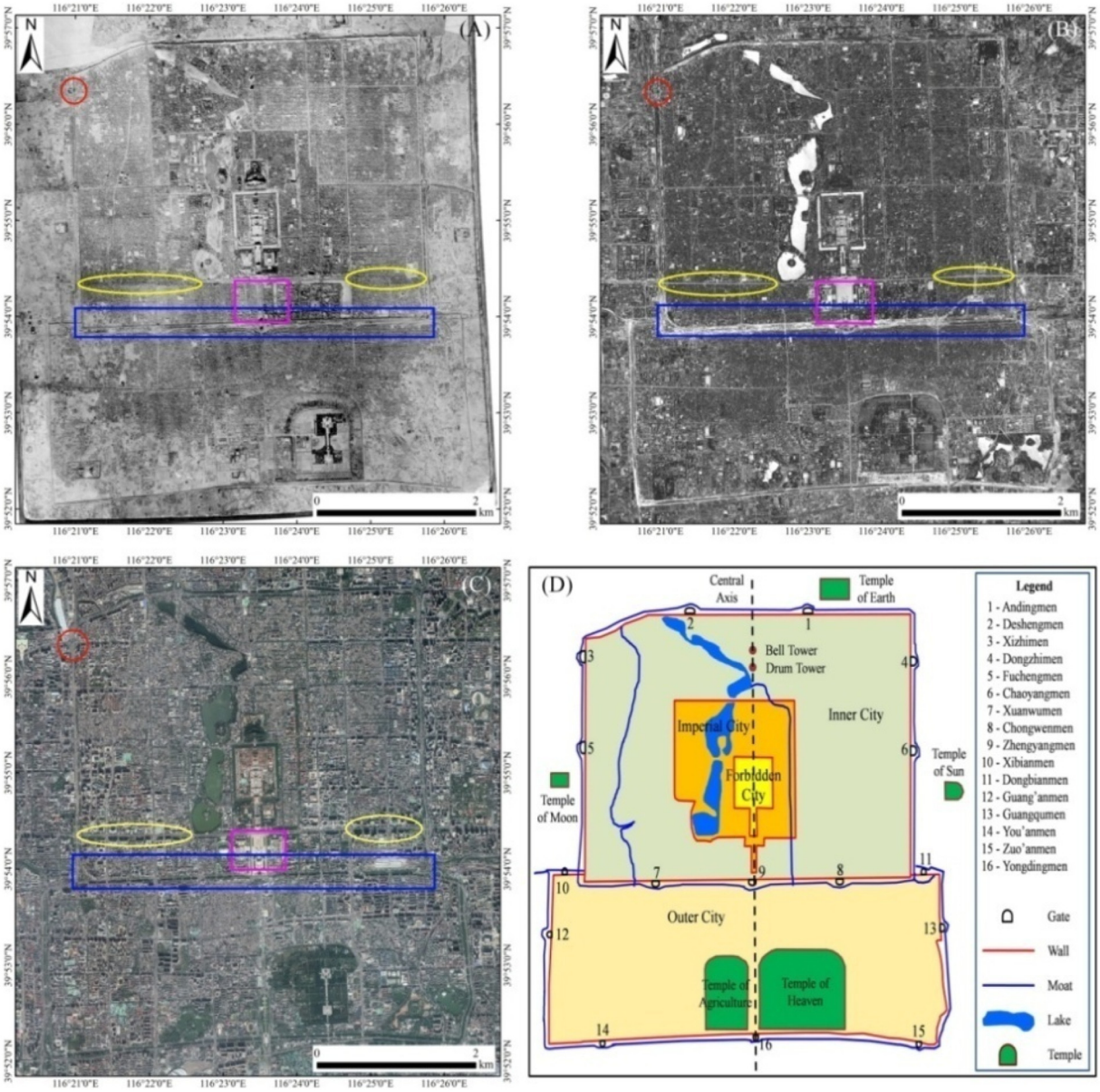

Fig. 4. Reconstruction of the walled Beijing old city (BOC) based on historical photographs. (A) Aerial photograph in 1945; (B) 0.6 m CORONA spy photograph in 1967; (C) GE imagery (© 2019 Digital Globe, acquired on 18 October 2018); (D) the layout of BOC. The red circle indicates the location of the disappeared Xizhimen Gate, the yellow ellipses show the extension of the Chang'an Avenue, and the pink and blue boxes indicate the landscape transformations. (For interpretation of the references to color in this figure legend, the reader is referred to the web version of this article.)

4.2. Multispectral and hyperspectral remote sensing

4.2.1. Background

Remote sensing images depict features (spectral, spatial, radiometric and temporal) of buried archaeological remains, most of them through the above-mentioned proxies such as crop or soil marks (Fig. 5). Since the 1900s, historical photographic data have made great contributions to our improved appreciation of the distribution and diversity of archaeological sites across the world and also to the discovery of these sites. However, photographing crop or soil marks is not equally effective in all regions of interest because of the particular imaging conditions and phenology needed before these marks become visible, which is highly unpredictable (Aqdus et al., 2012). Vertical and oblique photography, even when executed in color, thus significantly reduce the detection sensitivity of crop or soil marks. Despite their potentially high spatial resolution, photography spectrally under-samples the at-sensor radiation and masks spectral features that are too narrow to be distinguished (Verhoeven, 2017). Also, the timing of photography campaigns for archaeological prospecting is therefore crucial and, often, the optimal conditions for detection may not occur for a long period. Given that the appearance of crop or soil marks is linked to the nature of the local landscape matrix, these marks are potentially detectable at bandwidths outside the visible spectrum before they become apparent there. As a result, nowadays, spectral imaging data are commonly used in ACH applications.

4.2.2. Spectrarchaeology: spectral imaging for archaeological prospection

In this review, 'spectral imaging' generally refers to passive optical remote sensing techniques that capture a specific part of the Earth's reflected solar energy or self-emitted thermal energy from space, and then turn this into an image (Verhoeven, 2018). Since buried archaeological remains can change the chemical, physical and biological properties of the local soil matrix, their presence might be expressed by phenological differences in the spectral reflectance or height of

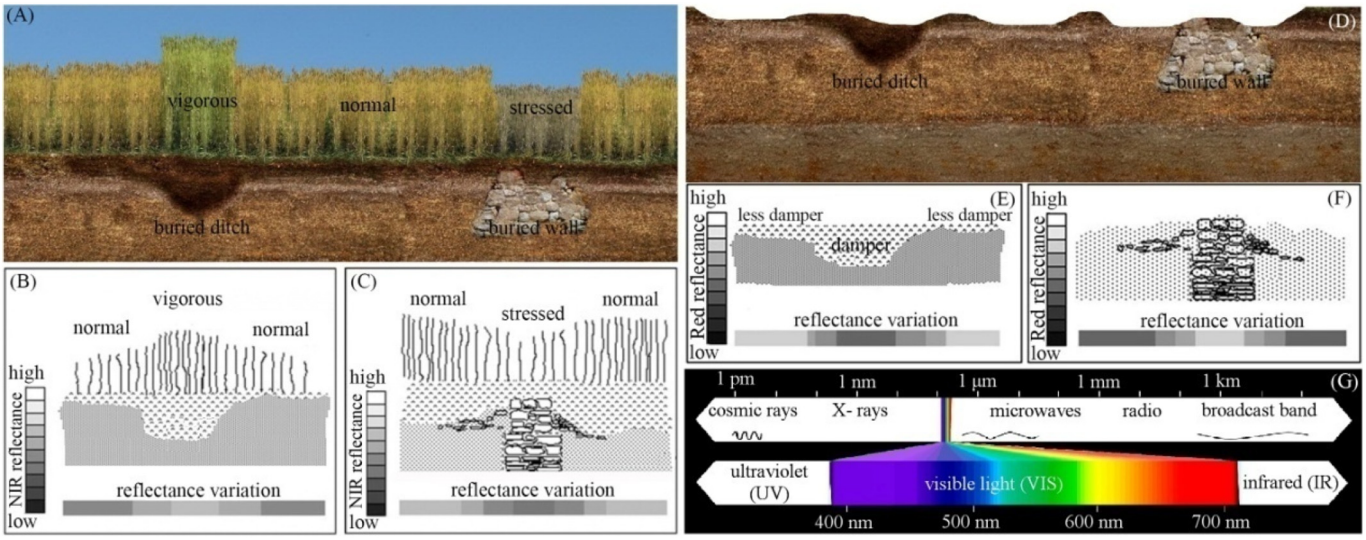

Fig. 5. Variations in reflectance due to the presence of crop marks (A) caused by buried ditch (B) and buried wall (C), and soil marks (D) caused by shallow buried ditch (E) and buried wall (F); electronic spectrum (G). ((B, C, E and F modified from Lasaponara and Masini (2012c)).

vegetation on top of the remains (crop marks) (Fig. 5A, B, C) (Agapiou et al., 2012; Beck, 2010; Lasaponara and Masini, 2007; Verhoeven, 2018) or in distinct tonal or textural differences in the ploughed soil (soil marks) (Kim et al., 2013; Luo et al., 2014a; Agapiou et al., 2016b) (Fig. 5D, E, F). Spectral imagers record the reflected energy for a number of sampled wavelength ranges — from the visible (VIS, 0.4 μm–0.7 μm) part of the electromagnetic spectrum (Fig. 5G), through the near infrared (NIR, 0.7 μm −1.1 μm), short-wave (SWIR, 1.1 μm–3 μm) and middle-wave infrared (MWIR, 3 μm–6 μm) to the thermal infrared (TIR, 6 μm–15 μm). Where vegetation cover is dominant, the VIS and NIR spectral regions are more sensitive to variations in spectral properties related to buried structures, whereas, where soil cover becomes relevant, the SWIR and the TIR regions resulted more sensitive. The selection of specific spectral channels for the detection of archaeological remains both in vegetated areas as well under bare soil has recently been discussed by Bassani et al. (2009). Variations in the spectra were the key to detecting archaeological marks. In specific cases where the dominant land cover type over archaeological sites is known, then the optimal spectral range can be selected in order to improve the efficiency of archaeological observations using remote sensing data (Agapiou et al., 2014a; Agapiou et al., 2014b; Cavalli et al., 2009).

4.2.3. Multispectral and hyperspectral imaging system

Broadband multispectral remote sensing involves the simultaneous acquisition of calibrated radiance units in a limited number (generally between 3 and 15) of non-contiguous broad (generally wider than 20 nm) spectral bands; in contrast, narrowband hyperspectral remote sensing involves the simultaneous acquisition of calibrated radiance in many (generally more than 100) narrow (generally 20 nm or smaller) spectrally contiguous channels (Agapiou et al., 2012; Beck, 2010; Veraverbeke et al., 2018). The current generation of airborne and spaceborne spectral imaging sensors easily enables a Ground Sampling Distance (GSD) below 50 cm and 2 m, respectively, with a spectral range from 400 nm to 1000 nm, respectively. The multispectral GSD can even reach 10 cm for low altitude unmanned aerial vehicles (UAVs). The fundamental differences between multispectral and hyperspectral imaging play an important role in archaeological prospecting. Obviously, more and narrower spectral bands have a greater potential for detecting subtle spectral reflectance differences in the soil and vegetation cover (Agapiou et al., 2012; Carter and Miller, 1994).

The earliest multispectral satellite imaging system for earth observation began in 1972 using the Landsat program, which had the highest (15 m) spatial resolution sensor available for civilian applications (Brivio et al., 2000; Dorsett et al., 1984). The latest Landsat satellite was launched in 2013. The importance of this system lies primarily in its potential for providing long-time series of systematic multispectral data of the earth surface features and the archaeolandscapes. A major improvement in earth observation was achieved by the end of the 20th century (1999) with the launch of IKONOS, the first commercial very high-resolution satellite with 1 m spatial resolution. Several airborne multispectral imaging systems, such as the Daedalus Airborne Thematic Mapper (ATM) (Pascucci et al., 2010; Winterbottom and Dawson, 2005), have been developed and used in archaeological research for the generation of corrected orthoimages and digital surface models (DSM). Up to now, a large number of multispectral imaging systems (Table 1) have been developed for multiscale and multi-temporal Earth-observation. Typically these systems have been exploited by satellite imaging platforms, such as Landsat MSS/TM/ETM + /OLI (Aminzadeh and Samani, 2006; Davies et al., 2016), SPOT (Fowler, 2002; Löhrer et al., 2013), IKONOS (Beck et al., 2007; De Laet et al., 2007; Garrison et al., 2008), ASTER (Altaweel, 2005; Cerra et al., 2016), QuickBird (Lasaponara and Masini, 2007; Mondino et al., 2012), GeoEye (Lin et al., 2011; Luo et al., 2017b), WorldView (Luo et al., 2014b; Parcak and Tuttle, 2016) and Sentinel-2 (Agapiou et al., 2014b; Tapete and Cigna, 2018).

Hyperspectral remote sensing has proven its utility in a wide range of Earth system science domains including ACH applications (Aqdus et al., 2012; Doneus et al., 2014; Sivitskis et al., 2018). Hyperspectral imaging, or imaging spectroscopy, refers to the acquisition of co-registered images over contiguous narrow spectral channels (Schaepman et al., 2009). Most hyperspectral ACH studies were mostly conducted based on airborne imagery, often obtained from the Airborne Imaging Spectrometer (AIS), Airborne Hyperspectral Scanner (AHS), Airborne Prism Experiment (APEX), Airborne Visible Infrared Imaging Spectrometer (AVIRIS), Compact Airborne Spectrographic Imager (CASI), or Multispectral Infrared and Visible Imaging Spectrometer (MIVIS) (Agapiou et al., 2012; Alexakis et al., 2009; Aqdus et al., 2012; Atzberger et al., 2014; Bassani et al., 2009; Cavalli et al., 2007; Cavalli et al., 2013; Cavalli et al., 2009; Cerra et al., 2018; Doneus et al., 2014; Giardino, 2012; Pascucci et al., 2010; Rowlands and Sarris, 2007; Savage et al., 2012; Sivitskis et al., 2018; Tan et al., 2005; Veraverbeke et al., 2018). Although most satellite imaging systems are multispectral, hyperspectral imagers do also exist (Agapiou et al., 2012; Alexakis et al., 2009; Castaldi et al., 2016; Savage et al., 2012). To date, Hyperion, carried on the EO-1 platform, which acquired data between 2000 and 2017 and had 242 channels, has been the only spaceborne

Table 1
List of available satellite multispectral (VIS-NIR) imaging systems for ACH applications.

Satellite/sensor	VIS-NIR		Time span	Spatial resolution/m	
	Spectrum/nm	Channel no.		PAN	VIS-NIR
ALOS/PRISM	420–890	4	2006–	2.5	10
CBERS	450–890	5	2003–		20
EO-1/ALI	433–890	8	2000–	10	30
GeoEye	450–920	4	2008–	0.41	1.65
Gaofen-1/PMS	450–890	4	2013–	2	8
Gaofen-2/PMS	450–890	4	2014–	1	4
IKONOS	450–950	4	1999–2015	1	4
IRS-P6/Resourcesat-1	520–860	3	2003–	5.8	23.5
KOMPSAT-2/EOC	450–900	4	2006–	1	4
KOMPSAT-3/EOC	450–900	4	2012–	0.7	2.8
Landsat-1/MSS	500–1100	4	1972–1978	78	
Landsat-4/MSS	520–900	4	1982–1993	78	
Landsat-5/TM	450–900	4	1984–2013	30	
Landsat-7/ETM+	450–900	4	1999–	15	30
Landsat-8/OLI	443–885	5	2013–	15	30
Orbview-3	450–900	4	2003–	1	4
Pleiades-1	430–950	4	2011–	0.5	2
Pleiades-2	430–950	4	2012–	0.5	2
QuickBird	450–900	4	2001–	0.6	2.4
RapidEye	440–850	5	2008–	5	
Sentinel-2/MSI	450–900	4	2015–	10	
SPOT-1/HRV	500–890	3	1986–2003	10	20
SPOT-2/HRV	500–890	3	1990–2009	10	20
SPOT-3/HRV	500–890	3	1993–1996	10	20
SPOT-4/HRVIR	500–890	3	1998–	10	20
SPOT-5/HRG	500–890	3	2002–	5	10
SPOT-6/HRG	455–890	4	2012–	1.5	6
SPOT-7/HRG	455–890	4	2014–	1.5	6
Terra/ASTER	520–860	3	1999–	15	
WordView-2	400–1040	8	2009–	0.46	1.84
WordView-3	400–1040	8	2014–	0.31	1.24
Ziyuan-3	450–890	4	2012–	2.1	5.8

hyperspectral imager that acquired data in the visible to short-wave infrared spectral range (0.4 μm–2.5 μm) (Veraverbeke et al., 2018).

4.2.4. Airborne hyperspectral remote sensing in ACH applications

Airborne hyperspectral applications used in archaeology mainly fall into the detection of crop marks, in which the goal is to identify spectra containing archaeological anomalies (Agapiou et al., 2012; Alexakis et al., 2009; Aqdus et al., 2012; Cavalli et al., 2007; Cavalli et al., 2013; Cerra et al., 2018; Doneus et al., 2014; Savage et al., 2012; Tan et al., 2005). In the literature, many techniques for the detection of Earth surface features or objects (Schaepman et al., 2009; Veraverbeke et al., 2018) as well as archaeological anomalies related to buried remains (Bassani et al., 2009; Cavalli et al., 2009; Lasaponara and Masini, 2012c) have been developed. However managing and processing hyperspectral data is not a simple task, mainly because of the hundreds of spectral channels involved. Thus, it is imperative to carry out dimensionality reduction for speeding up the visual interpretation and identification of buried remains in airborne hyperspectral images to support further archaeological prospecting. For this purpose, many techniques have been proposed to reduce the dimensionality of hyperspectral images, preserving the variability in the original dataset (Huang et al., 2015; Lee et al., 1990; Plaza et al., 2005; Wang and Chang, 2006). Among these, Principal Components Analysis (PCA), a generic spectral enhancement technique used by remote sensing archaeologists, has been widely used to enhance visual interpretation (Fig. 6A, B) of the scene or as a way of increasing the computational efficiency of automated classification procedures (Cavalli et al., 2007; Cavalli et al., 2013; Doneus et al., 2014). In PCA, the vast majority of the variance in the original dataset (sometimes greater than 95%) is captured by the first principal component, and each new principal component is orthogonal to every other. Vegetation Indies (VIs) (Fig. 6C) have a certain potential to enhance the visibility of crop marks. The principle of VI based ACH applications will be discussed in detail in section §4.2.5 below. In addition to PCA and VIs, Doneus et al. (2014) investigated the red edge inflection point (REIP) (Fig. 6D) and distribution fitting (Fig. 6E, F) for analysing airborne narrowband spectral data. Their examples showed that, when compared to the true color imagery, distribution fittings and REIP visualizations can increase the contrast between healthy and stressed crops (Fig. 6H, G).

Besides dimensionality reduction, channel selection, image enhancement and classification are the main issues in hyperspectral applications for detecting archaeological features. Since buried remains generate slight differences in spectral features between the pixels containing archaeological marks and the background pixels, the capability of airborne hyperspectral sensors to distinguish spectral anomalies related to buried remains can be assessed by using the Spectral Separability Index (SSI), Spectral Angle Mapper (SAM) and Spectral Mixture Analysis (SMA) (Cavalli et al., 2009). SSI, also called M-statistics (Luo et al., 2018b), can be used to assess the separability between archaeological features and backgrounds by a channel-by-channel inspection of multispectral or hyperspectral data, and then also used to guide the selection of spectral channels for improving the ability to detect buried archaeological remains and reduce the computation time (Bassani et al., 2009; Cavalli et al., 2009; Lasaponara et al., 2016; Lasaponara and Masini, 2012c). The SAM determines the spectral similarity on the basis of the spectral shape. It describes the angular differences (expressed in radiance from 0 to $\pi/2$) between the spectrum of every quarantine pixel and the spectrum of one given endmember related to the archaeological features (Savage et al., 2012). Instead of placing each pixel in an image into one of a set of discrete classes, SMA starts with a set of endmembers, representing a spectral library, and then deconvolves the image through linear spectral unmixing to reveal the percentages of endmembers present in each analyzed pixel. SMA analysis provides the potential for covering a large spectral library of

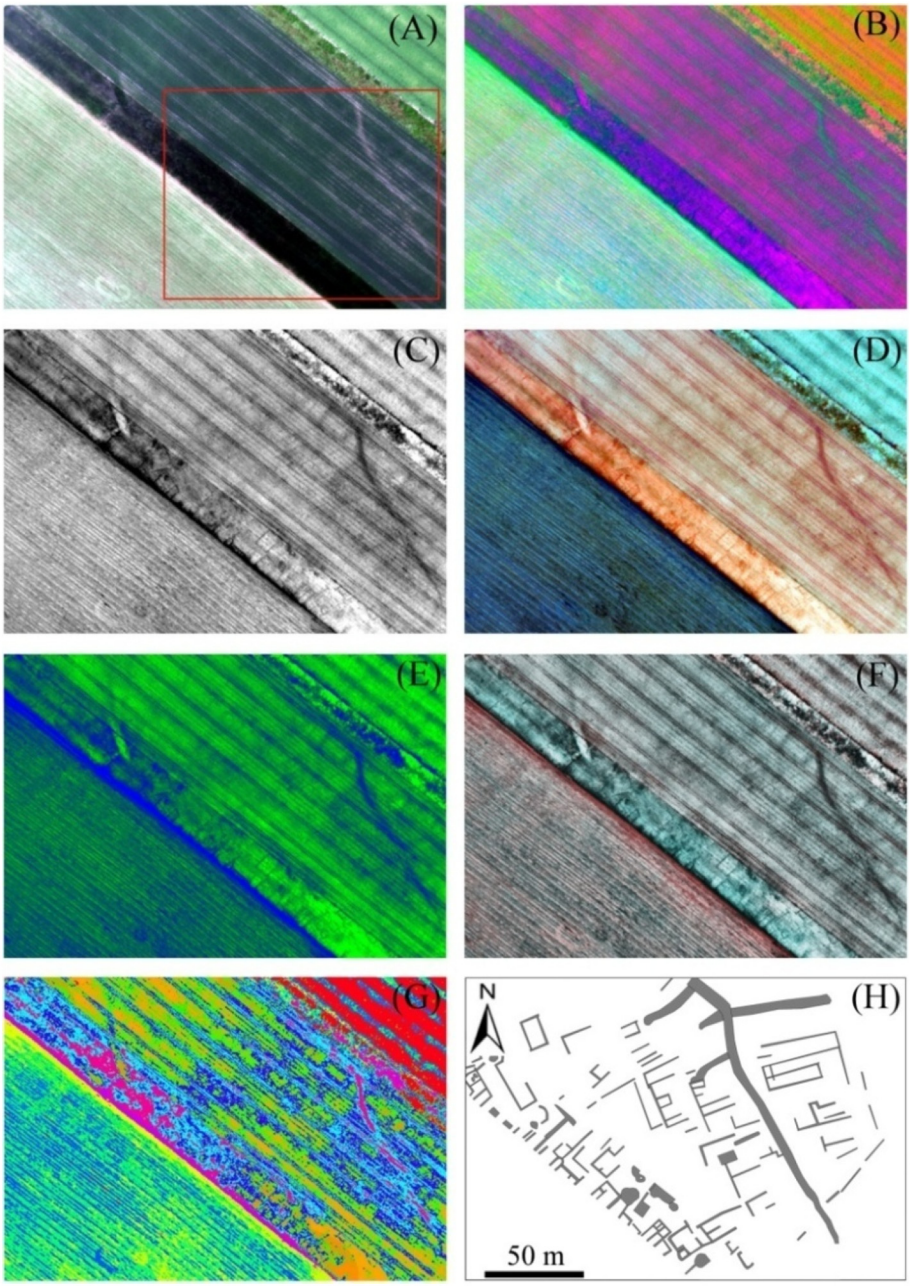

Fig. 6. Airborne hyperspectral data (64 spectral channels and 0.4 m GSD) from Carnuntum, Austria, acquired on May 262,011 (Data source: LBI-ArchPro and ABT GmbH). (A) True-color image; (B) false color composite created by the PCA (R = PC1, G = PC2, B = PC3); (C) NDVI; (D) false color composite created by the REIP (R = band 1 (wavelength), G = band 2 (slope), B = band 3 (reflectance value)); (E) gamma distribution fitting (R = none, G = band 2 (shape parameter α), B = band 1 (rate parameter β)); (F) normal distribution fitting ((R = band 4 (the upper bound of the confidence interval for mean (μ)), G = band 2 (standard deviation (σ)), B = band 2)); (G) unsupervised k-means classification results with 10 classes; (H) visual interpretations of archaeological traces (Roman Road) from (D) covering the area enclosed by red box in (A). All data processes were implemented in an open MATLAB®-based archaeological toolbox called ARCTIS (see Atzberger et al. (2014)). (For interpretation of the references to color in this figure legend, the reader is referred to the web version of this article.)

endmembers, including archaeological features and other land cover types. It is a useful tool for guiding surveys and for discovering unknown sites in a large region with actual ancient human occupations (Savage et al., 2012).

4.2.5. Satellite multispectral remote sensing in ACH applications

Satellite multispectral imaging, the most popular technique in the second half century of remote sensing archaeology, has been successfully applied in almost every field related to ACH (Pringle, 2010). Success stories include the detection and identification of archaeological features (Agapiou et al., 2014a; Baeye et al., 2016; De Laet et al., 2009; Lasaponara and Masini, 2007; Menze and Ur, 2014), archaeolandscape analysis and reconstruction (Banerjee and Srivastava, 2013; Canilao, 2017; Foglini et al., 2016; Gallo et al., 2009; Luo et al., 2017a), looting monitoring and assessment (Agapiou et al., 2017a; Contreras and Brodie, 2010; Lasaponara et al., 2012; Stone, 2008), urbanization mapping (Agapiou, 2017b; Agapiou et al., 2015a; Lefebvre, 2017), risk monitoring and assessment (Agapiou et al., 2016c; Hadjimitsis et al., 2013a; Lasaponara et al., 2017b; Reimann et al., 2018), and cultural heritage management and conservation (Agapiou et al., 2015b; Comer, 2012; Davies et al., 2016; Evans et al., 2007; Parry, 1992; Rayne and Donoghue, 2018).

Recently, VHR satellite multispectral imagery was used to track heritage loss across Middle East (such as Syria, Iraq, Egypt, Yemen, Oman, and Lebanon) and to assess the damage to Syria's World Heritage Sites caused by ISIS and the Syrian civil war (Casana, 2015; Luo et al., 2018a; Parcak et al., 2016). Several international organization and scientific communities, such as UNESCO, UNITAR and AAAS, have launched the satellite applications project during the past sensitive period, one of whose aims is to provide remote sensing support for the fast assessment and decision-making of the cultural heritages and archaeological sites (AAAS, 2014; Luo et al., 2018a). A well-known example is the Roman site of Dura Europos on the West bank of the Euphrates River. During the three years (2011–2014) that separate the two VHR satellite images (Fig. 7) that were analyzed, the site was subject to extremely serious looting. A long history of pre-war looting

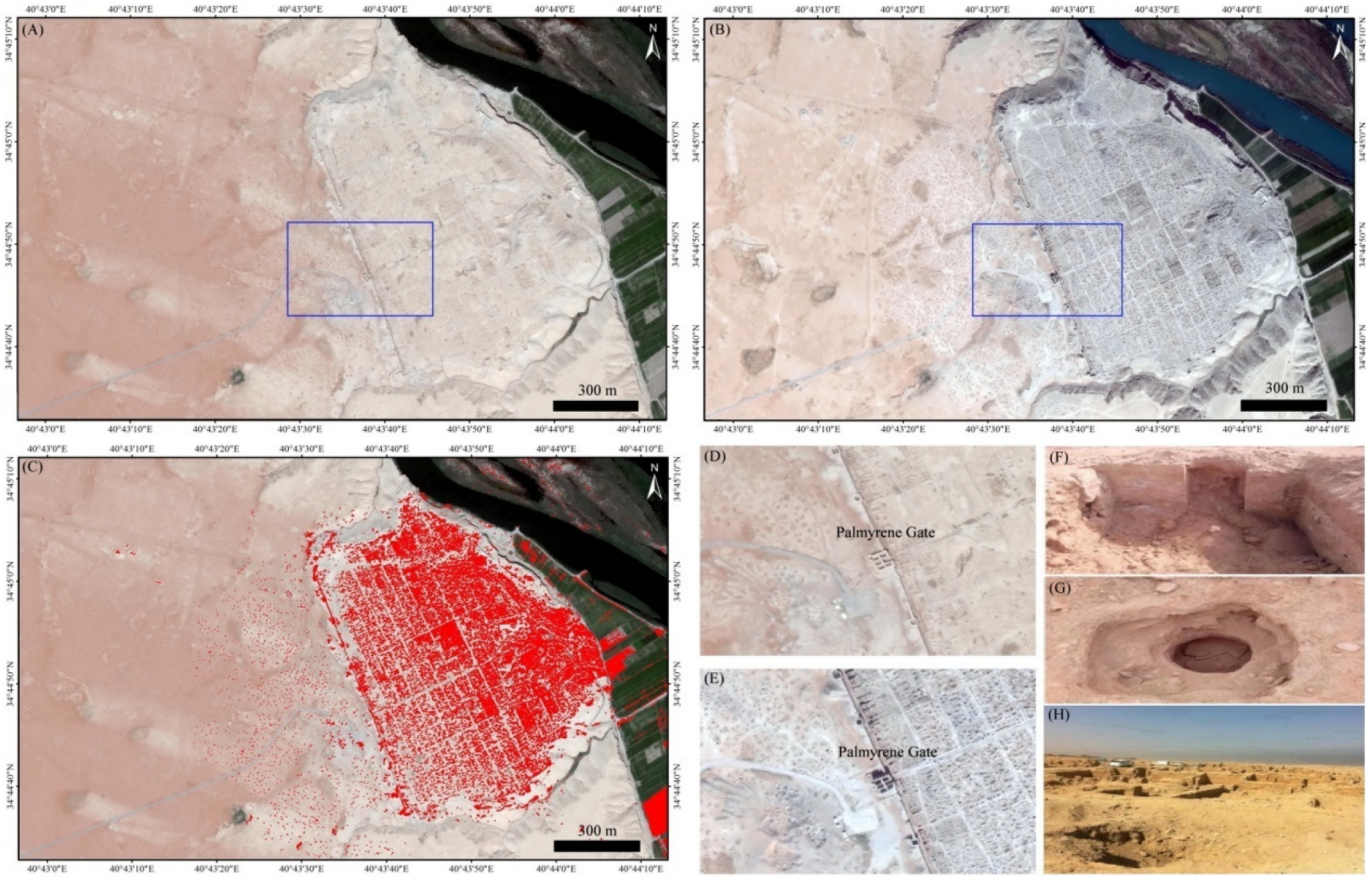

Fig. 7. Dura Europos, eastern Syria, as it appears in VHR satellite images (© 2019 Digital Globe) from August 2011 (A) and April 2014 (B). The VHR satellite image from 2011 was displayed with detected looting changes in red (C); the sub-image correspond to the area marked by the blue box in A, dozens of old looting pits are visible around the Palmyrene Gate (D); the sub-image correspond to the area marked by the blue box in B, a renewed phase of severe, war-related looting with fresh pits clearly visible in the same area (E); and ground views (© AAAS (2014)) of looting at Dura Europos site (F–H). (For interpretation of the references to color in this figure legend, the reader is referred to the web version of this article.)

extending back several decades is visible in an early 2011 VHR satellite image (Fig. 7A) of the site, but in 2014 (Fig. 7B), the site was further damaged by looting, with thousands of new looting pits visible across the entire site. Fig. 7C shows the changes caused by looting between 2011 and 2014, which were identified in ENVI 5.3 by using the change-detection tool. These applications have primarily exploited broadband multispectral remote sensing data. As Giardino (2011) and Agapiou and Lysandrou (2015) argues, multispectral sensors carried on satellite platforms have provided new and important dataset for the investigation, discovery, delineation and analysis of ACH sites worldwide (Agapiou et al., 2014a; Agapiou et al., 2014b; Alexakis et al., 2009; Aminzadeh and Samani, 2006; Deroin et al., 2011; Garrison et al., 2008; Luo et al., 2017b).

The sensitivity of satellite multispectral sensors was systematically assessed and used in a series of studies by Agapiou (Agapiou et al., 2014a; Agapiou and Hadjimitsis, 2011; Agapiou et al., 2013b; Hadjimitsis et al., 2013b) that focused on (1) the investigation and assessment of the spectral sensitivity of satellite multispectral sensors intended for use in the detection of archaeological crop marks, (2) ground spectroscopy and ground-truthing campaigns for quantitative archaeological applications, and (3) establishment and validation of orthogonal equations to multispectral satellite imagery for the identification of archaeological features. For instance, a series of new linear orthogonal equations for different multispectral data derived from QuickBird, IKONOS, WorldView, GeoEye, ASTER, and Landsat sensors was developed to enhance the exposure of archaeological marks (Agapiou, 2017a; Agapiou et al., 2013a). In the last decade, most satellite multispectral studies have focused on identifying archaeological features from very high resolution (VHR) imagery (Agapiou et al., 2012; Hadjimitsis et al., 2013b; Lambers, 2018; Lasaponara and Masini, 2012a; Noviello et al., 2013). However, traces of archaeological features are very hard to observe due to multiple factors. As a result of coarse spectral and spatial resolution, image degradation, the presence of obstacles (trees, man-made objects, etc.), and unfavorable preservation, they are often only partially visibility. In order to improve the visibility of archaeological features, many enhancement techniques that can be applied to the spatial, spectral and frequency domains (e.g., data fusion, VIs, orthogonal equations, convolution and morphology, PCA, Kauth-Thomas (K-T), and Wavelet) have been adopted (Lasaponara et al., 2016; Luo et al., 2017a; Tapete and Cigna, 2018). This is because viewed from above, the presence of buried remains appears as subtle spatial discontinuities or variations in the reflectance values of vegetation or soil cover (Agapiou and Hadjimitsis, 2011; Agapiou and Lysandrou, 2015; Beck, 2010; Lasaponara and Masini, 2007; Rowlands and Sarris, 2007; Traviglia and Cottica, 2011; Verhoeven, 2012).

Data fusion and pansharpening can be considered suitable for improving the visibility of archaeological features in multispectral data (Lasaponara and Masini, 2012b; Noviello et al., 2013). Several studies have presented the results of applying different pansharpening techniques (Fig. 8) for better identification of buried remains (De Laet et al., 2015; Lasaponara and Masini, 2012b; Lasaponara and Masini, 2014; Traviglia and Cottica, 2011). The reason for the multiplicity of techniques is that either the spatial or the spectral properties of the image are always compromised during the pansharpening process (Opitz and Herrmann, 2018). VIs are mathematical combinations of reflectance

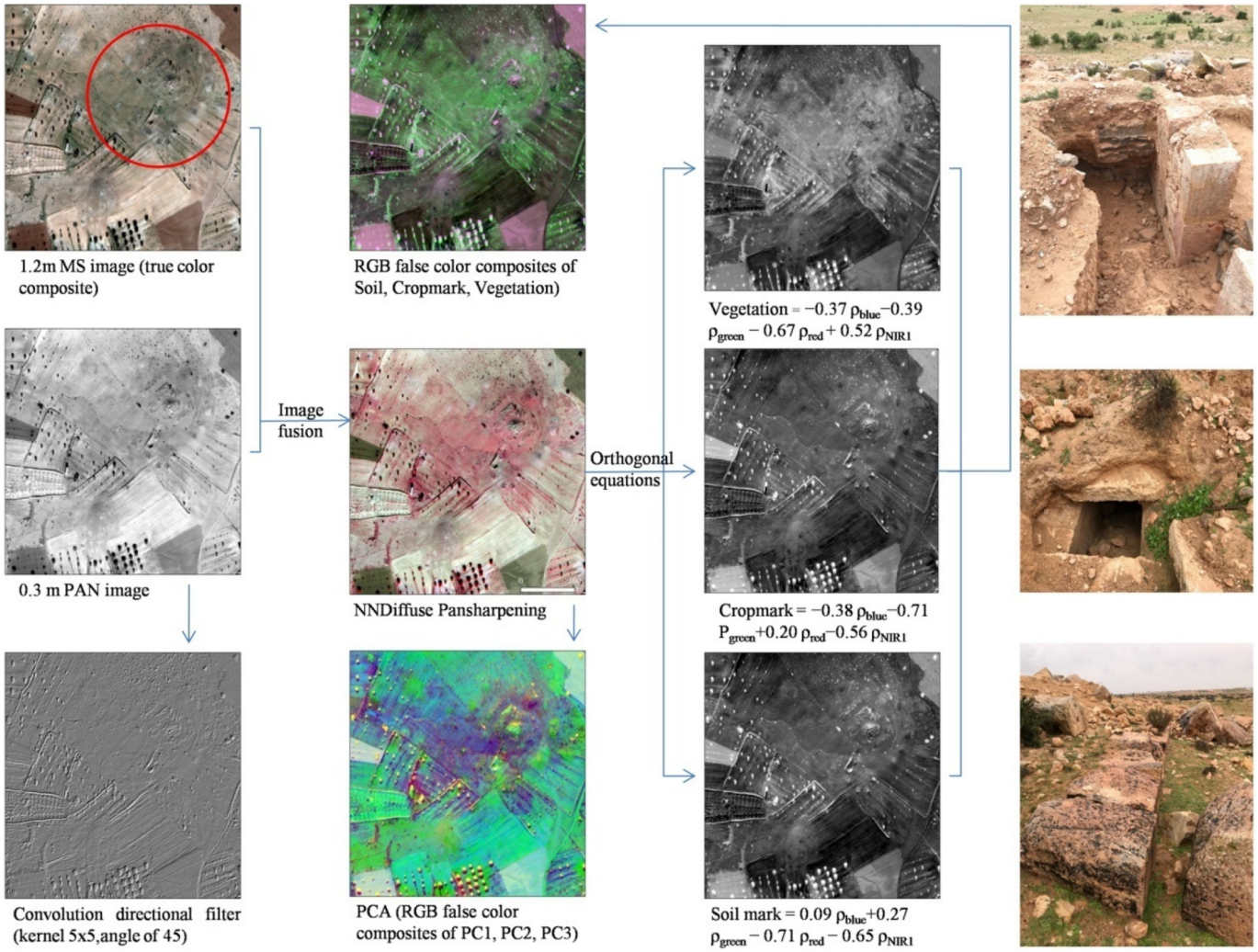

Fig. 8. The image processing results from WorldView-3 multispectral data allowed us to discover buried archaeological remains near the site of the Roman Port City Gigthis (Tunisia).

values from two or more spectral channels of multispectral or hyperspectral data. These combinations highlight a specific feature of the vegetation while reducing the perturbing effects caused by solar geometry as well as atmosphere, topography, viewing angle and exposed soil (Verhoeven, 2012). There exists a variety of VIs, each of them using different datasets and optimized for specific purposes (Agapiou et al., 2013a; Agapiou et al., 2013b; Atzberger et al., 2014). As a result, they all have their advantages and disadvantages as well as appropriate operational scales. As such, not all of these VIs are of benefit to archaeology and the NDVI remains the most popular index (Lasaponara and Masini, 2007; Masini and Lasaponara, 2007). A comprehensive analysis that included 38 vegetation indices, object-oriented classification and segmentation, PCA, and color transformation, was applied to the detection of looting marks in WorldView-2 imagery and the results interpreted (Agapiou et al., 2017a). Lasaponara and Masini (2014) proposed a novel enhancement approach based on local indicators of spatial autocorrelation applied to ASTER and QuickBird data, which allowed them to visually identify traces of a possible ancient hydrographic network.

However, the spatial resolution of hyperspectral satellite data is much lower than that of multispectral satellite data and so, of limited application to the fine-scale study of ACH sites. The satellite EO-1 Hyperion has a spectral and spatial resolution of 10 nm and 30 m, respectively. There is an extreme paucity of studies exploring the capabilities of hyperspectral satellite data in ACH application. Savage et al. (2012) guided an archaeological survey and found several potential ore-processing areas with similar spectral signatures by visually interpreting the results of applying PCA to Hyperion imagery. Another exception is the research published by Agapiou et al. (2013b) which demonstrated that their proposed Archaeological Index was suitable for the enhancement of crop marks in Hyperion imagery. However, so far, this study stands alone.

5. Active remote sensing in ACH applications

5.1. Synthetic aperture radar (SAR)

5.1.1. Background

In contrast to passive optical remote sensing, SAR actively transmits radar signals and then receives backscattering radiation for imaging. It can provide a major contribution to overcoming the limits of passive optical data: being an active technique, SAR is able to sense a target at any time of day or night under all-weather conditions and, to some extent, 'penetrate' soil and vegetation depending on the imaging frequency (C-, L-, X-, and P-band), surface characteristics (ice, desert sand, close canopy, etc.) and conditions (texture, moisture content, compactness, etc.). Backscattering amplitude and phase are two components of a SAR image (Franceschetti and Lanari, 2016). The former is influenced by speckle, layover, shadow and foreshortening, and the latter by the variation in backscattering and movements of terrain

(Chen et al., 2017c). The characteristics of surface objects, such as landcover type, relief, geometry, moisture, conductivity and roughness, can be retrieved by exploring the amplitude information (backscattering coefficient σ^0); topographic data and subtle deformation can be derived by exploiting the phase information from interferometric analyses of multiple SAR images. In addition, the radiometric component of SAR data, i.e. the intensity (*I* value), can serve as an additional feature in archaeological prospecting.

5.1.2. SARchaeology: SAR in archaeology

In general, the ability of SAR to discriminate archaeological objects is an issue closely related to both the signal-to-noise ratio and to the differential scattering behavior of target objects and their surroundings (Chan and Koo, 2008; Chapman and Blom, 2013; Chen et al., 2017c; Holcomb, 2007). Compared with passive optical remote sensing, large numbers of studies have demonstrated that SAR is superior at detecting buried features, soil-marks and micro/medium-relief (occurring as shadow-marks in optical imagery with a low solar elevation angle) for archaeological purposes (Adams et al., 1981; Chen et al., 2017c; Guo, 1997; Lasaponara et al., 2017a; McCauley et al., 1982; Moore et al., 2007; Stewart et al., 2013; Tapete et al., 2016). Several publications have also tried to demonstrate the potential of SAR in prospecting for crop-marks (Chen et al., 2015; Jiang et al., 2017; Stewart, 2017) but with little success in spite of years of effort. Fig. 9 shows a general model of the basic scattering mechanisms between the radar signal and typical archaeological objects (soil marks and micro/medium-relief). The configuration of the SAR system (frequency, polarization, incidence angle and viewing geometry) will additionally influence the visibility of archaeological features. It is worth noting that different frequencies are characterized by different 'penetration capabilities', with higher frequencies exhibiting greater penetration capabilities (Lasaponara and Masini, 2013). The penetration capability is strongly limited by surface characteristics and significantly influenced by tree canopy and moisture content.

The interferometric SAR (InSAR) technique, which is based on the processing of two or more SAR images covering the same scene, has the ability to detect changes occurring between acquisitions (Cigna et al., 2014; Hanssen, 2001; Tang et al., 2016; Tapete et al., 2012). A high-resolution DEM, one of the most common and popular InSAR-derived products, provided an insight into settlement patterns in ancient times and allowed discovery of new structures (Bubenzer and Bolten, 2008; Garrison et al., 2011; Menze et al., 2006). Therefore, InSAR-derived subtle deformations have great potential for preventive diagnosis of the structural instability and vulnerability of ACH sites and their surrounding environments and providing early warnings of these problems (Chen et al., 2017a; Tapete et al., 2012). Movements not perceivable with the naked eye can be revealed through estimates of displacement only along the radar line of sight (LOS) (Fig. 10) (Tapete et al., 2012). Differential InSAR (D-InSAR) techniques date back to 1989, when L-band SEASAT SAR data was first exploited for this purpose (Gabriel et al., 1989). Since 2001, the capability of D-InSAR has been considerably improved by using Multi-Temporal InSAR (MT-InSAR) (Crosetto et al., 2016; Lin et al., 2017) to enhance accuracy and retrieve consistent estimates, with millimeter precision being achieved for single measurements.

5.1.3. Airborne and spaceborne SAR system

Airborne SAR systems, which are generally equipped with dual antennas, can map regions of interest at high spatial resolution and with faster repeat times than satellite SAR systems and thus play a key role when cloud cover, bad weather or the need for nighttime acquisition restrict other approaches. These advantages have been used in planned archaeological prospecting (Garrison et al., 2011; Moore et al., 2007). Currently, several relatively mature airborne SAR systems-E-SAR, OrbiSAR-1, Eco-SAR, AIRSAR and UAVSAR (Garrison et al., 2011) - are available. E-SAR identifies the DLR airborne experimental SAR system which has been operated on their Dornier DO228-212 aircraft since 1988. This system has polarimetric and interferometric flexibility and is capable of emitting a radar signal at four separate frequencies. The fully polarimetric SAR data acquired by E-SAR L- and P-band radar, together with X- and C-band E-SAR data, has been collected to estimate surface topography. UAVSAR, a NASA/JPL L-band airborne experimental SAR platform that uses quad-polarization to image, has been in operation since 2009. UAVSAR is designed to collect fully polarimetric SAR data from an aircraft that can fly near-exact-repeat flight lines for interferometry research and applications. This radar system is designed to operate on an Unpiloted Aerial Vehicle (UAV) but was initially demonstrated on a NASA Gulfstream III aircraft (C-20A/G-III) (Comer et al., 2017).

Spaceborne SAR systems can be mounted on space shuttles, space stations or satellites. SEASAT, the first spaceborne SAR system, was launched in 1978 by NASA, to carry out demonstration studies focused on the oceans. Later, the Shuttle Imaging Radar (SIR) systems consisting of SIR-A, SIR-B and SIR-C were launched one after another and acquired data that gradually came to be used for archaeological purposes. Since the first use of SAR imagery acquired by the space shuttle in the 1990s, satellite SAR systems, such as ENVISAT and RADARSAT, developed by ESA and CSA, respectively, have been introduced and their products have also been used by archaeologists. In 2000, the Shuttle Radar Topography Mission (SRTM) was designed for interferometric

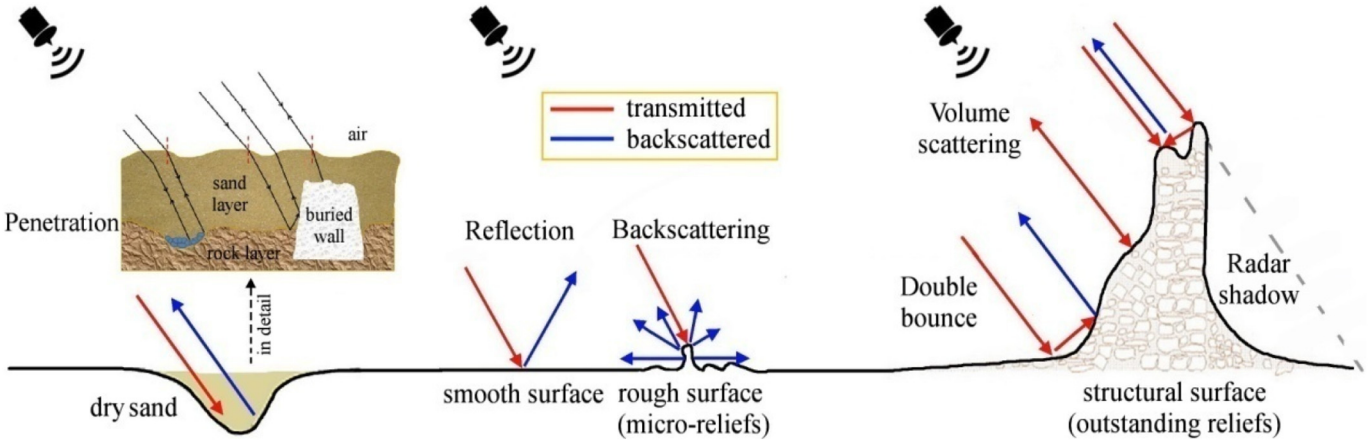

Fig. 9. Model of the response of basic scattering mechanisms: from left to right, simplified models of volume scattering in soil penetration, single bounce (smooth surface), back scattering (surface roughness for archaeological microrelief) and double bounce volume scattering (walls or other outstanding reliefs). (Modified from Lasaponara and Masini (2013)).

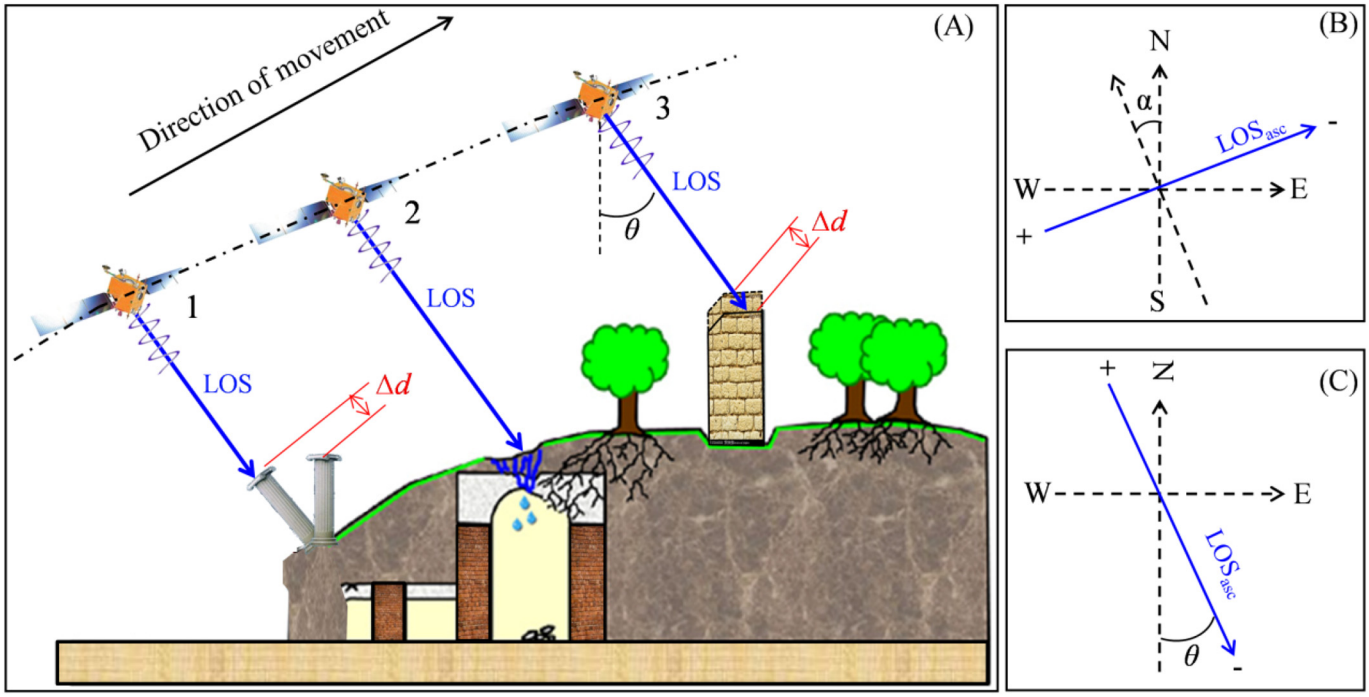

Fig. 10. Estimation scheme, along the line of sight (LOS), of the displacement (Δd) that occurred in the elapsed time between two consecutive acquisitions (Δt), (A) in cases of: (1) toppling outstanding relief, (2) terrain deformation correlated with instability of buried structures, and (3) building collapse due to land subsidence and ground motions; (B, C) LOS geometry for the ascending acquisition mode, with orbit inclination, α, and look angle, θ, indicated. (Modified from Tapete et al. (2012)).

applications and measuring large-scale surface changes. The Digital elevation models (DEMs) derived from SRTM data have been and still are one of the most useful and most often used SAR-based products in landscape archaeology (Bubenzer and Bolten, 2008; Menze et al., 2006). Since 2007, satellite SAR has witnessed a revolution as the first generation of satellites (e.g., ERS-1/2, JERS-1, ENVISAT, ALOS-1, and RADARSAT-1/2) has been followed by the second (e.g., COSMO-SkyMed, TerraSAR-X, Sentinel-1, ALOS-2 and Gaofen-3). Satellite SAR systems have been developed to provide multi-frequency, multi-polarization, multi-mode, variable incidence angle, and high-resolution data. Furthermore, a number of user-friendly commercial and open-source software or toolkits have recently been developed. As a result, space-borne SAR systems have ushered in a new era of ACH applications mainly due to the increasing availability of large historical archives and active satellite platforms.

5.1.4. SAR for archaeological prospecting

SAR-based archaeological investigations date back to the 1980s and undoubtedly have enabled numerous important discoveries and provided new insights in forested areas and desert environments, as in the cases of the Maya Lowlands (Adams et al., 1981) and the Sahara (McCauley et al., 1982). Since then, more and more studies have uncovered buried features and paleo-landscapes by exploiting the peculiar penetration capability of SAR (Blom et al., 1997; Blom et al., 1984; Chen et al., 2016; Evans et al., 2007; Gould, 1987; Guo, 1997; Lasaponara and Masini, 2013; Moore et al., 2007) at different acquisition frequencies. In the eastern Sahara Desert (Ghoneim et al., 2012; McCauley et al., 1982), southern Taklimakan Desert (Holcomb, 1992) and Gobi Desert (Guo et al., 2000; Wang et al., 2004), subsurface linear features related to paleo-channels were discovered using space shuttle SAR data. These discoveries had significant implications for the geoarchaeology and landscape evolution of paleo-environments in the research regions. In other cases, the paleo-landscapes and water management systems of prehistoric and ancient Angkor lying under tropical forests were revealed using AIRSAR data (Evans et al., 2007; Moore and Freeman, 1996; Moore et al., 2007).

SAR's sensitivity to structures makes it more useful than passive optical data for detecting archaeological microrelief or outstanding relief. Taking Peru's Nasca Cultural Landscape as an example, C-band ENVISAT, L-band PALSAR and X-band COSMO-SkyMed imagery (Cigna et al., 2013; Lasaponara et al., 2017a; Tapete et al., 2013) were separately used to detect earthen structures that are only partially above ground; visually, these structures would be difficult to distinguish from the surrounding landscape. Several researches assessed the sensitivity of satellite SAR to buried or microrelief archaeological features in terms of frequency, polarization, incidence angle and scale based on an analysis of SAR imagery from both single- and multi-date (Chen et al., 2017b; Chen et al., 2016; Lasaponara and Masini, 2013; Patruno et al., 2013; Stewart et al., 2014; Tapete and Cigna, 2017b). Stewart et al. (2014) assessed the sensitivity to buried archaeological structures of C- and L-band SAR with various polarizations in the eastern outskirts of Rome, including single and dual-polarization PALSAR and quad-polarization Radarsat-2 SAR data. The results showed that by identifying the polarimetric bases that yielded the greatest backscatter over anomalous features and subsequently changing the polarimetric bases of the time series, features of interest in the study area could be highlighted. The multi-frequency polarimetric SIR-C/X-SAR data (Guo et al. 1997) have been used to uncover the buried remains of two generations of the earthen Great Wall in northwestern China (Fig. 11). The colors in the composite image below (Fig. 11B) have been assigned to different radar frequencies and polarizations as follows: red is L-band, horizontally transmitted, horizontally received (L-HH); green is L-band, horizontally transmitted, vertically received (L-HV); and blue is C-band, horizontally transmitted, vertically received (C-HV). Fig. 11C shows that the L-band HH image provides the clearest image of the wall, and that the two generation of the earthen Great Wall are seen less distinctly in the L-HV image and C-HH image.

Generally, most archaeological applications have directly utilized SAR imagery for visual interpretation and identification of buried features, microrelief or outstanding relief (earthworks, walls and other structures) by using the backscatter, which provides information about surface characteristics according to the wavelength frequency,

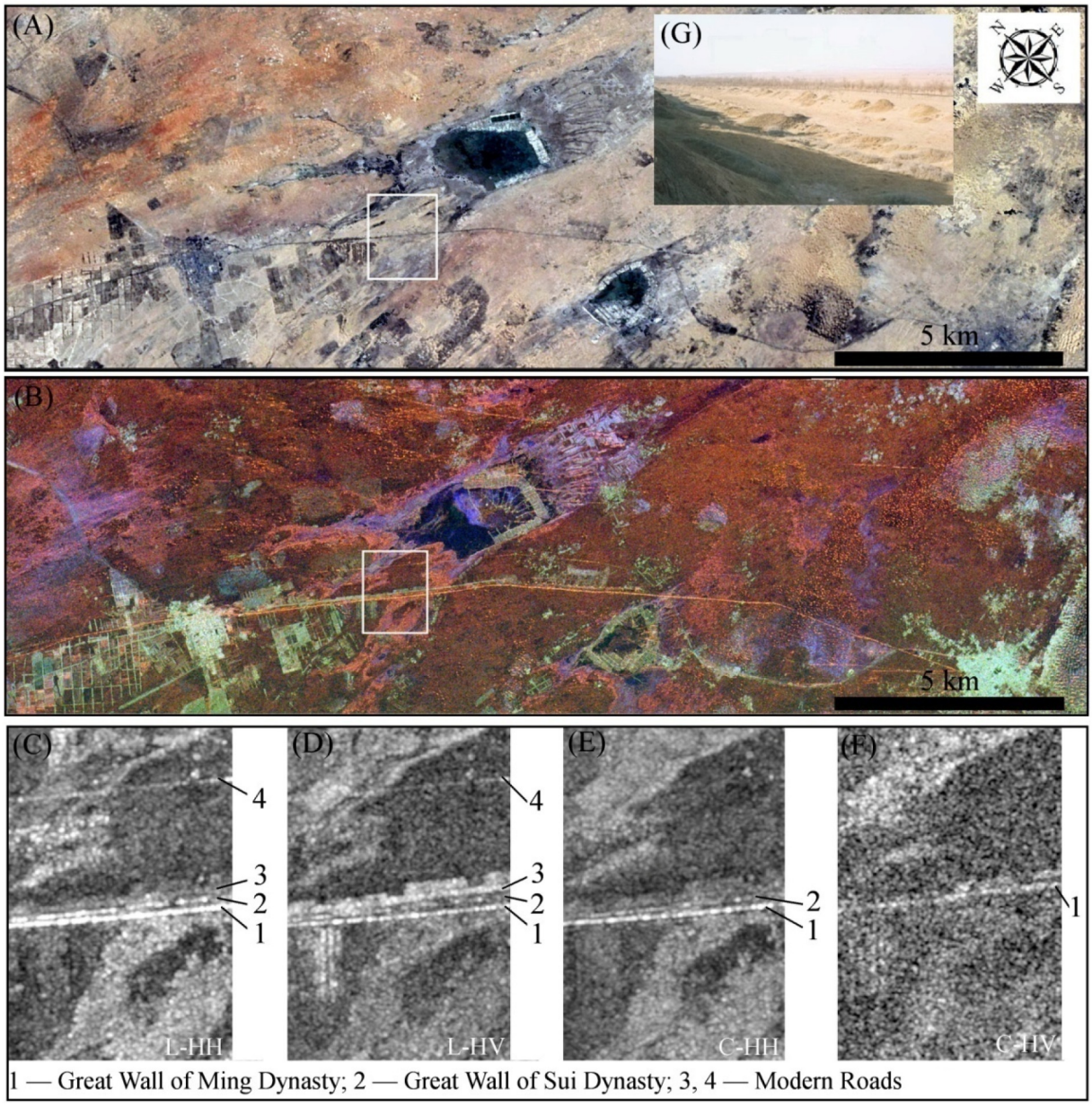

Fig. 11. SIR-C/X-SAR polarimetric images showing the buried segments of the earthen Great Wall in northwestern China. (A) Landsat-5 TM imagery; (B) false color composite of SAR SIR-C/X-SAR polarimetric images, the trace of Great Wall appears as a thin orange band, running from the right to the left; (C–F) the sub-images correspond to the area marked by the white box in A and B, and are the four frequency-polarization channels; (G) field photo of archaeological remains of the Great Wall. (SAR SIR-C/X-SAR images courtesy of JPL).

polarization and incidence angle. However, the effect of the viewing geometry and radar illumination on the visibility of archaeological features should be taken into consideration. Both Patruno et al. (2013) and Chen et al. (2016) provided pilot cases and interesting discussions on how different bands, incidence angles and imaging modes (spatial resolutions) can be used in a polarimetric analysis to detect buried archaeological features in arid environments. Additionally, in order to reduce speckle and improve the visibility of archaeological features, certain enhancement methods included multi-looking, filtration and multi-temporal averaging have been applied to archived SAR data. Further processing may involve multi-temporal coherence, analysis of target decompositions, and study of the polarimetric signatures over areas of suspected buried structures and changing the polarimetric bases in an attempt to enhance the visibility (Tapete and Cigna, 2017b).

For archaeological purposes, SAR-derived DEM products are most often used for surface analysis (Bubenzer and Bolten, 2008; Chen et al., 2016; Erasmi et al., 2014; Garrison et al., 2011; Ghoneim et al., 2012; Hillier et al., 2007; Luo et al., 2017b; Menze et al., 2006; Rajani and Rajawat, 2011) in order to provide new insights into the understanding of archaeolandscapes or paleo-environments. The near-global availability of the SRTM product offers specialists the opportunity of carrying out large-scale surveys for landscape archaeology and geoarchaeology (Ghoneim et al., 2012). Based on a groundwater model provided in the hydrological analysis tools under the GIS environment, Luo et al. (2017b) discovered the moat system of the ancient Longcheng site using the SRTM product. After the launch of the TanDEM-X mission, a 3D product with an unprecedented resolution could be derived for archaeological identification (Tapete and Cigna, 2017b) and palaeoenvironmental reconstruction (Erasmi et al., 2014). Chen et al. (2016) discovered a rectangular-shaped anomaly by employing an entire radar interferometry procedure for generating the TanDEM-X DEM product at the desert Niya site. The AIRSAR is now capable of detecting

archaeological sites, with notable implications for archaeology in tropical forests (Moore et al., 2007). Garrison et al. (2011) successfully detected and mapped ancient Maya settlements beneath jungle canopy in Guatemala by using AIRSAR radar elevation data.

5.1.5. SAR for cultural heritage monitoring and conservation

Multi-date SAR products, such as interferometric coherence, multi-temporal features of radar signatures (e.g. ratio, summed, mean, median, gradient and standard deviation) and RGB multi-temporal composites, have been effective at sharpening archaeological traces as well as in change monitoring and detection (Chen et al., 2016; Cigna et al., 2013; Stewart et al., 2013; Stewart et al., 2014; Tapete and Cigna, 2017b; Tapete et al., 2016). Tapete et al. (2016) developed an alternative solution for quantifying the magnitude, spatial distribution and rates of looting at the Apamea site in Syria based on the successful recognition of looting marks within ratio maps of radar backscatter derived using two consecutive TerraSAR-X scenes. In order to detect and measure landscape disturbances that are threatening the world-renowned archaeological features and ecosystems of Peru's Nasca Cultural Landscape, Comer et al. (2017) employed algorithms to calculate correlations between pairs of SAR images and to generate correlation images for both airborne UAVSAR and satellite Sentinel-1 SAR data (Fig. 12). High coherence values indicate high homogeneity with no change of surface characteristics such as moisture content, vegetation cover, roughness, elevation or geometry, while low values are found over altered surfaces. Therefore, correlation images together with further analysis (e.g. ratio of correlation images) can be used to identify archaeological features and to detect changes in these features (Comer et al., 2017; Garrison et al., 2011; Tapete and Cigna, 2017b).

Due to the wide spatial coverage and the high accuracy provided, MT-InSAR can be considered an efficient and cost-effective technique for monitoring ground subsidence. It has been widely used to preserve and management historic city centres or traditional urban landscapes (e.g. in Mexico, Beijing, Rome, Angkor, Athens, and Venice, etc.) for monitoring deformations and instability in buildings and assessing the risk (Chen et al., 2017a; Chen et al., 2017d; Cigna et al., 2014; Da Lio and Tosi, 2018; Osmanoğlu et al., 2011; Parcharidis et al., 2006; Sowter et al., 2016; Tang et al., 2016; Tapete et al., 2012; Tosi et al., 2018; Zhu et al., 2018) of damage due to ground subsidence. For example, Cigna et al. (2014) carried out a comprehensive study focused on SAR-based investigations of Rome over time. In particular, outputs from COSMO-SkyMed time series processed using the Stanford Method for Persistent Scatterer InSAR (PS-InSAR) confirmed the persistence of ground motion affecting monuments and of subsidence in southern residential quarters adjacent to the Tiber River (see Fig. 13). The movements and potential risk of collapse of the monuments at the Angkor World Heritage Site, along with changes in surface elevation, have been monitored with high-resolution TerraSAR/TanDEM-X data and PS-InSAR approach (Chen et al., 2017a).

Until now, of all the proposed MT-InSAR techniques, Persistent Scatterer InSAR (PS-InSAR) (Ferretti et al., 2001) and Small BAseline Subset InSAR (SBAS-InSAR) (Berardino et al., 2002), which are based on processing long stacks of satellite SAR imagery and identification of coherent or persistent scatterers, have been the most popularly employed to detect and analyse surface stability, structural deformation and changes occurring in areas where ACH sites are present (Alberti et al., 2017; Chaussard et al., 2014; Confuorto et al., 2016; Da Lio and Tosi, 2018; Evans and Farr, 2007; Le et al., 2016; Osmanoğlu et al., 2011; Tapete and Cigna, 2017a; Tapete and Cigna, 2017b). Tapete et al. (2012) verified the capabilities of the PS-InSAR and SqueeSAR approaches for the preventive diagnosis of deformation threatening the structural stability of archaeological monuments and buried structures in Historic Centre of Rome. By combining the PS-InSAR technique with 55 ERS-1/2 SAR scenes, a precise average annual deformation rate-map of Athens was generated for the period 1992–2002, the results showed a rate of 2–3 mm/yr in some part of the city centre (Parcharidis et al.,

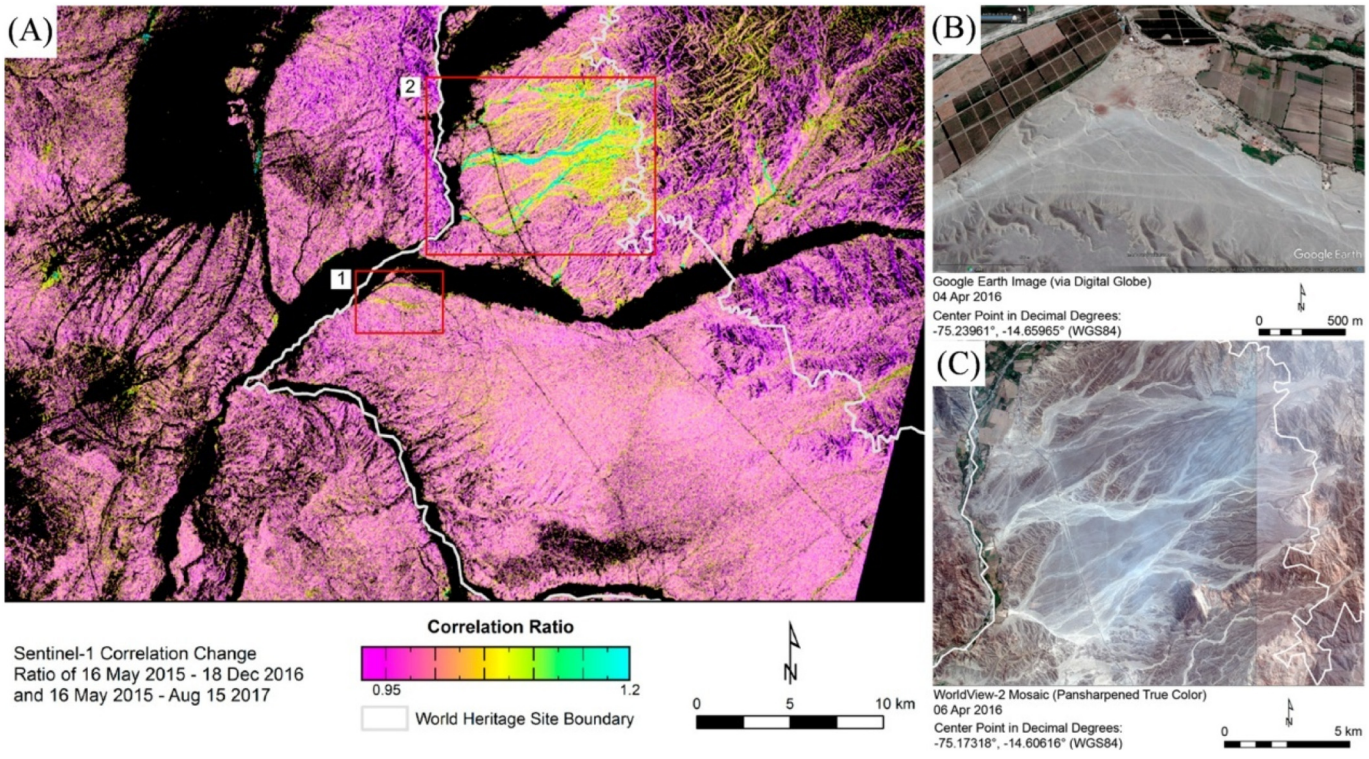

Fig. 12. The correlation change image in (A) compares two correlation images. The red and orange areas experienced a relatively constant level of disturbance between May 2015 and August 2017. Yellow to green indicates that decorrelation during the 2016–2017 period was 5% to 20% higher than during the 2015–2016 period. Panel (B) is a satellite image of the area delineated and labeled 1 in (A); (C) is a satellite image of area 2. (Following Comer et al. (2017)). (For interpretation of the references to color in this figure legend, the reader is referred to the web version of this article.)

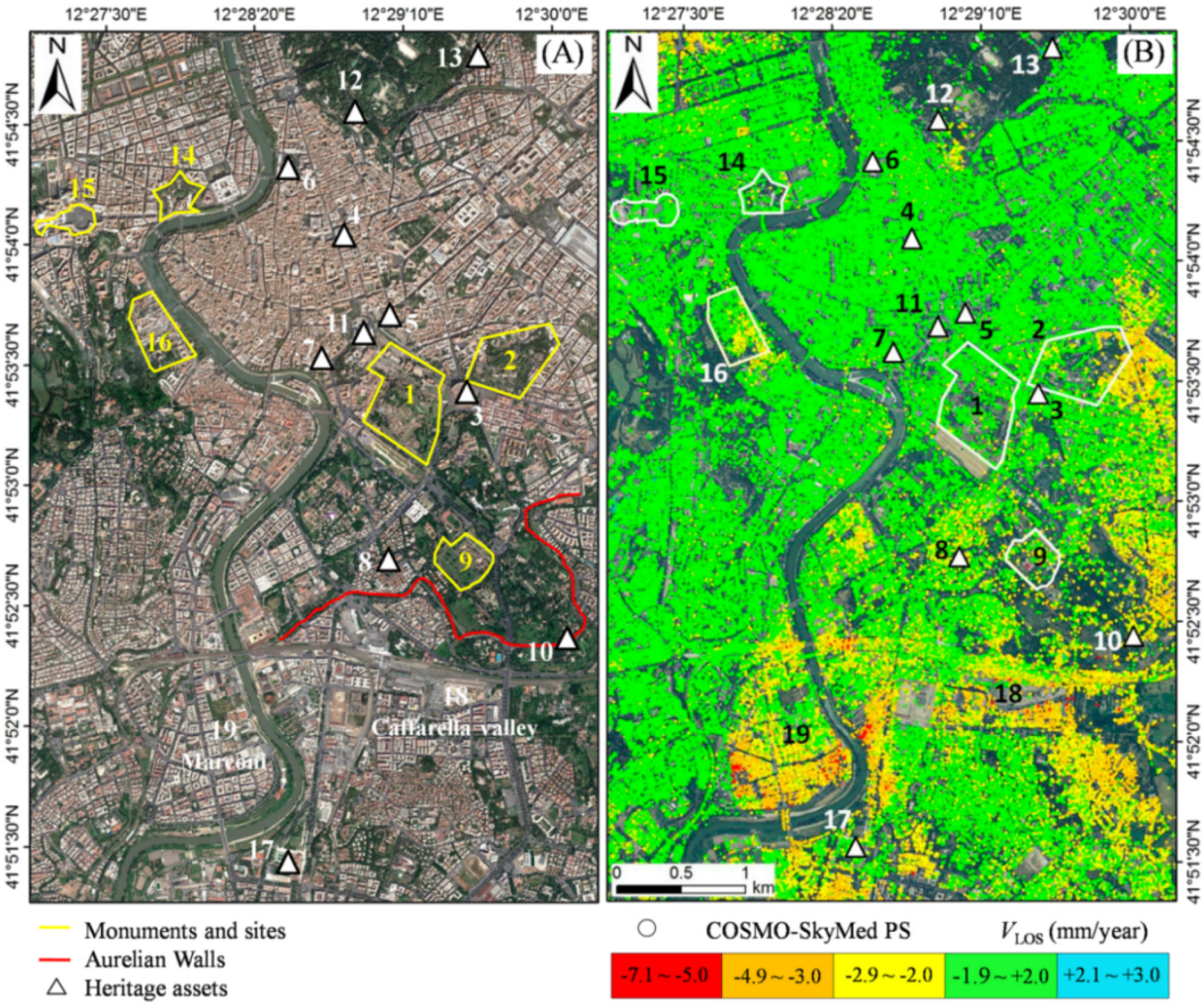

Fig. 13. (A) GE VHR imagery (© 2019 Digital Globe, acquired on 4 June 2010) of the historic centre of Rome, with the locations of the monuments, heritage assets and linear walls marked; (B) Spatial distribution and associated estimates of LOS velocities obtained using COSMO-SkyMed PSs (March 2011–June 2013) and StaMPS-InSAR processing (Modified from Cigna et al. (2014)).

2006). Recently, based on the results of an intermittent SBAS time-series analysis of 18 Sentinel-1 scenes of Mexico City, Sowter et al. (2016) revealed a serious subsidence rate of 40 cm/yr and demonstrated the potential of Sentinel-1 to support wide-area land subsidence surveys.

5.2. Light detection and ranging (LiDAR)

5.2.1. Background

In principle, LiDAR is similar to SAR in that LiDAR systems send out light pulses and record both how long it takes their backscattered echoes to return and how much of the original energy comes back (White, 2013). LiDAR can measure range and orientation, and identify target characteristics through position, radial velocity, reflection and scattering characteristics (Yan et al., 2015). LiDAR instruments can be mounted on ground platforms (e.g. Terrestrial Laser Scanning, (TLS)), airborne platforms (e.g. Airborne Laser Scanning, (ALS)) or satellites (e.g. freely available data from ICESat (Wang et al., 2016)), and come in two common models – discrete return and full-waveform systems (Lefsky et al., 2002; Vierling et al., 2008). The former records a discrete number of echoes and measures the time taken for a pulse to travel to an object and is used to determine height. The latter digitize the complete waveform of each backscattered echo, thus allowing improvements in the classification of terrain and off terrain objects (Doneus et al., 2008; Wagner, 2010; Yan et al., 2015). TLS is more suitable for 3D recording archaeological excavations and architectural heritages in site-scale. At the same time, due to the limited spatial resolution of satellite LiDAR data, it is little used for ACH applications.

5.2.2. LiDARchaeology: LiDAR in archaeology

At present, airborne LiDAR-based ACH applications concentrated on the uses of full-waveform systems, which enable highly accurate surface models to be obtained and archaeological structures, earthworks or submerged sites even under dense vegetation cover or underwater to be detected (Crow et al., 2007; Doneus et al., 2008; Doneus et al., 2013; Masini and Lasaponara, 2013; Menna et al., 2018; Shih et al., 2014; Wang and Philpot, 2007; Yan et al., 2015). However, there are several cases of archaeological prospecting (Challis, 2006; Holden, 2001) that have been successful using discrete model LiDAR, which was described as a “conventional” system by Doneus et al. (2008) and Lasaponara et al. (2011). Generally, a near-infrared LiDAR system (wavelength of 1064 nm or 1550 nm), also called topographic mapping LiDAR, penetrates the tree canopy to obtain terrain information (Fig. 14a); a green LiDAR system (wavelength of 532 nm), also called bathymetric LiDAR, penetrates the water column to survey the seafloor (Fig. 14b). Several recent publications have shown how airborne LiDAR can be used to detect, record, and even discover; archaeological features at both site and landscape scales (Chase et al., 2012; Chase et al., 2011; Chase et al., 2017; Evans et al., 2013; Fisher et al., 2017; Grammer et al., 2017; Lasaponara et al., 2010; Masini et al., 2018; White, 2013). In this

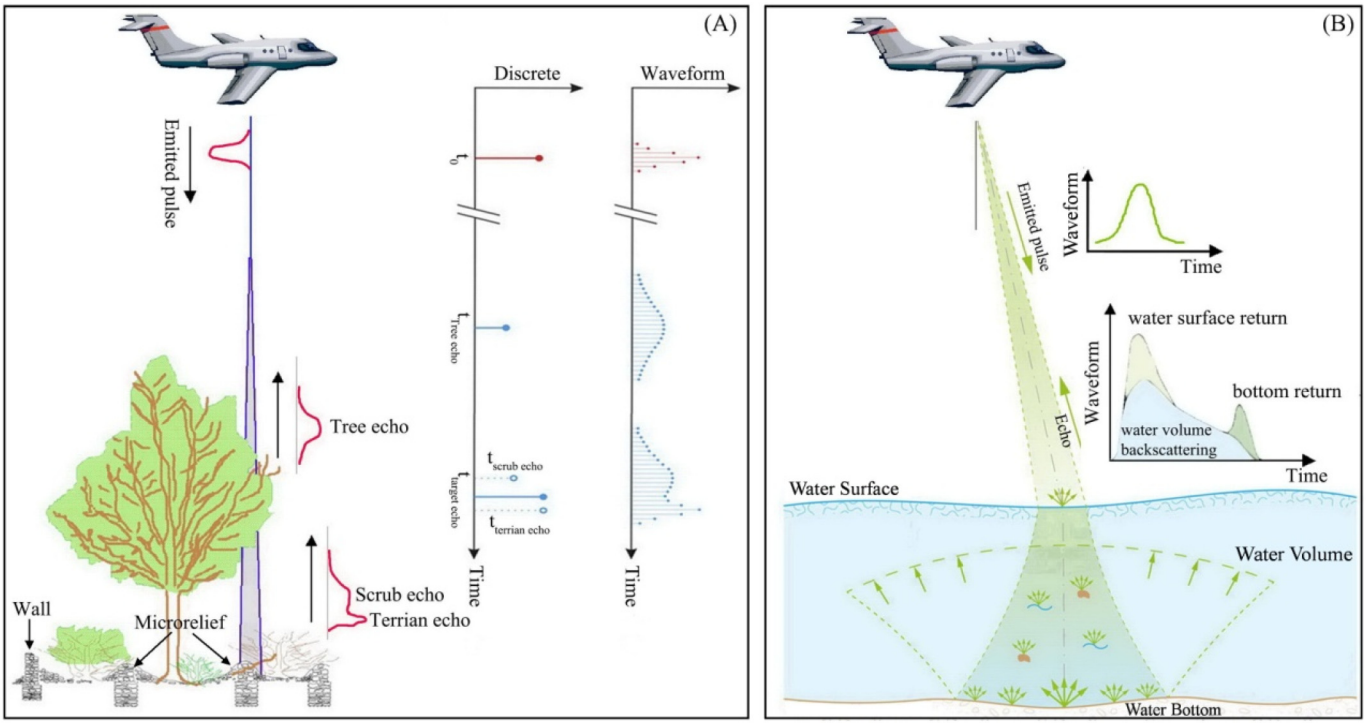

Fig. 14. Airborne LiDAR in archaeology: (A) diagram explaining airborne topographic LiDAR (ATL) in discrete mode and full-waveform mode (modified from Masini and Lasaponara (2013) and Doneus et al. (2008)); (B) diagram explaining airborne bathymetric LiDAR (ABL) in full-waveform mode (Modified from Doneus et al. (2013)).

context, this review focuses on the full-waveform type for prospecting ACH sites. In products derived from classified airborne LiDAR point cloud, there are usually two datasets: a digital surface model (DSM) providing an estimate of the top of canopy, manmade structures or water surface height, and a DTM showing the topographic variability of the bare-earth, seafloor or other water body bed.

5.2.3. Airborne LiDAR systems

Airborne LiDAR, also called ALS, is a laser profiling and scanning system used in topographic and bathymetric applications that emerged commercially in the mid-1990s (Chase et al., 2011; Evans et al., 2013; Lasaponara et al., 2011; Stott et al., 2018). In contrast to 2D remote sensing data, LiDAR point cloud data provide 3D information about the topography of the Earth's surface (Huisman et al., 2016; Yan et al., 2015). Other benefits of airborne LiDAR include the lack of effects due to relief, the ability to penetrate the tree canopy, and insensitivity to lighting conditions (Freeland et al., 2016; Lefsky et al., 2002; Rosenswig et al., 2015; Wagner, 2010). During the past two decades, the development of airborne LiDAR has led to a gradual improvement in both pulse rates and flying heights (Guo et al., 2011; Singh et al., 2012), which has made large-area coverage and mapping easier (Yan et al., 2015). Since LiDAR sensors used for commercial topographic mapping usually utilize a multichannel laser source, which operates at wavelengths of 532 nm, 1064 nm, and 1550 nm, high separability of spectral reflectance between different land cover materials in the visible and near-infrared spectrum is possible. Fernandez-Diaz et al. (2014) assessed the effects of the data density, flying height, pulse repetition frequency and scan angle on ACH applications.

5.2.4. Airborne LiDAR for archaeological prospecting

As a result of the work of archaeologists and specialists in understanding the physical basis of LiDAR echo returns (Devereux et al., 2008; Devereux et al., 2005; Doneus et al., 2013; Masini and Lasaponara, 2013), airborne LiDAR has been successfully applied to detect archaeological features and to analyse patterns in these features across the world-from Europe (Bernardini et al., 2013; Bewley et al., 2005; Devereux et al., 2005; Hesse, 2010; Masini et al., 2018; Masini and Lasaponara, 2013) to North America (Gallagher and Josephs, 2008; Harmon et al., 2006; Johnson and Ouimet, 2014; Krasinski et al., 2016; Rochelo et al., 2015) to Mesoamerica (Chase et al., 2012; Chase et al., 2011; Rosenswig et al., 2013; Von Schwerin et al., 2013; Weishampel et al., 2012) to Asia-Pacific region (Cheng et al., 2016; Evans et al., 2013; Ladefoged et al., 2011; McCoy et al., 2011; Wang and Philpot, 2007; Wang et al., 2017a) to South Africa (Sadr, 2016). The series of studies carried out in the Maya Lowlands can perhaps be considered representative of LiDARchaeology, not only in terms of the identification of monuments (Fig. 15) (Chase et al., 2011; Garrison et al., 2011; Hare et al., 2014; Von Schwerin et al., 2016a), but also in terms of the understanding and analysis of social pattern and paleo-landscape (Chase et al., 2014; Chase and Chase, 2017; Evans, 2016; Garrison et al., 2019; Inomata et al., 2018; Weishampel et al., 2011). Chase et al. (2011) used the LiDAR DTM product to accurately portray not only the topography of the Mayan landscape, but also structures, causeways, and agricultural terraces that has a relatively low relief of 5–30 cm.

All of the above-mentioned studies inevitably involve two key steps – effective filtering and classification of point clouds, and appropriate generation and visualization of the DTM – for LiDAR-based archaeological interpretation. The filtering and classification of ground and non-ground points is crucial for the discrimination of archaeological features and subsequent interpretation. Therefore, it is essential to apply adequate filtering methods that allow accurate DTMs for archaeological interpretation to be generated. Researchers have developed a wide range of filters to discriminate between ground and non-ground in raw LiDAR point clouds (Fernandez-Diaz et al., 2014; Sithole and Vosselman, 2004). According to Meng et al. (2010), based on the characteristics of ground filters, filtering methods can be categorized into six groups: segmentation/cluster-based, morphological-based, directional scanning, contour-based, TIN-based, and interpolation-based. Each method has its own hypothesis, so the factors affecting the accuracy of DTM are different. Remote sensing archaeologists should choose

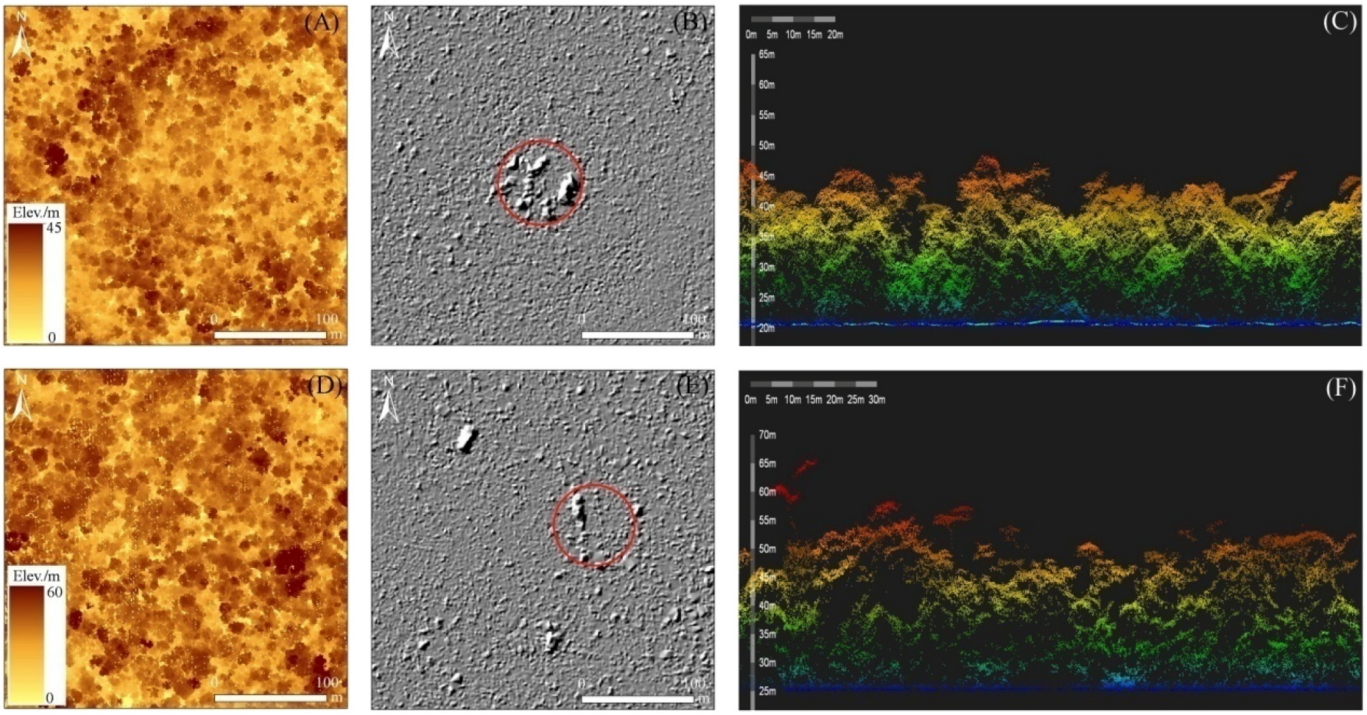

Fig. 15. Two suspected Mayan public architectures (red circles in B and E) in the south Caracol, Belize. LiDAR data represented in DSM (left panels), hillshaded maps of DTM (middle panels), and point cloud profile (right panels). LiDAR point cloud data (Data Source: Open Topography, LiDAR data were collected in 2013) have been normalized and average density is reach up to 20/m^2. (For interpretation of the references to color in this figure legend, the reader is referred to the web version of this article.)

suitable filtering methods according to the characteristics of their research areas. When remote sensing archaeologists get a DTM, if they know the merits and demerits of the DTM filtering method, they will also be helpful to grasp where the error is large and where the error is small, and to distinguish some “true” and “false” archaeological features. An active TIN-based model developed by Axelsson (2000) has been the most popular algorithm and also the most widely applied by archaeologists across the world (Hare et al., 2014; Harmon et al., 2006; Lasaponara et al., 2010; O'Reilly et al., 2017; Opitz et al., 2015; Štular et al., 2012; Von Schwerin et al., 2016a). Lasaponara et al. (2011) presented the threshold-based algorithm for the filtering and classification of ground and non-ground points and for the discrimination of canopy, understory and micro-topographic relief of archaeological interest. Evans et al. (2013) uncovered archaeological sites at Angkor based on filtration, culminating in a ground classification routine that used an iterative triangulation approach.

However, for ease of archaeological interpretation, visualization and analysis, DSM or DTM elevation rasters have often been created and used. These elevation rasters are created by interpolating the elevation values from the irregularly spaced point clouds to a single elevation value for each raster element (Fernandez-Diaz et al., 2014). There are many mature interpolation algorithms that can be used to generate a DTM. Among the most common are inverse distance weighting (IDW), Kriging, minimum curvature, the modified Shepard's method, natural neighbor, nearest neighbor, polynomial regression, radial basis function, triangulation with linear interpolation, moving average, and local polynomial. Each of these will produce slightly different in surface models or representations of reality based on the available information (Guo et al., 2010). Thus it is important to know the differences between the methods and the results they produce and also when a given method might be better than another at answering a particular research question (Fernandez-Diaz et al., 2014). The Kriging algorithm (Cressie, 1990) and its derivatives are the methods most used for archaeological DTM generation, and have been widely used by archaeologists for LiDARchaeology (Canuto et al., 2018; Chase et al., 2014; Chase et al., 2012; Doneus et al., 2008; Evans et al., 2013). To reduce the effects due to residual non-terrain points in the classified data, Devereux et al. (2008) used a hierarchical method focusing on the technique of robust interpolation with an eccentric and a symmetrical weight function (Kraus and Pfeifer, 1998). Based on the LiDAR-derived DTM product, Johnson and Ouimet (2014) have positively identified numerous archaeological sites (Fig. 16) in forested areas of New England that have not been previously recorded by archaeological studies.

For archaeological purposes, most research has focused on using visual maps of the DTM for manual or automatic interpretation (Chase et al., 2017; Devereux et al., 2008; Freeland et al., 2016; Guyot et al., 2018; Masini et al., 2018; Trier and Pilø, 2012; Wang et al., 2017a). Different visualization techniques for post-processing the classified data are used by archaeologists (Challis et al., 2011); the traditional methods include hillshaded maps, images where the changes in elevation are represented by a color gradient, slope analysis, 3D models, and contour maps (Fernandez-Diaz et al., 2014). And the Local Relief Model (Hesse, 2010), Sky View Factor (Štular et al., 2012) and Openness (Doneus, 2013) are among many new methods highlight the natural and man-made features of the terrain that have been proposed for archaeological applications. Štular et al. (2012) proposed that interpreters should choose different techniques for different terrain types by comparing thirteen visualization methods. The hillshaded map (Fig. 16B) (Chase et al., 2014; Chase et al., 2011; Corns and Shaw, 2009; Devereux et al., 2005; Evans et al., 2013; Fernández-Lozano et al., 2015; Gallagher and Josephs, 2008; Hare et al., 2014; Inomata et al., 2017; Johnson and Ouimet, 2014; Lasaponara et al., 2010; Opitz et al., 2015; Quintus et al., 2015; Tapete et al., 2017) is the most common visualization technique in LiDARchaeology. Doneus et al. (2015) generated a DSM of the underwater topography at depths of up to 11 m in Kolone, Croatia. The shaded DSM and its visualizations allowed several ancient fish-catching structures to be identified and the result were verified during underwater surveys (Fig. 17). It is worth noting that the use of micro-

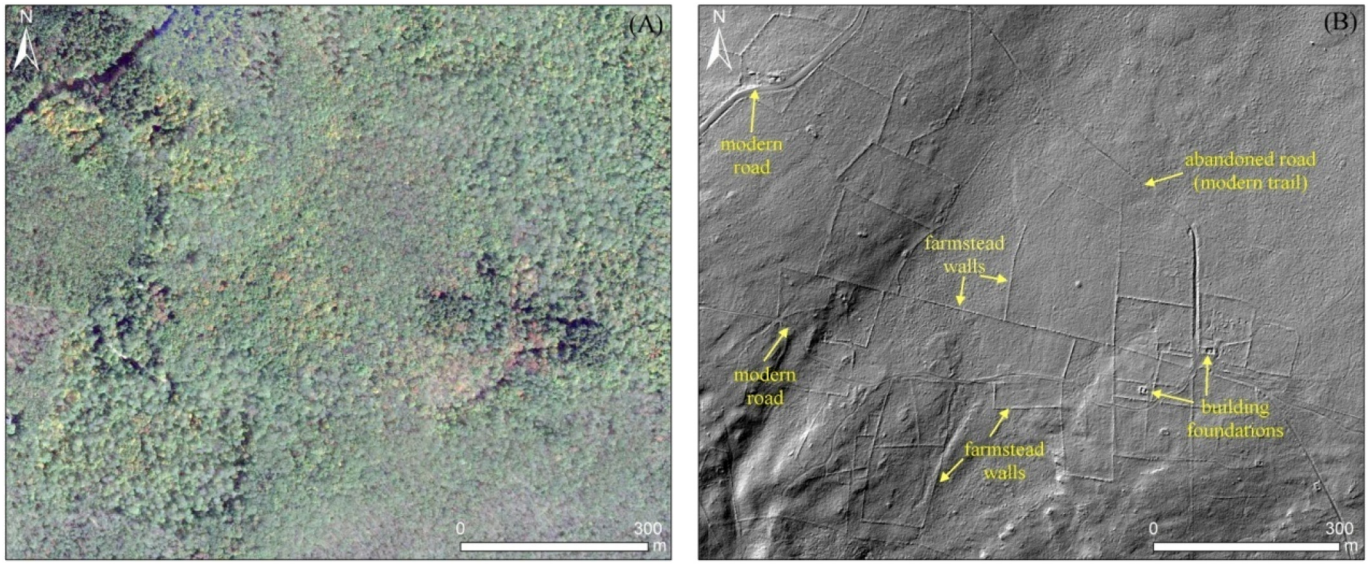

Fig. 16. ATL for re-discovering archaeological features under the canopy in New England, USA. (A) shows leaf-on GE VHR imagery (© 2019 Digital Globe, acquired on 11 October 2016) with a modern road superimposed on the northwest corner of the image for reference; (B) shows a hillshaded DTM created from 1 m resolution LiDAR data (Data Source: USIEI, LiDAR data were collected in 2016 and average point spacing is about 0.7 m), quite clearly depicting many features that can then be identified.

topographical relief as archaeological proxies could benefit of SVF and Openness (Masini et al., 2018) for the reconstruction of the urban shape of ancient villages, as showed in Fig. 18 which depicts LiDAR-derived models of a medieval village in South of Italy.

6. Discussion: limitations and challenges

6.1. Archaeological and cultural heritage (ACH) remote sensing

6.1.1. Passive photography remote sensing in ACH

Historical aerial and spy satellite photographs are revealing more than those who took them could have imagined because now, a century or more later, they are proving to be of enormous benefit in revealing lost ACH sites (Leisz, 2013; Menze and Ur, 2012; Stott et al., 2018). Archaeological relief such as structures, earthworks and walls can be seen on aerial or spy satellite photographs at an appropriate scale and viewing angle. However the use of these data is limited to the manual interpretation of grayscale images, which can be improved by image enhancement methods including filtering, fusion, edge detection techniques, etc. Agapiou et al. (2016a) presented a methodology for improving the interpretation of CORONA images by adding color from recently acquired satellite or airborne imagery. The methodology followed in their article, is based on the use of pansharpening algorithms which are applied to a set of an archived grayscale image and a recent color image taken of the same area. Also, 3D information extracted by photogrammetry from historic photographic stereo-pairs is of particular value, allowing high-resolution historic Digital Elevation Models (hDEMs) to be generated for archaeological purposes (Casana and Cothren, 2008; Casana et al., 2012; Rayne and Donoghue, 2018). Orengo et al. (2015) introduced a novel workflow for the topographic

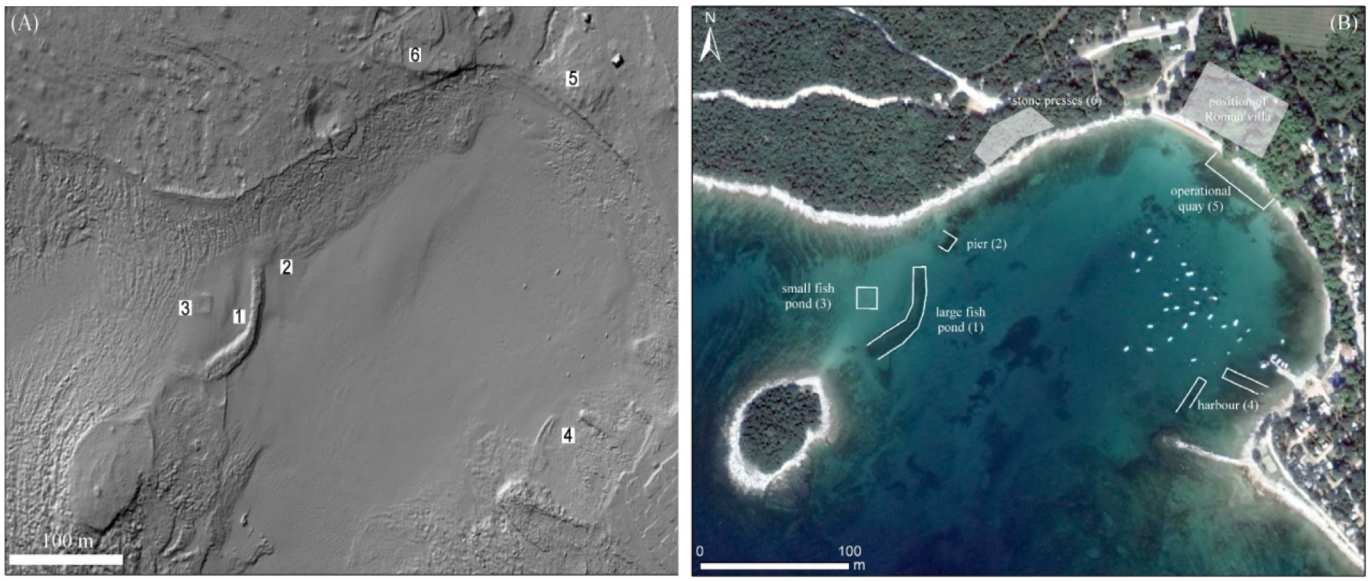

Fig. 17. ABL for underwater archaeological purposes. (A) Shaded DSM generated from filtered and strip-adjusted ABL point cloud of the Roman harbour site at Kolone; and (B) interpretation drawing based on ABL derived visualizations and underwater survey. (Reproduction after Doneus et al. (2015), the base-map in B is the GE imagery (© 2019 Digital Globe, acquired on 29 August 2018).

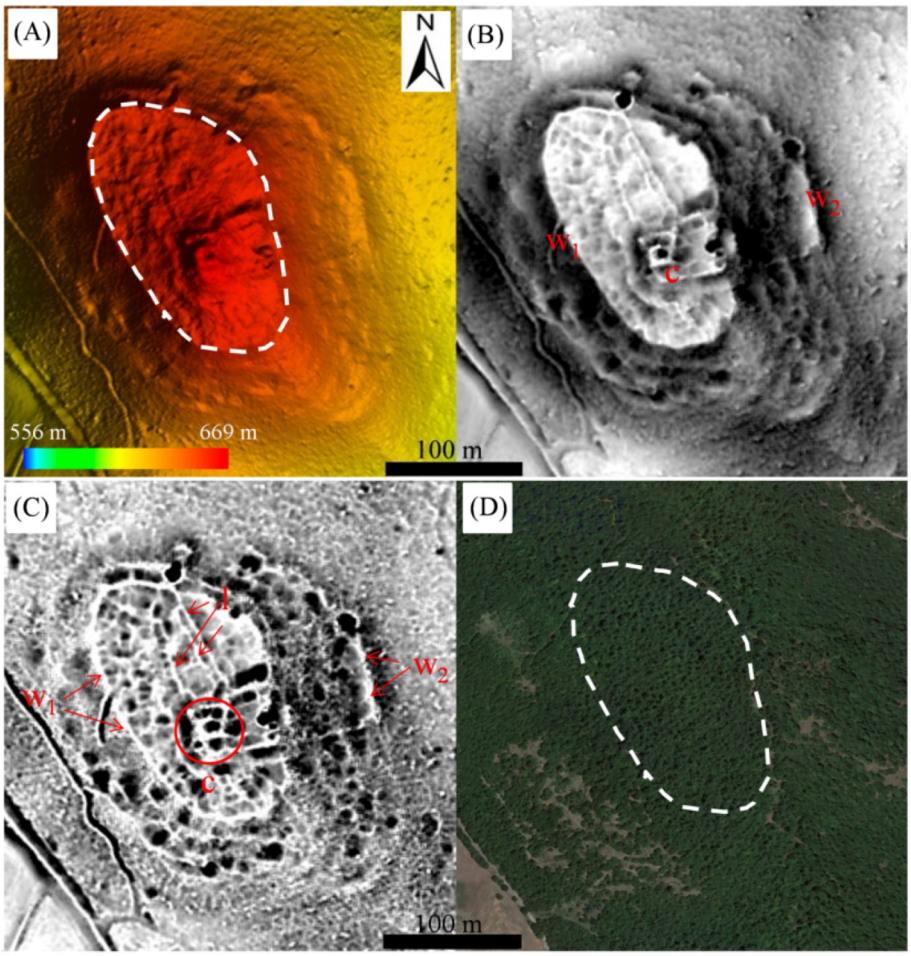

Fig. 18. LiDAR based reconstruction of urban shape of a medieval village near Matera (Southern Italy). (A) DTM; (B) SVF; (C) Openness; (D) GE imagery (© 2019 Digital Globe, acquired on 4 July 2014). The LiDAR data were collected on 10 October 2014 and average point density is about 25 points/m^2. w_1 and w_2 are related to potential city walls and extramural walls, c indicates the castle, and l refers to potential streets of the village.

reconstruction of now-lost archaeolandscapes based on the digital photogrammetric extraction of morphological information from historic aerial photographs. Galiatsatos et al. (2008) set out analyses of the orthorectification of satellite CORONA images in order to use its stereo feature to create a DEM by calculating the degree of parallax between conjugate points in each image using dedicated software.

In recent years, Structure from Motion (SfM) complemented by dense image-matching algorithms embedded in Multi-View Stereo (MVS) approaches (Szeliski, 2010; Ullman, 1979), particularly those employing aerial photography imagery, has become an important tool for passively generating point clouds and topographic data for ACH sites and small-scale landscapes (Green et al., 2014; José Luis et al., 2019; Mozas-Calvache et al., 2012; Orengo et al., 2015; Papworth et al., 2016; Remondino et al., 2011; Verhoeven et al., 2012). The SfM-MVS technique allows the generation of 3D models without any knowledge of the imaging parameters and network geometry; this is in contrast to traditional photogrammetry, where the positions of the cameras, or the position of some points that are visible in more than one image must be known (Green et al., 2014; Szeliski, 2010; Verhoeven and Vermeulen, 2016). Sevara et al. (2018) presented refinements to an SfM-MVS-based workflow for the extraction of 3D data from aerial imagery, using specific image preprocessing techniques and in-field measurement observations to mitigate some of the shortcomings of archival imagery and to improve extraction of topographic data for change analysis of archaeolandscapes. Whether the end product is a DSM or DTM, aerial image-based dense point cloud generation as a means of digitizing surfaces with a specific elevation can now be considered a suitable alternative to active airborne LiDAR approaches (Verhoeven and Vermeulen, 2016). In addition, the creation of 3D models for larger areas by processing historical aerial photographs not collected explicitly with photogrammetric processing in mind, as demonstrated by Opitz and Herrmann (2018), Risbøl et al. (2015) and Sevara et al. (2018), shows the potential of SfM for supporting multi-temporal landscape analysis by allowing archaeologists to reconstruct hDEMs that have since been transformed, and by providing new products for high-resolution tracking of landscape change when satellite data are limited or not available.

6.1.2. *Passive multi- and hyperspectral remote sensing in ACH*

The most commonly used archaeological proxies for guiding archaeological prospecting are crop and soil marks, which can be detected through contrasts in spectral reflectance (Bewley et al., 2005; Gaffney and Gater, 2003; Scollar et al., 1990; Scudder et al., 1996) in spectral imagery. The visibility of crop marks often depends on the crop type and soil conditions and their expression is dictated by crop's phenological cycles. Soil marks develop due to subtle differences in localized soil properties and their expression depends on physical, chemical and biological conditions, particularly soil moisture and composition. Spectral imaging largely addresses these problems because it is able to image at a wide range of different wavelengths simultaneously. In broadband multispectral imagery, subtle spectral details can be lost due to averaging; however, because images are generally recorded at well-placed spectral positions in the NIR and SWIR, they are still suitable for discriminating the reflectance

differences between different soils types and vegetations health states (Agapiou et al., 2014a; Lasaponara and Masini, 2007; Verhoeven, 2018). Narrowband hyperspectral imagery can often support the enhancement or discrimination of archaeological features from the landscape matrix, or provide fine information on their state of health or ambient conditions according to the particular absorption and reflectance properties or spectral signature of the features. Although spectral signatures have been used to accurately identify crop or soil marks in multi- and hyperspectral images, archaeological features do not, in fact, exhibit specific or special spectral signatures that can be used for generic detection purposes (Altaweel, 2005).

As has been shown here, when compared to using aerial imagery for ACH applications, both broadband multispectral and narrowband hyperspectral imagery can increase the contrast between normal and stressed (or vigorous) crops, and improve the visibility of crop marks can be improved by data enhancements. This applies, however, only when the data are acquired at a high spatial resolution and at the correct moment in the crop growing cycle. Once the crop marks are clearly visibly, the specific advantages of the hyperspectral imaging technique are seriously reduced and aerial photographs or multispectral images are able to show most archaeological information in very high detail (Doneus et al., 2014). Conversely, sometimes the subtle effects of buried remains on variations in crop, soil and topography are not detectable using NIR and SWIR spectra (Winterbottom and Dawson, 2005). By using the TIR spectrum, the chances of detecting these subtle patterns may be greatly improved. In addition, a combination of predawn and mid-day thermal images can be used to determine variations in the thermal inertia of the ground surface (Beck, 2010) which may be strongly affected by buried remains or moisture differences in the soil. Lunden (1985) highlighted the considerable potential of thermal imaging for the detection of buried remains, although recent cases have demonstrated that the capability of aerial thermography to reveal surface and buried archaeological features is limited (Casana et al., 2014; McLeester et al., 2018; Poirier et al., 2013; Thomas, 2018). Technological and cost barriers have prevented the widespread application of thermal imaging in archaeology (Šedina et al., 2019).

6.1.3. Active LiDAR remote sensing in ACH

More attention is now being paid to LiDARchaeology across the world and there have been many successful cases where it has been used to reveal archaeolandscape and in cultural resource management (Evans et al., 2007; Gheyle et al., 2018; Lasaponara et al., 2011; Siart et al., 2008; Wang et al., 2017a); however, LiDARchaeology lags far behind the use of LiDAR in a wide variety of other geosciences disciplines (e.g. forestry, oceanology, and agriculture). For instance, LiDAR intensity data have been widely employed in land cover classification (Yan et al., 2015) but not for archaeological purposes. Although this review has covered a wide range of archaeological prospecting using airborne LiDAR data, further investigation and analysis of the use of the archaeological information thus derived has been lacking. It is expected that forthcoming studies will include deeper archaeological analyses from the micro- to the landscape-scale. For example, airborne LiDAR DTM data can be used to analyse and reconstruct ancient urban and settlement patterns in vegetated areas (Chase et al., 2014), and to guide the active automatic discovery of unknown archaeological sites (Wang et al., 2017a).

As the majority of existing airborne LiDAR systems operate at a single wavelength, the invention of a multi- or hyperspectral airborne LiDAR sensor is required; this is likely to be realized in the next few years (Yan et al., 2015). As has been reported recently (Fernandez-Diaz et al., 2016; Wei et al., 2012; Woodhouse et al., 2011), there are some experimental multi- or hyperspectral LiDAR sensors being developed. Although most of the preliminary studies have focused on forest canopy modeling and monitoring, the introduction of a multi- or hyperspectral LiDAR sensor would provide new feature spaces to further enhance the capability of detecting and understanding archaeolandscapes. Recently, Canuto et al. (2018) utilized a Titan MultiWave multispectral LiDAR system at three wavelengths (532 nm, 1064 nm, and 1550 nm) to map natural terrain and archaeological features over several areas in the Maya Lowlands of northern Guatemala, successfully uncovering interconnected urban settlements and landscapes containing extensive infrastructural development. In addition to multi- or hyperspectral LiDAR, Geiger-mode and single-photon LiDAR are also new commercial systems for increasing the number of light beams. These two novel systems are useful in improving the density of point clouds, the coverage of the regions of interest, and the efficiency of data acquisition.

The reduction of signal distortion and misclassification is crucial for the identification of archaeological features and for their interpretation, and the development of novel filtering and classification methods is expected in the near future. Semantic segmentation, serves as a novel classification method to 3D LiDAR point clouds, is mostly used in urban or even indoor scenes. The field archaeological environment is generally complex, and semantic segmentation is difficult to be applied at present. However, with the development of artificial intelligence (AI) and big data, it is possible migrate it to archaeological scenes in the future. At the same time, driven by the promotion and distribution of LiDAR data and its derived products, a fast and robust 3D rendering and visualization platform that is not restricted to one operating platform needs to be developed (Torres-Martínez et al., 2016; Von Schwerin et al., 2013; Von Schwerin et al., 2016b; Yan et al., 2015). Additionally, it is worth noting that it still too early for the use of either topographic or bathymetric LiDAR systems mounted on UAVs, although this is likely to change in the next decade (Menna et al., 2018; Risbøl and Gustavsen, 2018).

6.1.4. Active SAR remote sensing in ACH

SAR backscattering provides information about surface characteristics according to the imaging parameters of frequency, incidence angle, and polarization. Thus, it can be a very useful tool for supporting archaeological prospecting; however, compared to VHR optical imagery, the ability to detect ACH sites is limited. Due to the speckling effect, the discrimination of ACH sites and natural structures in SAR images is, especially in comparison with the ability to detect more recent man-made structures, quite limited. Compared to optical imagery, Balz et al. (2016) estimated that SAR would require approximately a spatial resolution that is two- to three-times-higher for the clear identification of burial mounds. Integration and comparative analysis of the use of optical and SAR in the prospecting of ACH sites will become part of mainstream remote sensing archaeology. Furthermore, the penetration capability of SAR is strongly limited by surface characteristics and significantly by moisture content. This is the main reason why most applications of spaceborne SAR have focused on (semi-) arid areas. To date the lack of high resolution SAR data at bands with greater penetration capability (i.e. the L- and P-band) has limited the use of SAR for detecting buried remains (Chen et al., 2017c). Fortunately, L-band ALOS-2/PALSAR-2 data, which has higher resolution, has recently become available and could open encouraging perspectives in the field of archaeological prospecting. Both airborne and spaceborne SAR systems have been widely employed for archaeological prospecting by specialists in many countries, with the latter type becoming more and more popular. Satellite SAR has provided and continues to provide advanced tools and data for archaeological purposes ranging from archaeological investigation, buried detection, understanding of paleoenvironments and monitoring of looting (Balz et al., 2016; Chen et al., 2017c; Cigna et al., 2013; Comer et al., 2017; Garrison et al., 2011; Jiang et al., 2017; Lasaponara and Masini, 2013; Stewart et al., 2014; Tapete and Cigna, 2017a; Tapete and Cigna, 2017b; Tapete et al., 2016).

Due to the emergence of space-ground integrated platforms and new data processing techniques, fine instability monitoring and preventive diagnosis for cultural heritage sites has become increasingly feasible with the development of Differential Tomography SAR (D-TomoSAR), Ground-Based Interferometric SAR (GB-InSAR) and Distributed

Scatterer InSAR (DS-InSAR) techniques. Fornaro et al. (2010) applied D-TomoSAR in 4D imaging experiment (3D positioning and 1D deformation velocity) in Rome. Intrieri et al. (2015) proposed and assessed a GB-InSAR system for sinkhole monitoring and early warning in Elba Island, Italy. DS-InSAR provides a new high-resolution method for the precise detection of surface motion change. In contrast to the first generation of MT-InSAR technology, the DS-based method focuses both on pointwise targets with high phase stability and distributed targets with moderate coherence, the latter being more suitable in complex environments (Dong et al., 2018; Liu et al., 2019). The use of MT-InSAR for monitoring and conservation of ACH sites can further developed, benefitting from the increasingly consistent data archives that have increasing spatial resolution and temporal frequency. It is worth pointing out that satellite-based InSAR has dominated in the field of cultural heritage monitoring and conservation, especially for monitoring the deformation of architectural heritage sites and related mapping of potential risks. In contrast to satellite-based D-InSAR or MT-InSAR, the application of such techniques to airborne data has not, as of yet, been well-established. Several airborne campaigns, involving mainly P-/L-/C- and X-band systems, have been planned in the last 15 years to exploit the potential for deformation monitoring (Gray and Farrismanning, 2003; Perna et al., 2008; Reigber and Scheiber, 2003).

6.2. Data availability

It is widely acknowledged that, over the past century, the coverage and availability of ASRS data has improved significantly. Because archaeological work is carried out with obvious localized characteristics and under localized conditions, most remote sensing archaeologists wish to know if high-quality (e.g. higher resolution and cloud-free) ASRS data is available for their area of interest. Although some ACH applications might still be possible at lower or medium spatial resolutions, in most situations, archaeologists' use of VHR ASRS data trends towards freely available archive imagery. At the same time, archive ASRS data are widely used to prospect ACH sites, especially for warzones or in other sensitive areas where aerial and ground campaigns are not allowed or would be difficult to carry out. Moreover, today, the historical aerial photograph archives acquired during the two world wars represent a “unique data source” that can be used for detecting ACH features later destroyed by urbanization, intensive agricultural production and other anthropogenic activities. Thus, historical data can be considered a low-cost alternative to modern aerial photography or commercial satellite products for archaeological purposes. An enormous amount of important sources of archaeological information are also buried in the millions of aerial photographs taken for the purposes of military reconnaissance or cartography collected in major national archives (Cowley and Stichelbaut, 2012; Hanson and Oltean, 2013; Lambers, 2018). These examples could help archaeologists to use these data more in ACH applications. While imaging techniques for data acquisition have advanced significantly, archaeological communities and scientific institutes continue to struggle with the uneven availability of these technologies and the data produced using them, and with the ability to manage, maintain and make use of the data once they have been acquired. These challenges are not unique to remote sensing in ACH, but the scale, variability and complexity of the data involved make them acute.

6.3. Data interpretation

For archaeologists, obtaining information (location, shape, structure, and pattern) about features from remote sensing images is one of the most important purposes of archaeological research. Until now, remote sensing archaeologists have given priority to visual interpretation which is usually limited in three spectral channels at a time. Both visual interpretation and automatic detection techniques have their strengths and shortcomings. Visual interpretation, an accurate method, is time-consuming and strongly dependent on the digitization experience of the archaeologist using it; however, it has the advantage that the naked eye can identify subtle differences between archaeological features and backgrounds that a computer cannot. Inevitably, the biases in the knowledge of archaeologists limit the accuracy of visualization procedures and can lead to omission errors (Davis, 2018). At the same time, with the application of digital image processing in archaeology, some (semi-) automatic methods have also been proposed (Dorazio et al., 2012; Freeland et al., 2016; Luo et al., 2014a; Orazio et al., 2015; Sonnemann et al., 2017; Trier and Pilø, 2012; Witharana et al., 2018). Generally, in these automated applications, the experimental and test images are chosen for the great variable of the archaeological remains that they contain and the marked contrast between them and their surroundings. For instance, in the case studied by Figorito and Tarantino (2014), the lengths of the linear archaeological traces that were the targets for the semi-automatic method were only a hundred meters and the background were homogeneous. Although existing (semi-) automatic detection techniques save time and manpower, they are not very successful except at an extremely limited range of spatial scales and spectral contrasts. Compared to generic visual interpretation, the biggest weakness of automatic methods is that they are not applicable to the detection of archaeological features with heterogeneous backgrounds at a large scale (Opitz and Herrmann, 2018). Automatic detection of archaeological features is a challenging task in itself and further analysis of the features requires even more effort.

6.4. Unmanned aerial vehicles (UAVs)

The use of Unmanned Aerial Vehicles (UAVs) or drones for ACH applications is becoming ever more popular, especially for oblique photography, spectral imaging and LiDAR in inaccessible areas (Campana, 2017; Lin et al., 2011). In contrast to conventional airborne and satellite remote sensing, sensors onboard UAVs are capable of generating imagery with a GSD of up to 1 cm (Fig. 19A). As a result, these novel vehicles and data have motivated researchers to explore new methods for ACH applications, such as the use of aerial thermography (Casana et al., 2014) and photography (Verhoeven and Schmitt, 2010). It is worth noting that, previously, aerial photogrammetry was one of the main techniques used for the 3D documentation and reconstruction of archaeolandscape and architectural cultural heritage (Peak, 1978; Smith, 1989). Since 2010, UAV-based oblique photogrammetry has been the main method used and has continued to increase in popularity (Achille et al., 2015; Chen et al., 2018; Chiabrando et al., 2011; Fernández-Hernandez et al., 2015; Nikolakopoulos et al., 2017) for documenting excavations and 3D modeling of architecture heritage. Together with the popularity of UAVs in the field of ACH, the SfM-MVS mentioned above enables the fast and cost-effective creation of VHR topographic models over ACH sites of interest and their surrounding areas (Fig. 19B).

Furthermore, the use of close-range SfM-MVS for the on-site recording of stratigraphy during archaeological excavations is gradually becoming popular (Dellepiane et al., 2013; Waagen, 2019), as is the practice of documenting the landscape surrounding an excavation (Opitz and Herrmann, 2018). The main advantages of UAVs platform are flexibility, the very high resolution, low flight altitude and small footprint as well as the far-reaching field of view. The disadvantages are related to battery capacity, the size of the area covered and, particularly, the requirement to have line of sight between the operator and the UAV, a fact that restricts efficiency in terms of mapping large areas. Their unavoidable growth in archaeological research notwithstanding, non-military and affordable UAVs currently still suffer from too many restrictions to consider them a viable alternative to large-area archaeological prospecting from a low-flying manned aircraft (Verhoeven and Sevara, 2016). However, it is predicted that the increased use of UAVs will be one of the next trends for remote sensing archaeology (Agapiou and Lysandrou, 2015).

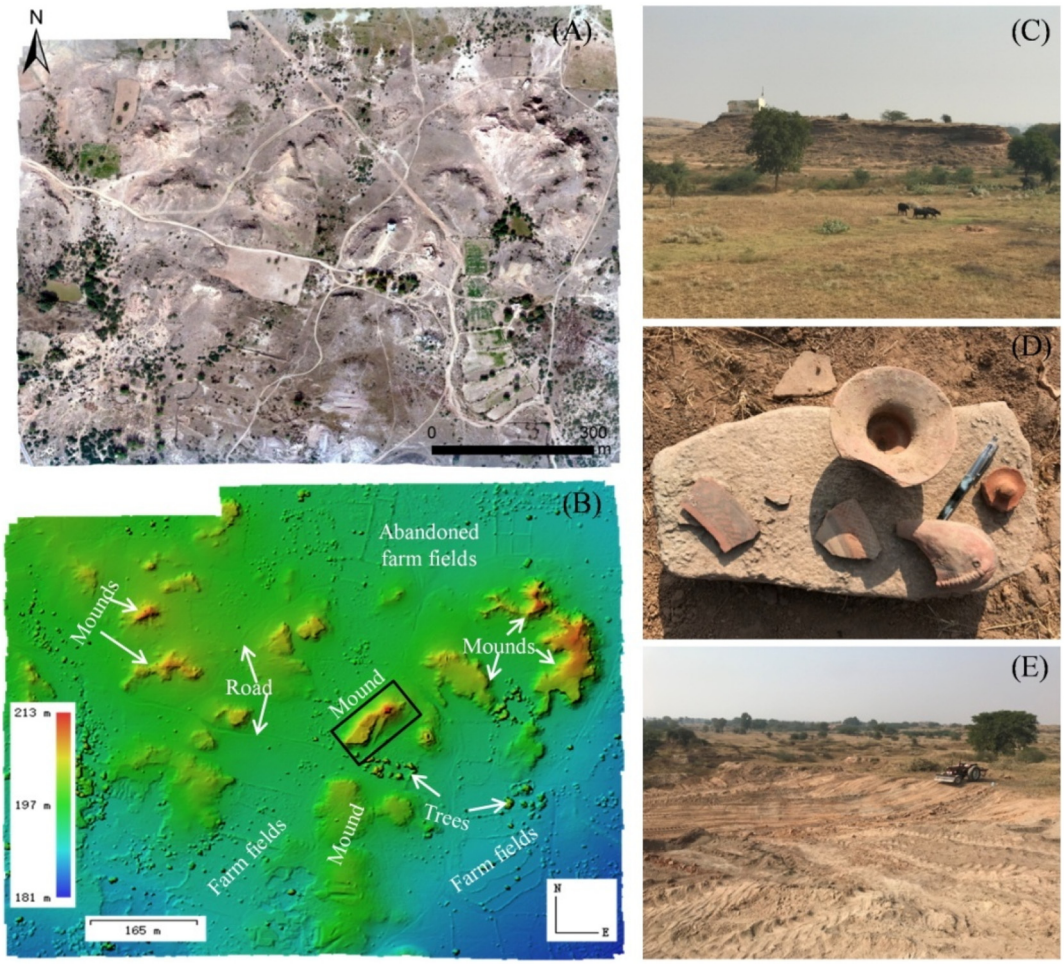

Fig. 19. The UAVs derived orthoimage (A) and topographical model (B) of ancient Bhera site (related to the Eastern Expedition (334 BCE–324 BCE) of Alexander the Great) in the north bank of the River Jhelum, Northern Pakistan; the ground view of the military mound (C) marked by the black box in B; the pottery fragments on the site surface (D) and the mechanical opening up wasteland for farming (E).

7. Trends and perspectives

7.1. Towards (semi-) automatic feature detection

Generally, archaeological features can be extracted from imagery as statistical and morphological data using GIS-aided manual interpretation or automatic detection following image enhancement. At present, ACH applications are still focused on the analysis of multi-sensor image interpretation results using artificial visualization or human-computer interaction. This means that archaeological researchers are still required to intervene manually, which requires a lot of time, manpower and material resources (Luo et al., 2014a; Luo et al., 2018b). At the beginning of 21st century, the automatic detection of ACH features was mainly carried out using different pixel-based approaches supported by single sensor imagery (Aminzadeh and Samani, 2006; De Laet et al., 2007; Garrison et al., 2008; Lasaponara and Masini, 2007). Fortunately, with the application of digital image processing technology in archaeology, some (semi-) automatic applications based on pixel-based classification or object-based image analysis (OBIA) are also available. A comparison between conventional per-pixel classification and OBIA classification was performed by De Laet et al. (2007), who concluded that the OBIA method resulted in a significant improvement in identification accuracy. Thus, there has been an increase in archaeological features detection using OBIA procedures applied to high-resolution multisensor imagery during the 2010s: for example, Figorito and Tarantino (2014) extracted ancient linear man-made relics indicative of vegetation markers by combining aerial images with active contour model segmentation; using ENVI's FX algorithm, Lasaponara et al. (2016) semi-automatically extracted information about farmland relics at Turkey's Hierapolis site. These studies proved that pixel-based classification can be quite useful. However, when compared to object-based approaches, OBIA methods are more accurate for detecting ACH features (Davis, 2018; Luo et al., 2018b).

OBIA is a method of assessing remote sensing data that uses morphometric and spectral parameters simultaneously to identify features in remote sensing imagery (Blaschke, 2010; Blaschke et al., 2014; Davis, 2018). It generally consists of two key steps: segmentation and then classification. Improvements in accuracy have been attained by using a greater number of morphometric variables for segmentation and multi-scale feature analysis for classification. Over the past decade, OBIA methods have been introduced to automatically detect archaeological features from multisensor datasets (Cerra et al., 2016; Figorito and Tarantino, 2014; Freeland et al., 2016; Jahjah and Ulivieri, 2010; Lasaponara et al., 2016; Lasaponara and Masini, 2018; Luo et al., 2014a; Luo et al., 2018b; Orazio et al., 2015; Trier et al., 2018; Trier and Pilø, 2012). By utilizing multiple parameters simultaneously, OBIA is well suited for identifying features that are small, structurally homogeneous, and that display differences with the local topography (Davis, 2018). OBIA is a useful and potential tool for ACH research. However, owing to the complexity of and multiple possible solutions for ACH features in different physical and cultural contexts, it is crucial to support the development of approaches that integrate OBIA with

archaeological expert experience. In addition, the development and testing of approaches for pattern recognition are undoubtedly another key but difficult topic that requires more investigation, although recent research based on optical imagery (Dorazio et al., 2012), SAR data (Tapete et al., 2016) and LiDAR data (Trier et al., 2018) has shown that great progress has already been made in this regard (Tapete and Cigna, 2017b). It is to be hoped these pilot studies will provide the stimulus for further examination of the use of machine-learning methods (even AI) to identify ACH sites from ASRS data.

7.2. Towards big remote sensing data

This review of the century for various categories of direct and indirect applications of remote sensing in the field of archaeology and cultural heritage has indicated that various remote sensing archaeologists have collected and employed megabyte- or gigabyte- scale ASRS data to carry out their studies in the regions of interest (Gumerman and Lyons, 1971; Lambers, 2018). Recently, two petabyte-scale remote sensing applications have been presented by Agapiou (2017b): the first one was an evaluation of the sue of multi-temporal Landsat image stacks and linear orthogonal equations for the detection of buried Neolithic Tells in Greece; the second exploited European-scale multi-temporal DMSP-OLS night-time light time-series to visualize the impact of urban sprawl in the vicinity of UNESCO World Heritage sites and monuments. Both applications highlight the considerable opportunities that big remote sensing data can offer the fields of archaeology and cultural heritage (Agapiou, 2017b). Great challenges, including the development of automatic detection and analysis algorithms and cloud computing platforms for archaeological purposes (Liss et al., 2017; McCoy, 2017) still need to be overcome in order to make the exploitation of big remote sensing data manageable and fruitful for future ACH applications.

However, the true value of ASRS archaeology lies in the integrated utilization of different imaging techniques and in the comparison and correlation of archaeological interpretations derived from the big remote sensing data that these techniques provided (Deroin et al., 2012; Křivánek, 2017; Kvamme and Ahler, 2007; Lin et al., 2011; Luo et al., 2014b; Piga et al., 2014). There is no one all-purpose remote sensing dataset on which the archaeologist can rely that will uncover all evidence of human occupation. This is determined by the nature (buried, weak, complex, and have multiple solutions) of archaeological features and the archaeologists' subjective perceptions when interpreting the data (Luo et al., 2018b). For maximum data mining and archaeological knowledge discovery, it is necessary that archaeologists collect and employ as many different types of remote sensing data under as many different environmental conditions as their resources and skill will allow. Thus, a conventional approach is for archaeologists to build local databases using multiple remote sensing datasets. In ACH applications, such databases can be built by integrating historical photographs, satellite data and aerial imagery that require further processing. Only then can the use of big remote sensing data led to a comprehensive understanding of the archaeological and cultural purposes of their regions of interest.

Since the turn of the 21st century, the progressive improvements in imaging sensors in terms of spectral and spatial resolution, temporal frequency and coverage, and the renewed enthusiasm for ASRS as the data the sensor provided became finer and more sensitive to ACH features, has meant that archaeologists' preoccupation with detail and feature detection has been highlighted. However, ASRS imagery generally fails to reveal buried features in significant detail, which can negatively affect archaeological interpretation. A novel space-air-ground integrated database is needed to respond to this archaeological question. It should be acknowledged openly that ground remote sensing is very useful in archaeology. In terms of ground remote sensing, ground spectroscopy, geophysical prospecting, and synthetic aperture sonar (SAS) can be used alone or in combination to supplement and support the results of ASRS applications. Field spectroradiometers can be used to provide calibrated and accurate reflectance measurements since these instruments are often accompanied by a calibrated Lambertian surface (Agapiou, 2017a). Multi-frequency Ground Penetrating Radar (GPR), a popular geophysical tool, can produce 3D full-waveform maps of the subsurface (Keay et al., 2014; Lasaponara et al., 2016). SAS data can serve as the reference data for validating bathymetric LiDAR products (Menna et al., 2018). It is worth pointing out that while geophysics and SAS belong to generalized remote sensing technology, as ASRS does, there are obvious differences in their application to ACH. SAS collects and records the acoustic characteristics of underwater ACH targets almost truly, while geophysical prospecting collects and records the attribute differences between buried ACH targets and their surrounding media. At the same time, the fusion of ground and ASRS data is one of the main barriers to the realization of integrated space-air-ground applications (Agapiou and Lysandrou, 2015; Sarris et al., 2013; Wang and Guo, 2015).

7.3. Towards complexes of ACH sites and their supporting environments

Since the 1950s, tremendous advances in Earth observation technology have led to the development of ASRS sensors that can be applied to surveying, conserving and managing ACH sites (Luo et al., 2017b). However, the development of imaging techniques has evolved independently, with little understanding of the small- or large-scale environmental conditions and processes that determine whether ACH features or risks will be identified by any sensor (Beck, 2010; Tapete and Cigna, 2017b; Wang and Guo, 2015). ACH features and the conditions in which they were preserved have been formed and transformed by local natural and human processes. Generally, these ACH features can be expressed through, for example, topographic, spectral reflectance or thermal variations. Hence, it is hypothesized that archaeological remains produce localized contrasts in their supporting environment (landscape matrix) which can be detected using an appropriate sensor under appropriate conditions. For example, the spectral imaging of ACH features reviewed in this paper has shown that, when compared to aerial imagery, broadband multispectral and narrowband hyperspectral imagery can increase the contrast between normal and stressed (or vigorous) crops, and can improve the visibility of crop marks following data enhancement. However, little is known about how different archaeological remains contrast with their supporting environment, how these contrasts are expressed in the electromagnetic spectrum, or how localized environmental factors such as soil moisture or vegetation types impact on contrast magnitude over space and time (Beck, 2010). Uncontrollable environmental variables (moisture, nutrients, landcover, relief, etc.) all play an important role in the utility of remote sensing to the archaeologist, who needs rich experience of studying ACH sites and their supporting environments.

From the perspective of landscape-scale archaeology, which is generally provided by lower spatial resolution imagery, is frequently as necessary in interpretation as the identification of individual small ACH features from high spatial resolution data. While an improved ability to detect small features of interest is clearly important for ACH applications, the strong emphasis placed on working with high spatial resolution data may lead to neglecting the potential for lower-resolution data to continue to shed important light on land-use patterns, areas of activity, and the geological and morphological contexts constraining appearance, and development and disappearance of the archaeolandscape or cultural phenomenon, as well as affecting preservation of the corresponding ACH sites (Opitz and Herrmann, 2018; Verhoeven, 2017). Stated more simply, the remote sensing archaeologist most certainly must see the “forest” (the supporting environment or landscape) as well as the “individual trees” (ACH sites) (Gumerman and Lyons, 1971). Taking Miran *tuntian* irrigation landscape on the Silk Road as an example, this landscape has been co-controlled by the Altyn Mountain Ecosystem, the Miran Oasis System and the Taklimakan

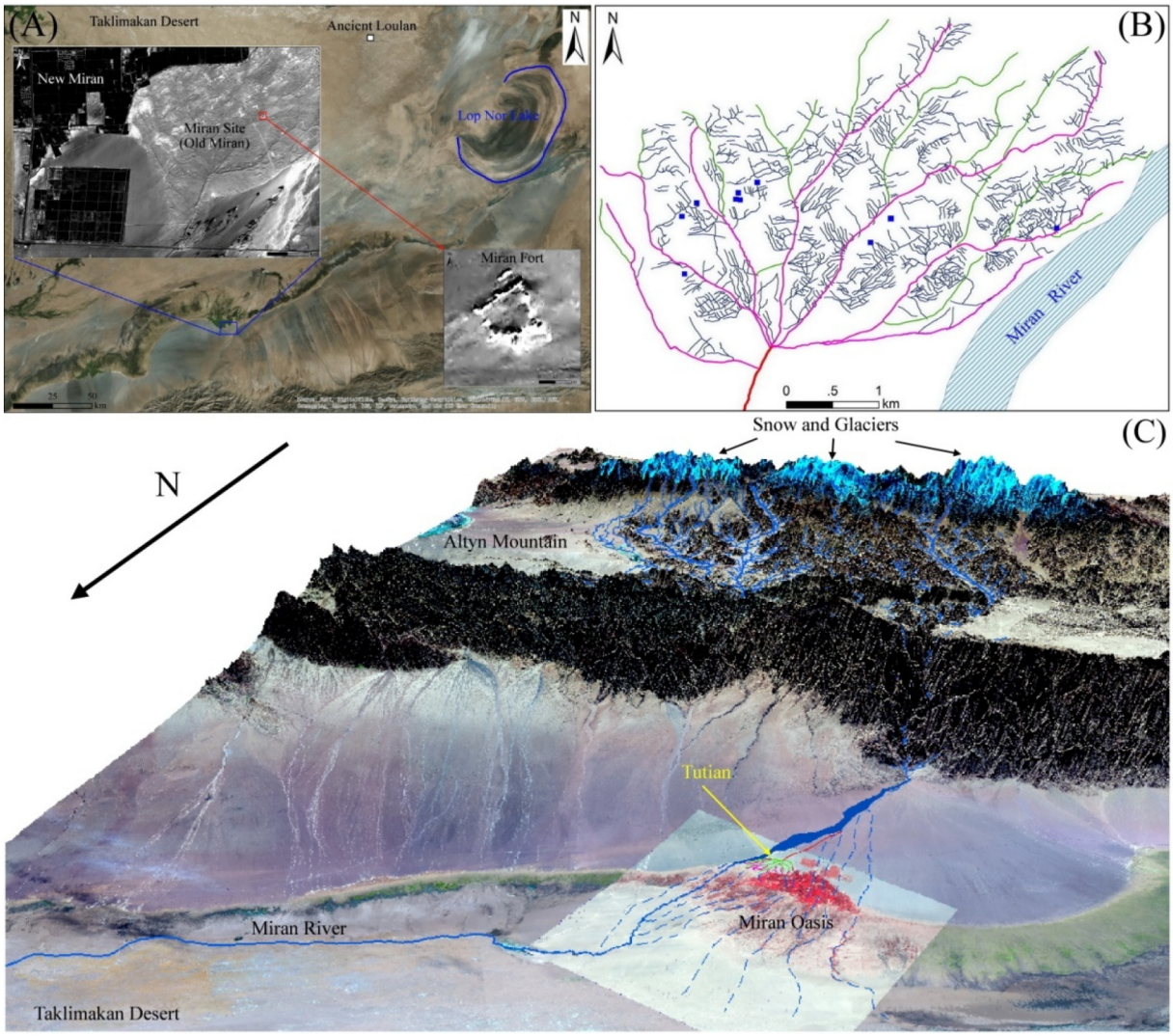

Fig. 20. Miran *Tuntian* Irrigation Landscape. (A) Miran site; (B) A fan-shaped complex including trunk (red), primary (pink), secondary (green) and tertiary canals (blue) which have been automatic detected from Gaofen-1 PAN data (following Luo et al. (2018b)); (C) 2.5D view of the Mountain–Oasis–Desert Ecosystem (MODES) of the Miran Tuntian Irrigation Landscape as viewed from the north, in this view, Gaofen-1 PMS (false color composites, RGB 432) and Landsat-8 OLI (false color composites, RGB 654) pansharpened data have been laid over an ASTER GDEMV2 DEM product; the drainage system of the Miran River is also shown. (For interpretation of the references to color in this figure legend, the reader is referred to the web version of this article.)

Desert System (Luo et al., 2017b), which were connected by the Miran River and together constituted a coupled mountain–oasis–desert ecosystem (MODES) (Fig. 20). Thus, it is important to explore the spatial patterns in Miran tuntian irrigation system at a landscape-scale for understanding its changes and declines. Landscape-scale archaeology is a very challenging field for remote sensing archaeologists (Luo et al., 2017b; Verhoeven, 2017) because not only do they need a good understanding of multi-sensor imagery but also detailed knowledge of the ACH sites that they are studying. They also need to know about the supporting environment and the human activities that took place there, altogether thus including the geographic, geomorphic and hydrological conditions, the historical origins of the sites and the associated socio-cultural characteristics.

On the other hand, using data merely derived from remote sensing techniques, archaeologists often can only detect the archaeological anomalies, but hard to understand the essence of abnormality. The multiplatform remote sensing products should be combined with other geospatial data (e.g. archaeological, cultural, historical, geological, hydrological, environmental, ecological, social and economic, etc.) to provide new insight and contextual information about anomalies in multiple layers of data (Tapete et al., 2017). By combining satellite SAR image stacks with local grounder water data and architectural parameters, for example, Chen et al. (2017a) not only uncovered the serious situations of monument collapse at site-scale, but provided new evidences for understanding the water crisis of Angkor in a landscape-scale.

7.4. Towards a down-to-earth tool for ACH applications

Undoubtedly, ASRS is a very effective, low-cost, and readily accessible tool that provides direct perception of the geographical situations at ACH sites with a relatively high accuracy. It is the major reason that ASRS has become widely open to both the public and archaeologists. However, over-reliance on ASRS imagery might lead to the danger that archaeologists become too remote from the people that they are researching (Luo et al., 2018a). The characteristics of archaeological features strongly depend on localized factors (Beck, 2010; Crawford, 1923). It can be said that archaeological features create spatial anomalies but those features that show spatial anomalies may not be archaeological features. After all, an ASRS image is both an abstraction and a particular, situated representation (McCoy and Ladefoged, 2009). In addition, as far as remote sensing archaeology is concerned,

archaeologists are faced more with a social problem than a technical one (Opitz and Herrmann, 2018). Too many projects attempt to get everything out of remote sensing data and start off with unrealistic expectations, resulting in a general frustration with remote sensing as an approach (Lasaponara et al., 2017a; Linck et al., 2013). Although ASRS is a powerful tool for studying ACH sites, traditional and novel ground-based survey methods, including excavation, ground remote sensing measurements and instrumental observation of chemical, physical, biological and meteorological factors, must be employed as well to distinguish false positives from areas of interest or objects related to actual ancient human occupations, and to discover ACH sites too small to be detected reliably by ASRS sensors (Luo et al., 2018a). As evidenced by many successful studies where ASRS images were validated by ground-truthing data at a resolution appropriate to the scale of the features, the archaeological aims can be reached if this is done (Agapiou et al., 2017b; Balz et al., 2016; Banerjee and Srivastava, 2013; Campana et al., 2009; Garrison et al., 2008; Verhoeven and Sevara, 2016).

Ground-truthing is the key to remote sensing archaeology and it can be emphasized too much that researchers have to be able to confirm what they are identifying in an image or other type of scene. ASRS is not a straightforward substitute for field archaeology and should ideally be integrated with ground-truthing and expert knowledge obtained from both the public and archaeologists (McCoy and Ladefoged, 2009). Where this is not possible, caution must be used when putting forward interpretations of sites and features. It is certain that ASRS alone cannot identify all ACH sites in a given region. Taking mountainous areas as an example, due to the existence of shadows and terrain distortions, anomalies often cannot be identified from remote sensing imagery but can be identified by field survey (Brown Vega et al., 2011). Ideally, ASRS-based ACH applications are a two-pronged approach that entails image interpretation followed by GPS-based ground-truthing, or a field survey of spatial anomalies. For deeply buried archaeological features, small-scale invasive boring is a good alternative when excavation is not allowed. Zong et al. (2018) used archaeological boring to map stratigraphic sequences on the basis of color, compactness, and the inclusions contained in the soil, and then to provide detailed confirmation of the results produced by the remote sensing data and GPR surveys. ASRS data will not replace the traditional field survey or ground measurement, but, used judiciously, data gathered by spaceborne and airborne platforms can reveal many archaeological features and the early signals of damage risks in cultural heritage whose existence would not be unsuspected from the ground.

7.5. Capitalize the experience of all the existing networks for the benefit of the society

ACH, one of the core carriers of cultural diversity on our planet, is a driver and enabler of sustainable development of the society (ICOMOS, 2017). Discovering, documenting and understanding ACH sites and their changes in space and time are crucial to promptly provide monitoring and management practices against damage and cultural diversity loss (Vaz et al., 2019). This is explicitly taken into account by the SDGs of the United Nations (Guo, 2018; Guo et al., 2017, 2018; UN, 2015), with Goal 11.4 explicitly aiming to “strengthen efforts to protect and safeguard the world's cultural and natural heritage to make our cities inclusive, safe, resilient and sustainable”. However, ACH management and monitoring is mainly based on field observations related to physical survey, considering different geographical settings, under the proper methods of in situ analysis. Such a method is time and cost consuming and does not allow in most cases to get temporal replicates. This led to the urgent need of developing novel and low-cost methods and stakeholders' networks to face above-mentioned issues at various levels.

Fortunately, to the scientific community, many local, national, regional and global (Table 2) networks or organizations such as University of Arkansas, University of Alabama, University of Central Florida, Cyprus University of Technology, LBI-ArchPro, CNR-IMAA, CNR-IBAM, CAS-RADI, National Aeronautics and Space Administration (NASA), European Space Agency (ESA), Italian Space Agency (ASI), International Centre on Space Technologies for Natural and Cultural Heritage (HIST), and International Society for Photogrammetry and Remote Sensing (ISPRS) are not only platforms providing huge volumes of freely available RS imagery or 3D views of the ACH sites, but more importantly are effective channels to communicate and share data, research findings and experiences. We need and should make full use of the experience of existing networks and organizations for the benefit of the society. For example, since the early 2010s, HIST launched several research projects to refine and validate the use of passive and active remote sensing for archaeological purposes (Wang et al., 2017b). In the beginning of 21st century, NASA formally solicited “Space Archaeology” proposals through its Earth Science Directorate and continues to assist archaeologists and cultural resource managers in doing their work more efficiently and effectively (Giardino, 2011). Moreover, the Center for Advanced Spatial Technologies at the University of Arkansas set up methods for the reliable and efficient orthorectification of CORONA imagery and provides free public access to their imagery database (covering the Near East and surrounding areas) and GIS tools for non-commercial use in archaeology (Casana and Cothren, 2013).

7.6. From remote sensing archaeology to space archaeology

With the rapid development of science and technology, especially the combination of applications in the natural sciences and the humanities and social sciences, archaeology has developed into several new subfields, such as historical archaeology, remote sensing archaeology, environmental archaeology, and other multidisciplinary approaches. Conventional archaeology generally believes that it is a science with “time” as its core, while remote sensing is a technology with “space” as its core. Remote sensing is of particular interest for specialists and the public as it combines three key essences of archaeological research: objects, space, and time (Luo et al., 2018a). It has become an important tool for helping archaeologists to prospect and understand ACH sites, for discovering and monitoring archaeological sites, for documenting and preserving cultural heritage, and for resolving real archaeological problems. The object of study is, of course, the ACH feature buried underground or, sometimes surface remains. Whether they are underground or surface remains, remote sensing archaeology starts with the cognition of its attributes in “space”, including the micro-space (site scale) and macro-space (landscape scale). Both the horizontal scale and vertical depth of archaeological prospecting have been extended with the rise of spatial technology (McCoy and Ladefoged, 2009) and computer science since the 1950s. Recently, the research focus of ASRS-based ACH applications has moved away from investigation, mapping, monitoring and documentation to the mining of big geospatial data, archaeological knowledge discovery and understanding, and landscape pattern analysis and reconstruction (Agapiou and Lysandrou, 2015; Wang and Guo, 2015). These improvements and transformations are jointly pushing remote sensing archaeology towards a new stage of space archaeology.

8. Conclusions

Even though remote sensing technology, especially ASRS, was not originally designed for archaeological purposes, it has become an indispensable and powerful tool in ACH and is being applied for miscellaneous purposes. Archive and novel ASRS data allow multi-temporal and multi-scale prospecting and change analysis of ACH sites. Historical photographs constitute a highly valuable resource as many of them show sites and landscapes that have since been heavily altered damaged or destroyed because of, for example, land consolidation, irrigation, urban sprawl, or armed conflict. Multi- and hyperspectral remote sensing is cheaper, more intuitive and has wider applications than

Table 2
Main existing global networks for RS-based ACH applications.

Networks or organizations	Date	References
Computer Application and Quantitative Methods in Archaeology (CAA)	Since 1973	CAA (2019)
Global Heritage Network (GHN), Global Heritage Fund (GHF)	Since 2010	GHF (2011)
Group on Earth Observation (GEO)	Since 2017	GEO (2017)
Int'l Committee for Documentation of Cultural Heritage (CIPA), ICOMOS/ISPRS	Since 1968	CIPA (2019)
HIST, UNESCO	Since 2011	HIST (2011)
Heritage Working Group, Digital Belt and Road Program (DBAR)	Since 2017	DBAR (2017)

active remote sensing for archaeological prospecting and feature identification. SAR now has the great potential to provide suitable resolution for prospecting, mapping and monitoring, condition assessment and documentation, as well as conservation and management. Airborne LiDAR generally serves the purposes of exploration below the vegetation canopy or underwater and for carrying out landscape analysis better than spectral imaging, SAR, or photography can. Aerial photography and UAVs can be used to collect centimeter-level VHR data that is typically captured at the site or site scale to support the detailed mapping and monitoring. As an emerging force in aerial archaeology, UAVs play an increasingly important role in ACH applications. ASRS is a useful tool when combined with field campaigns, and it is a valuable and low-cost method for archaeological investigations in remote or inaccessible regions (e.g. tropical forests, deserts, Gobi, underwater or war-zones). It can also be used to help accentuate spatial, spectral, temporal and structural features (e.g. small or large buried ACH sites, slight spectral differences and architectural micro-deformations) that are invisible to direct observation by the human eye.

When going back to the above-mentioned landscape archaeology as the study of the geo-cultural or man-land spaces between the sites and their supporting environments, ASRS is in many research contexts a valid and helpful way to accomplish this (Verhoeven, 2017). However, remote sensing data stem from the worlds of quantification and generalization, to which the qualitative and subjective aspects of humanity defended by the broadly labeled post-processual movement, represents a partial reaction (Witcher, 1999). Post-processual archaeologists mainly critiqued the scientific, analytical approach to reach objective conclusions, in that light, it is unsurprising that remote sensing was generally of little interest to them (Verhoeven, 2017). In addition, it should be acknowledged frankly and openly that all the existing applications mentioned in this review have proved that ASRS has substantial contribution to studying 'space' dimension in Archaeology, but the drawbacks in 'time' dimension are also obvious. ASRS would effectively response and solve the spatial problems (e.g. location, distribution pattern and man-land relationship) in the specific archaeological investigation, but it is often helpless on the temporal issues (e.g. human society evolution, the origin and rise and fall of culture, and paleoclimate change) of archaeological research per se.

This review has not only notes the major milestones in ASRS as used in ACH applications but also provided in-depth discussion on methods, current developments, challenges and trends. ASRS represents an invaluable set of powerful tools for prospecting, monitoring and documentation and also for supporting the assessment and conservation of ACH sites and their supporting environments. ASRS is not always suitable in all environmental situations at any time and for all types of ACH features. The reflection or emission properties of ACH sites distinguishable by various types of imaging sensors may perhaps be one of their most characteristic features, and yet the meaning of the differential discrimination of features has not been determined for the most part, since such spectral and backscattering properties are inadequately understood at this date. ASRS provides big data related to archaeological objects, but data without interpretation is of no value. Opportunities to access archive and novel data acquired by spaceborne and airborne platforms are increasing, and training on how to integrate these data and demonstration of their potential value for ACH study appear to be practical ways forward to fill the gap between the ASRS technology and archaeological communities (Tapete and Cigna, 2017b; Wang and Guo, 2015), and to support the transfer of ASRS technology into archaeological practice. This review has shown that the different ASRS imaging techniques and the corresponding output images vary in their applicability to ACH applications; however, their applications are far broader than this review has indicated. Their full potential, to a considerable extent, remains unexplored.

Acknowledgments

The authors thank three anonymous reviewers for their helpful comments and suggestions, which improved this manuscript. Many thanks are due to the DigitalGlobe, NASA/JPL, USGS, USIEI, ESA, Open Topography, LBI-ArchPro, ABT GmbH and CRESDA for providing the multisource remote sensing data that were used in this study. Also appreciated was the field survey assistance of Touil Lamia from IRA and Zain Ul Abedin from CUI, and the technical assistance of Meng Wang, Lanwei Zhu, Jie Liu, Biao Deng, Bangsen Tian, Wei Zhou and Lei Liang from RADI, CAS. This work was supported by the Strategic Priority Research Program of the CAS (Grant No. XDA19030504), the National Natural Science Foundation of China (Grant No. 41801345, 61860206004) and the International Partnership Program of the CAS (Grant No. 131C11KYSB20160061). The views and conclusions expressed in this article are those of the authors and do not necessarily represent the views of CAS, CNR, UNESCO, IRA and universities.

References

AAAS, American Association for the Advancement of Science, 2014. Ancient history, modern destruction: assessing the status of Syria's Tentative World Heritage sites using high-resolution satellite imagery. https://www.aaas.org/resources/ancient-history-modern-destruction-assessing-status-syria-s-tentative-world-heritage-sites-7, Accessed date: 15 March 2019.

Achille, C., Adami, A., Chiarini, S., Cremonesi, S., Fassi, F., Fregonese, L., Taffurelli, L., 2015. UAV-based photogrammetry and integrated technologies for architectural applications—methodological strategies for the after-quake survey of vertical structures in Mantua (Italy). Sensors 15, 15520–15539.

Adams, R., Brown, W., Culbert, T., 1981. Radar mapping, archaeology, and ancient Maya land use. Science 213, 1457–1463.

Agapiou, A., 2017a. Orthogonal equations for the detection of hidden archaeological remains de-mystified. J. Archaeol. Sci. Rep. 14, 792–799.

Agapiou, A., 2017b. Remote sensing heritage in a petabyte-scale: satellite data and heritage Earth Engine© applications. International Journal of Digital Earth 10, 85–102.

Agapiou, A., Hadjimitsis, D.G., 2011. Vegetation indices and field spectroradiometric measurements for validation of buried architectural remains: verification under area surveyed with geophysical campaigns. J. Appl. Remote. Sens. 5, 053554.

Agapiou, A., Lysandrou, V., 2015. Remote sensing archaeology: tracking and mapping evolution in European scientific literature from 1999 to 2015. J. Archaeol. Sci. Rep. 4, 192–200.

Agapiou, A., Hadjimitsis, D.G., Alexakis, D.D., 2012. Evaluation of broadband and narrowband vegetation indices for the identification of archaeological crop marks. Remote Sens. 4, 3892–3919.

Agapiou, A., Alexakis, D.D., Sarris, A., Hadjimitsis, D.G., 2013a. Orthogonal equations of multi-spectral satellite imagery for the identification of un-excavated archaeological sites. Remote Sens. 5, 6560–6586.

Agapiou, A., Hadjimitsis, D.G., Sarris, A., Georgopoulos, A., Alexakis, D.D., 2013b. Optimum temporal and spectral window for monitoring crop marks over archaeological remains in the Mediterranean region. J. Archaeol. Sci. 40, 1479–1492.

Agapiou, A., Alexakis, D.D., Hadjimitsis, D.G., 2014a. Spectral sensitivity of ALOS, ASTER, IKONOS, LANDSAT and SPOT satellite imagery intended for the detection of archaeological crop marks. International Journal of Digital Earth 7, 351–372.

Agapiou, A., Alexakis, D.D., Sarris, A., Hadjimitsis, D.G., 2014b. Evaluating the potentials of sentinel-2 for archaeological perspective. Remote Sens. 6, 2176–2194.
Agapiou, A., Alexakis, D.D., Lysandrou, V., Sarris, A., Cuca, B., Themistocleous, K., Hadjimitsis, D.G., 2015a. Impact of urban sprawl to cultural heritage monuments: the case study of Paphos area in Cyprus. J. Cult. Herit. 16, 671–680.
Agapiou, A., Lysandrou, V., Alexakis, D.D., Themistocleous, K., Cuca, B., Argyriou, A., Sarris, A., Hadjimitsis, D.G., 2015b. Cultural heritage management and monitoring using remote sensing data and GIS: the case study of Paphos area, Cyprus. Comput. Environ. Urban. Syst. 54, 230–239.
Agapiou, A., Alexakis, D.D., Sarris, A., Hadjimitsis, D.G., 2016a. Colour to greyscale pixels: re-seeing greyscale archived aerial photographs and declassified satellite CORONA images based on image fusion techniques. Archaeol. Prospect. 23, 231–241.
Agapiou, A., Lysandrou, V., Lasaponara, R., Masini, N., Hadjimitsis, D.G., 2016b. Study of the variations of archaeological marks at Neolithic Site of Lucera, Italy using high-resolution multispectral datasets. Remote Sens. 8, 723.
Agapiou, A., Lysandrou, V., Themistocleous, K., Hadjimitsis, D.G., 2016c. Risk assessment of cultural heritage sites clusters using satellite imagery and GIS: the case study of Paphos District, Cyprus. Nat. Hazards 83, 5–20.
Agapiou, A., Lysandrou, V., Hadjimitsis, D.G., 2017a. Optical remote sensing potentials for looting detection. Geosciences (Switzerland) 7, 98.
Agapiou, A., Lysandrou, V., Sarris, A., Papadopoulos, N., Hadjimitsis, D.G., 2017b. Fusion of satellite multispectral images based on ground-penetrating radar (GPR) data for the investigation of buried concealed archaeological remains. Geosciences (Switzerland) 7, 40.
Alberti, S., Ferretti, A., Leoni, G., Margottini, C., Spizzichino, D., 2017. Surface deformation data in the archaeological site of Petra from medium-resolution satellite radar images and SqueeSAR™ algorithm. J. Cult. Herit. 25, 10–20.
Alexakis, D., Sarris, A., Astaras, T., Albanakis, K., 2009. Detection of neolithic settlements in Thessaly (Greece) through multispectral and hyperspectral satellite imagery. Sensors 9, 1167–1187.
Alexakis, D., Agapiou, A., Hadjimitsis, D., Sarris, A., 2012. Remote sensing applications in archaeological research. In: Escalante, B. (Ed.), Remote Sensing – Applications. InTech, pp. 435–462.
Aliphat Fernandez, M., 1996. Arqueología y paisajes del alto usumacinta. Arqueología Mexicana 4, 24–29 (in Spanish).
Alizadeh, K., Ur, J.A., 2007. Formation and destruction of pastoral and irrigation landscapes on the Mughan Steppe, north-western Iran. Antiquity 81, 148–160.
Altaweel, M., 2005. The use of ASTER satellite imagery in archaeological contexts. Archaeol. Prospect. 12, 151–166.
Aminzadeh, B., Samani, F., 2006. Identifying the boundaries of the historical site of Persepolis using remote sensing. Remote Sens. Environ. 102, 52–62.
Aqdus, S.A., Hanson, W.S., Drummond, J., 2012. The potential of hyperspectral and multi-spectral imagery to enhance archaeological cropmark detection: a comparative study. J. Archaeol. Sci. 39, 1915–1924.
Atzberger, C., Wess, M., Doneus, M., Verhoeven, G., 2014. ARCTIS - a MATLAB® toolbox for archaeological imaging spectroscopy. Remote Sens. 6, 8617–8638.
Axelsson, P., 2000. DEM generation from laser scanner data using adaptive TIN models. International Archives of Photogrammetry and Remote Sensing XXXIII (Part B4), 110–117.
Baeye, M., Quinn, R., Deleu, S., Fettweis, M., 2016. Detection of shipwrecks in ocean colour satellite imagery. J. Archaeol. Sci. 66, 1–6.
Ballard, R.D., 2007. Archaeological oceanography. In: Wiseman, J., El-Baz, F. (Eds.), Remote Sensing in Archaeology. Springer, New York, pp. 479–497.
Balz, T., Caspari, G., Fu, B., Liao, M., 2016. Discernibility of burial mounds in high-resolution X-band SAR images for archaeological prospections in the Altai mountains. Remote Sens. 8, 817.
Banerjee, R., Srivastava, P.K., 2013. Reconstruction of contested landscape: detecting land cover transformation hosting cultural heritage sites from Central India using remote sensing. Land Use Policy 34, 193–203.
Bassani, C., Cavalli, R., Goffredo, R., Palombo, A., Pascucci, S., Pignatti, S., 2009. Specific spectral bands for different land cover contexts to improve the efficiency of remote sensing archaeological prospection: the Arpi case study. J. Cult. Herit. 10 (Suppl. 1), e41–e48.
Beazeley, G., 1919. Air photography in archaeology. Geogr. J. 53, 330–335.
Beck, A., 2010. Archaeological applications of multi-/hyper-spectral data-challenges and potential. In: Cowley, D. (Ed.), Remote Sensing for Archaeological Heritage Management. Europae Archaeological Consilium, Brussel, Belgium, pp. 87–98.
Beck, A., Philip, G., Abdulkarim, M., Donoghue, D., 2007. Evaluation of Corona and Ikonos high resolution satellite imagery for archaeological prospection in western Syria. Antiquity 81, 161–175.
Berardino, P., Fornaro, G., Lanari, R., Sansosti, E., 2002. A new algorithm for surface deformation monitoring based on small baseline differential SAR interferograms. IEEE Trans. Geosci. Remote Sens. 40, 2375–2383.
Bernardini, F., Sgambati, A., Montagnari Kokelj, M., Zaccaria, C., Micheli, R., Fragiacomo, A., Tiussi, C., Dreossi, D., Tuniz, C., De Min, A., 2013. Airborne LiDAR application to karstic areas: the example of Trieste province (north-eastern Italy) from prehistoric sites to Roman forts. J. Archaeol. Sci. 40, 2152–2160.
Bewley, R.H., 2003. Aerial survey for archaeology. Photogrammetric Record 18, 273–292.
Bewley, R.H., Crutchley, S.P., Shell, C.A., 2005. New light on an ancient landscape: Lidar survey in the Stonehenge world heritage site. Antiquity 79, 636–647.
Bindschadler, R., Vornberger, P., 1998. Changes in the West Antarctic ice sheet since 1963 from declassified satellite photography. Science 279, 689–692.
Bitelli, G., Girelli, V.A., 2009. Metrical use of declassified satellite imagery for an area of archaeological interest in Turkey. J. Cult. Herit. 10 (Suppl. 1), e35–e40.
Blaschke, T., 2010. Object based image analysis for remote sensing. ISPRS J. Photogramm. Remote Sens. 65, 2–16.
Blaschke, T., Hay, G.J., Kelly, M., Lang, S., Hofmann, P., Addink, E., Queiroz Feitosa, R., Van der Meer, F., Van der Werff, H., Van Coillie, F., Tiede, D., 2014. Geographic object-based image analysis - towards a new paradigm. ISPRS J. Photogramm. Remote Sens. 87, 180–191.
Blom, R., Crippen, R., Elachi, C., 1984. Detection of subsurface features in SEASAT SAR images of means valley, Mojave Desert, California. Geology 12, 346–349.
Blom, R., Clapp, N., Zarins, J., Hedges, G., 1997. Space technology and the discovery of the lost city of Ubar. In: Paper Presented at the IEE Aerospace Conference, Snowmass at Aspen, USA (1–8 February, 1997), pp. 19–28.
Bradford, J., Williams-Hunt, P., 1946. Siticulosa Apulia. Antiquity 20, 191–200.
Brivio, P.A., Pepe, M., Tomasoni, R., 2000. Multispectral and multiscale remote sensing data for archaeological prospecting in an alpine alluvial plain. J. Cult. Herit. 1, 155–164.
Brown Vega, M., Craig, N., Lindo, G.A., 2011. Ground truthing of remotely identified fortifications on the Central Coast of Perú. J. Archaeol. Sci. 38, 1680–1689.
Bubenzer, O., Bolten, A., 2008. The use of new elevation data (SRTM/ASTER) for the detection and morphometric quantification of Pleistocene megadunes (draa) in the eastern Sahara and the southern Namib. Geomorphology 102, 221–231.
CAA, Computer Application and Quantitative Methods in Archaeology, 2019. CAA history. https://caa-international.org/about/history/, Accessed date: 10 June 2019.
Campana, S., 2017. Drones in archaeology. State-of-the-art and future perspectives. Archaeol. Prospect. 24, 275–296.
Campana, S., Dabas, M., Marasco, L., Piro, S., Zamuner, D., 2009. Integration of remote sensing, geophysical surveys and archaeological excavation for the study of a medieval mound (Tuscany, Italy). Archaeol. Prospect. 16, 167–176.
Canilao, M.A.P., 2017. Early historical gold trade networks in Northwestern Luzon, as reconstructed from ethnohistorical accounts, WorldView2 satellite remote sensing and GIS predictive modelling: the Gasweling case. J. Archaeol. Sci. Rep. 16, 127–148.
Canuto, M.A., Estrada-Belli, F., Garrison, T.G., Houston, S.D., Acuna, M.J., Kovac, M., Marken, D., Nondedeo, P., Auld-Thomas, L., Castanet, C., Chatelain, D., Chiriboga, C.R., Drapela, T., Lieskovsky, T., Tokovinine, A., Velasquez, A., Fernandez-Diaz, J.C., Shrestha, R., 2018. Ancient lowland Maya complexity as revealed by airborne laser scanning of northern Guatemala. Science 361, eaau0137.
Capper, J., 1907. Photographs of Stonehenge as seen from a war balloon. Archaeologia 60, 571.
Carter, G., Miller, R., 1994. Early detection of plant stress by digital imaging within narrow stress-sensitive wavebands. Remote Sens. Environ. 50, 295–302.
Casana, J., 2013. Radial route systems and agro-pastoral strategies in the Fertile Crescent: new discoveries from western Syria and southwestern Iran. J. Anthropol. Archaeol. 32, 257–273.
Casana, J., 2015. Satellite imagery-based analysis of archaeological looting in Syria. Near Eastern Archaeology 78, 142–152.
Casana, J., Cothren, J., 2008. Stereo analysis, DEM extraction and orthorectification of CORONA satellite imagery: archaeological applications from the Near East. Antiquity 82, 732–749.
Casana, J., Cothren, J., 2013. The CORONA Atlas Project: orthorectification of CORONA satellite imagery and regional-scale archaeological exploration in the Near East. In: Comer, D., Harrower, M. (Eds.), Mapping Archaeological Landscapes from Space. Springer, New York, pp. 33–43.
Casana, J., Laugier, E.J., 2017. Satellite imagery-based monitoring of archaeological site damage in the Syrian civil war. PLoS One 12, e0188589.
Casana, J., Cothren, J., Kalayci, T., 2012. Swords into ploughshares: archaeological applications of CORONA satellite imagery in the Near East. Internet Archaeology(32). https://doi.org/10.11141/ia.32.2.
Casana, J., Kantner, J., Wiewel, A., Cothren, J., 2014. Archaeological aerial thermography: a case study at the Chaco-era Blue J community, New Mexico. J. Archaeol. Sci. 45, 207–219.
Castaldi, F., Palombo, A., Santini, F., Pascucci, S., Pignatti, S., Casa, R., 2016. Evaluation of the potential of the current and forthcoming multispectral and hyperspectral imagers to estimate soil texture and organic carbon. Remote Sens. Environ. 179, 54–65.
Cavalli, R., Colosi, F., Palombo, A., Pignatti, S., Poscolieri, M., 2007. Remote hyperspectral imagery as a support to archaeological prospection. J. Cult. Herit. 8, 272–283.
Cavalli, R.M., Pascucci, S., Pignatti, S., 2009. Optimal spectral domain selection for maximizing archaeological signatures: Italy case studies. Sensors 9, 1754–1767.
Cavalli, R., Licciardi, G., Chanussot, J., 2013. Detection of anomalies produced by buried archaeological structures using nonlinear principal component analysis applied to airborne hyperspectral image. IEEE Journal of Selected Topics in Applied Earth Observations and Remote Sensing 6, 659–669.
Ceraudo, G., 2004. Un secolo e un lustro di fotografia aerea archeologica in Italia (1899–2004), in Archeologia Aerea. In: Studi di Aerotopografia Archeologica I, Roma, pp. 47–68 (in Italian).
Cerra, D., Plank, S., Lysandrou, V., Tian, J., 2016. Cultural heritage sites in danger—towards automatic damage detection from space. Remote Sens. 8, 781.
Cerra, D., Agapiou, A., Cavalli, R., Sarris, A., 2018. An objective assessment of hyperspectral indicators for the detection of buried archaeological relics. Remote Sens. 10, 500.
Challis, K., 2006. Airborne laser altimetry in alluviated landscapes. Archaeol. Prospect. 13, 103–127.
Challis, K., Priestnall, G., Gardner, A., Henderson, J., O'Hara, S., 2004. Corona remotely-sensed imagery in dryland archaeology: the Islamic City of al-Raqqa, Syria. J. Field Archaeol. 29, 139–153.
Challis, K., Forlin, P., Kincey, M., 2011. A generic toolkit for the visualization of archaeological features on airborne LiDAR elevation data. Archaeol. Prospect. 18, 279–289.

Chan, Y., Koo, V., 2008. An introduction to synthetic aperture radar (SAR). Progress In Electromagnetics Research B 2, 27–60.
Chapman, B., Blom, R., 2013. Synthetic aperture radar, technology, past and future applications to archaeology. In: Comer, D., Harrower, M. (Eds.), Mapping Archaeological Landscapes from Space. Springer, New York, pp. 113–131.
Chase, D.Z., Chase, A.F., 2017. Caracol, Belize, and changing perceptions of Ancient Maya society. J. Archaeol. Res. 25, 185–249.
Chase, A.F., Chase, D.Z., Weishampel, J.F., Drake, J.B., Shrestha, R.L., Slatton, K.C., Awe, J.J., Carter, W.E., 2011. Airborne LiDAR, archaeology, and the ancient Maya landscape at Caracol, Belize. J. Archaeol. Sci. 38, 387–398.
Chase, A.F., Chase, D.Z., Fisher, C.T., Leisz, S.J., Weishampel, J.F., 2012. Geospatial revolution and remote sensing LiDAR in Mesoamerican archaeology. Proc. Natl. Acad. Sci. U. S. A. 109, 12916–12921.
Chase, A.F., Chase, D.Z., Awe, J.J., Weishampel, J.F., Iannone, G., Moyes, H., Yaeger, J., Brown, K., Shrestha, R.L., Carter, W.E., Diaz, J.F., 2014. Ancient Maya regional settlement and inter-site analysis: the 2013 West-central Belize LiDAR survey. Remote Sens. 6, 8671–8695.
Chase, A.S.Z., Chase, D.Z., Chase, A.F., 2017. LiDAR for archaeological research and the study of historical landscapes. In: Masini, N., Soldovieri, F. (Eds.), Sensing the Past. Springer, Cham, pp. 89–100.
Chaussard, E., Wdowinski, S., Cabral-Cano, E., Amelung, F., 2014. Land subsidence in central Mexico detected by ALOS InSAR time-series. Remote Sens. Environ. 140, 94–106.
Chen, F., Masini, N., Yang, R., Milillo, P., Feng, D., Lasaponara, R., 2015. A space view of radar archaeological marks: first applications of COSMO-SkyMed X-band data. Remote Sens. 7, 24–50.
Chen, F., Masini, N., Liu, J., You, J., Lasaponara, R., 2016. Multi-frequency satellite radar imaging of cultural heritage: the case studies of the Yumen Frontier Pass and Niya ruins in the western regions of the silk road corridor. International Journal of Digital Earth 9, 1224–1241.
Chen, F., Guo, H., Ma, P., Lin, H., Wang, C., Ishwaran, N., Hang, P., 2017a. Radar interferometry offers new insights into threats to the Angkor site. Sci. Adv. 3, e1601284.
Chen, F., Jiang, A., Tang, P., Yang, R., Zhou, W., Wang, H., Lu, X., Balz, T., 2017b. Multi-scale synthetic aperture radar remote sensing for archaeological prospection in Han Hangu Pass, Xin'an China. Remote Sensing Letters 8, 38–47.
Chen, F., Lasaponara, R., Masini, N., 2017c. An overview of satellite synthetic aperture radar remote sensing in archaeology: from site detection to monitoring. J. Cult. Herit. 23, 5–11.
Chen, F., Wu, Y., Zhang, Y., Parcharidis, I., Ma, P., Xiao, R., Xu, J., Zhou, W., Tang, P., Foumelis, M., 2017d. Surface motion and structural instability monitoring of Ming Dynasty City walls by two-step tomo-PSInSAR approach in Nanjing City, China. Remote Sens. 9, 371.
Chen, S., Wang, S., Li, C., Hu, Q., Yang, H., 2018. A seismic capacity evaluation approach for architectural heritage using finite element analysis of three-dimensional model: a case study of the limestone hall in the Ming Dynasty. Remote Sens. 10, 963.
Cheng, L., Wang, Y., Chen, Y., Li, M., 2016. Using LiDAR for digital documentation of ancient city walls. J. Cult. Herit. 17, 188–193.
Chiabrando, F., Nex, F., Piatti, D., Rinaudo, F., 2011. UAV and RPV systems for photogrammetric surveys in archaeological areas: two tests in the Piedmont region (Italy). J. Archaeol. Sci. 38, 697–710.
Cigna, F., Tapete, D., Lasaponara, R., Masini, N., 2013. Amplitude change detection with ENVISAT ASAR to image the cultural landscape of the Nasca region, Peru. Archaeol. Prospect. 20, 117–131.
Cigna, F., Lasaponara, R., Masini, N., Milillo, P., Tapete, D., 2014. Persistent scatterer interferometry processing of COSMO-SkyMed StripMap HIMAGE time series to depict deformation of the historic centre of Rome, Italy. Remote Sens. 6, 12593.
CIPA, International Committee for Documentation of Cultural Heritage, 2019. The international committee for documentation of cultural heritage. http://cipa.icomos.org/, Accessed date: 10 June 2019.
Coluzzi, R., Lanorte, A., Lasaponara, R., 2010. On the LiDAR contribution for landscape archaeology and palaeoenvironmental studies: the case study of Bosco dell'Incoronata (Southern Italy). Adv. Geosci. 24, 125–132.
Comer, D., 2012. Tourism and Archaeological Heritage Management at Petra. Springer-Verlag, New York, pp. 131–144.
Comer, D.C., Chapman, B.D., Comer, J.A., 2017. Detecting landscape disturbance at the Nasca lines using SAR data collected from airborne and satellite platforms. Geosciences (Switzerland) 7, 106.
Comfort, A., Ergeç, R., 2001. Following the Euphrates in antiquity: north-south routes around Zeugma. Anatol. Stud. 51, 19–50.
Conesa, F.C., Madella, M., Galiatsatos, N., Balbo, A.L., Rajesh, S.V., Ajithprasad, P., 2015. CORONA photographs in monsoonal semi-arid environments: addressing archaeological surveys and historic landscape dynamics over North Gujarat, India. Archaeol. Prospect. 22, 75–90.
Confuorto, P., Plank, S., Novellino, A., Tessitore, S., Ramondini, M., 2016. Implementation of DInSAR methods for the monitoring of the archaeological site of Hera Lacinia in Crotone (Southern Italy). Rendiconti Online Societa Geologica Italiana 41, 231–234.
Conn, V.S., Valentine, J.C., Cooper, H.M., Rantz, M.J., 2003. Grey literature in meta-analyses. Nurs. Res. 52, 256–261.
Connah, G., 1978. Aborigine and settler: archaeological air photography. Antiquity 52, 95–99.
Contreras, D.A., Brodie, N., 2010. The utility of publicly-available satellite imagery for investigating looting of archaeological sites in Jordan. J. Field Archaeol. 35, 101–114.
Cooper, A., Green, C., 2016. Embracing the complexities of 'big data' in archaeology: the case of the English Landscape and Identities Project. J. Archaeol. Method Theory 23, 271–304.
Corns, A., Shaw, R., 2009. High resolution 3-dimensional documentation of archaeological monuments & landscapes using airborne LiDAR. J. Cult. Herit. 10 (Suppl. 1), e72–e77.
Cowley, D., Stichelbaut, B., 2012. Historical aerial photographic archives for European archaeology. Eur. J. Archaeol. 15, 217–236.
Cox, C., 1992. Satellite imagery, aerial photography and wetland archaeology: an interim report on an application of remote sensing to wetland archaeology: the pilot study in Cumbria, England. World Archaeol. 24, 249–267.
Crawford, O., 1923. Air survey in archaeology. Geogr. J. 61, 342–360.
Cressie, N., 1990. The origins of kriging. Math. Geol. 22, 239–252.
Crosetto, M., Monserrat, O., Cuevas-González, M., Devanthéry, N., Crippa, B., 2016. Persistent scatterer interferometry: a review. ISPRS J. Photogramm. Remote Sens. 115, 78–89.
Crow, P., Benham, S., Devereux, B.J., Amable, G.S., 2007. Woodland vegetation and its implications for archaeological survey using LiDAR. Forestry 80, 241–252.
Crutchley, S., 2009. Ancient and modern: combining different remote sensing techniques to interpret historic landscapes. J. Cult. Herit. 10 (Suppl. 1), e65–e71.
Cuca, B., Hadjimitsis, D.G., 2017. Space technology meets policy: an overview of earth observation sensors for monitoring of cultural landscapes within policy framework for cultural heritage. J. Archaeol. Sci. Rep. 14, 727–733.
Da Lio, C., Tosi, L., 2018. Land subsidence in the Friuli Venezia Giulia coastal plain, Italy: 1992–2010 results from SAR-based interferometry. Sci. Total Environ. 633, 752–764.
Davies, K.P., Murphy, R.J., Bruce, E., 2016. Detecting historical changes to vegetation in a Cambodian protected area using the Landsat TM and ETM+ sensors. Remote Sens. Environ. 187, 332–344.
Davis, D.S., 2018. Object-based image analysis: a review of developments and future directions of automated feature detection in landscape archaeology. Archaeol. Prospect. 1–9. https://doi.org/10.1002/arp.1730. (early view, online).
DBAR, Digital Belt and Road Program, 2017. Natural and cultural heritage working group, DBAR. http://www.dbeltroad.org/index.php?m=content&c=index&a=show&catid=71&id=366/, Accessed date: 10 June 2019.
De Laet, V., Paulissen, E., Waelkens, M., 2007. Methods for the extraction of archaeological features from very high-resolution Ikonos-2 remote sensing imagery, Hisar (southwest Turkey). J. Archaeol. Sci. 34, 830–841.
De Laet, V., Paulissen, E., Meuleman, K., Waelkens, M., 2009. Effects of image characteristics on the identification and extraction of archaeological features from Ikonos-2 and Quickbird-2 imagery: case study Sagalassos (southwest Turkey). Int. J. Remote Sens. 30, 5655–5668.
De Laet, V., Van Loon, G., Van der Perre, A., Deliever, I., Willems, H., 2015. Integrated remote sensing investigations of ancient quarries and road systems in the Greater Dayr al-Barshā Region, Middle Egypt: a study of logistics. J. Archaeol. Sci. 55, 286–300.
De Meyer, M., 2004. Archaeological research using satellite remote sensing techniques (CORONA) in the valleys of Shirwan and Chardawal (Pusht-I Kuh, Luristan), Iran. Iran. Antiq. 39, 43–103.
Dellepiane, M., Dell'Unto, N., Callieri, M., Lindgren, S., Scopigno, R., 2013. Archeological excavation monitoring using dense stereo matching techniques. J. Cult. Herit. 14, 201–210.
Denbow, J.R., 1979. Cenchrus ciliaris: an ecological indicator of Iron Age middens using aerial photography in eastern Botswana. S. Afr. J. Sci. 75, 405–408.
Deng, B., Guo, H., Wang, C., Nie, Y., 2010. Application of remote sensing technique in archaeology: a review. Journal of Remote Sensing 14, 187–206.
Deroin, J.P., Téreygeol, F., Heckes, J., 2011. Evaluation of very high to medium resolution multispectral satellite imagery for geoarchaeology in arid regions - case study from Jabali, Yemen. J. Archaeol. Sci. 38, 101–114.
Deroin, J.P., Téreygeol, F., Cruz, P., Guillot, I., Méaudre, J.C., 2012. Integrated non-invasive remote-sensing techniques and field survey for the geoarchaeological study of the Sud Lípez mining district, Bolivia. J. Geophys. Eng. 9, S40–S52.
Devereux, B.J., Amable, G.S., Crow, P., Cliff, A.D., 2005. The potential of airborne lidar for detection of archaeological features under woodland canopies. Antiquity 79, 648–660.
Devereux, B.J., Amable, G.S., Crow, P., 2008. Visualisation of LiDAR terrain models for archaeological feature detection. Antiquity 82, 470–479.
Doneus, M., 2001. Precision mapping and interpretation of oblique aerial photographs. Archaeol. Prospect. 8, 13–27.
Doneus, M., 2009. Das Luftbild als Grundlage für Siedlungs- und Landschaftsarchäologie. In: Doneus, M., Griebl, M. (Eds.), Die Leitha – Facetten einer archäologischen Landschaft. Archäologie Österreichs Spezial, (Im Druck. (in German).
Doneus, M., 2013. Openness as visualization technique for interpretative mapping of airborne lidar derived digital terrain models. Remote Sens. 5, 6427–6442.
Doneus, M., Briese, C., Fera, M., Janner, M., 2008. Archaeological prospection of forested areas using full-waveform airborne laser scanning. J. Archaeol. Sci. 35, 882–893.
Doneus, M., Doneus, N., Briese, C., Pregesbauer, M., Mandlburger, G., Verhoeven, G., 2013. Airborne laser bathymetry – detecting and recording submerged archaeological sites from the air. J. Archaeol. Sci. 40, 2136–2151.
Doneus, M., Verhoeven, G., Atzberger, C., Wess, M., Ruš, M., 2014. New ways to extract archaeological information from hyperspectral pixels. J. Archaeol. Sci., 52, 84–96.
Doneus, M., Miholjek, I., Mandlburger, G., Doneus, N., Verhoeven, G., Briese, C., Pregesbauer, M., 2015. Airborne laser bathymetry for documentation of submerged archaeological sites in shallow water. ISPRS - International Archives of the Photogrammetry, Remote Sensing and Spatial Information Sciences XL-5/W5, 99–107.
Dong, J., Zhang, L., Tang, M., Liao, M., Xu, Q., Gong, J., Ao, M., 2018. Mapping landslide surface displacements with time series SAR interferometry by combining persistent

and distributed scatterers: a case study of Jiaju landslide in Danba, China. Remote Sens. Environ. 205, 180–198.
Donoghue, D., Shennan, I., 1988. The application of remote sensing to environmental archaeology. Geoarchaeology 3, 275–285.
Dorazio, T., Palumbo, F., Guaragnella, C., 2012. Archaeological trace extraction by a local directional active contour approach. Pattern Recogn. 45, 3427–3438.
Dorsett, J.E., Gilbertson, D.D., Hunt, C.O., Barker, G.W.W., 1984. The UNESCO Libyan Valleys Survey VIII: image analysis of Landsat satellite data for archaeological and environmental surveys. Libyan Studies 15, 71–80.
Elfadaly, A., Wafa, O., Abouarab, M.A.R., Guida, A., Spanu, P.G., Lasaponara, R., 2017. Geo-environmental estimation of land use changes and its effects on Egyptian temples at Luxor City. ISPRS International Journal of Geo-Information 6, 378.
Erasmi, S., Rosenbauer, R., Buchbach, R., Busche, T., Rutishauser, S., 2014. Evaluating the quality and accuracy of TanDEM-X digital elevation models at archaeological sites in the Cilician Plain, Turkey. Remote Sens. 6, 9475–9493.
Estes, J.E., 1966. Some applications of aerial infrared imagery. Ann. Assoc. Am. Geogr. 56, 673–682.
Evans, D., 2016. Airborne laser scanning as a method for exploring long-term socio-ecological dynamics in Cambodia. J. Archaeol. Sci. 74, 164–175.
Evans, D.L., Farr, T.G., 2007. The use of Interferometric Synthetic Aperture Radar (InSAR) in archaeological investigations and cultural heritage preservation. In: Wiseman, J., El-Baz, F. (Eds.), Remote Sensing in Archaeology. Springer, New York, pp. 89–102.
Evans, D., Pottier, C., Fletcher, R., Hensley, S., Tapley, I., Milne, A., Barbetti, M., 2007. A comprehensive archaeological map of the world's largest preindustrial settlement complex at Angkor, Cambodia. Proc. Natl. Acad. Sci. U. S. A. 104, 14277–14282.
Evans, D.H., Fletcher, R.J., Pottier, C., Chevance, J.B., Soutif, D., Tan, B.S., Im, S., Ea, D., Tin, T., Kim, S., Cromarty, C., De Greef, S., Hanus, K., Bâty, P., Kuszinger, R., Shimoda, I., Boornazian, G., 2013. Uncovering archaeological landscapes at Angkor using lidar. Proc. Natl. Acad. Sci. U. S. A. 110, 12595–12600.
Evers, R., Masters, P., 2018. The application of low-altitude near-infrared aerial photography for detecting clandestine burials using a UAV and low-cost unmodified digital camera. Forensic Sci. Int. 289, 408–418.
Fernandez-Diaz, J.C., Carter, W.E., Shrestha, R.L., Glennie, C.L., 2014. Now you see it... Now you don't: understanding airborne mapping LiDAR collection and data product generation for archaeological research in Mesoamerica. Remote Sens. 6, 9951–10001.
Fernandez-Diaz, J., Carter, W., Glennie, C., Shrestha, R., Pan, Z., Ekhtari, N., Singhania, A., Hauser, D., Sartori, M., 2016. Capability assessment and performance metrics for the titan multispectral mapping Lidar. Remote Sens. 8, 936.
Fernández-Hernandez, J., González-Aguilera, D., Rodríguez-Gonzálvez, P., Mancera-Taboada, J., 2015. Image-based modelling from Unmanned Aerial Vehicle (UAV) photogrammetry: an effective, low-cost tool for archaeological applications. Archaeometry 57, 128–145.
Fernández-Lozano, J., Gutiérrez-Alonso, G., Fernández-Morán, M.T., 2015. Using airborne LiDAR sensing technology and aerial orthoimages to unravel roman water supply systems and gold works in NW Spain (Eria valley, León). J. Archaeol. Sci. 53, 356–373.
Ferretti, A., Prati, C., Rocca, F., 2001. Permanent scatterers in SAR interferometry. IEEE Trans. Geosci. Remote Sens. 39, 8–20.
Figorito, B., Tarantino, E., 2014. Semi-automatic detection of linear archaeological traces from orthorectified aerial images. Int. J. Appl. Earth Obs. Geoinf. 26, 458–463.
Fisher, C.T., Cohen, A.S., Fernández-Diaz, J.C., Leisz, S.J., 2017. The application of airborne mapping LiDAR for the documentation of ancient cities and regions in tropical regions. Quat. Int. 448, 129–138.
Foglini, F., Prampolini, M., Micallef, A., Angeletti, L., Vandelli, V., Deidun, A., Soldati, M., Taviani, M., 2016. Late quaternary coastal landscape morphology and evolution of the Maltese Islands (Mediterranean Sea) reconstructed from high-resolution seafloor data. Geol. Soc. Spec. Publ. 411, 77–95.
Fornaro, G., Serafino, F., Reale, D., 2010. 4-D SAR imaging: the case study of Rome. IEEE Geosci. Remote Sens. Lett. 7, 236–240.
Fowler, M.J.F., 1996. High-resolution satellite imagery in archaeological application: a Russian satellite photograph of the Stonehenge region. Antiquity 70, 667–671.
Fowler, M.J.F., 2002. Satellite remote sensing and archaeology: a comparative study of satellite imagery of the environs of Figsbury Ring, Wiltshire. Archaeol. Prospect. 9, 55–69.
Fowler, M.J.F., 2004. Archaeology through the keyhole: the serendipity effect of aerial reconnaissance revisited. Interdiscip. Sci. Rev. 29, 118–134.
Fowler, M.J.F., 2011. Modelling the acquisition times of CORONA satellite photographs: accuracy and application. Int. J. Remote Sens. 32, 8865–8879.
Fowler, M.J.F., Fowler, Y.M., 2005. Detection of archaeological crop marks on declassified CORONA KB-4B intelligence satellite photography of Southern England. Archaeol. Prospect. 12, 257–264.
Franceschetti, G., Lanari, R., 2016. Synthetic Aperture Radar Processing. CRC Press, London.
Freeland, T., Heung, B., Burley, D.V., Clark, G., Knudby, A., 2016. Automated feature extraction for prospection and analysis of monumental earthworks from aerial LiDAR in the Kingdom of Tonga. J. Archaeol. Sci. 69, 64–74.
Gabriel, A., Goldstein, R., Zebker, H., 1989. Mapping small elevation changes over large areas - differential radar interferometry. Journal of Geophysical Research Solid Earth 94, 9183–9191.
Gaffney, C., Gater, J., 2003. Revealing the Buried Past: Geophysics for Archaeologists. Tempus Publishing, Stroud.
Galiatsatos, N., Donoghue, D., Philip, G., 2008. High resolution elevation data derived from stereoscopic CORONA imagery with minimal ground control: an approach using IKONOS and SRTM data. Photogramm. Eng. Remote. Sens. 74, 1093–1106.
Gallagher, J.M., Josephs, R.L., 2008. Using LiDAR to detect cultural resources in a forested environment: an example from Isle Royale National Park, Michigan, USA. Archaeol. Prospect. 15, 187–206.
Gallo, D., Ciminale, M., Becker, H., Masini, N., 2009. Remote sensing techniques for reconstructing a vast Neolithic settlement in Southern Italy. J. Archaeol. Sci. 36, 43–50.
Garrison, T.G., Houston, S.D., Golden, C., Inomata, T., Nelson, Z., Munson, J., 2008. Evaluating the use of IKONOS satellite imagery in lowland Maya settlement archaeology. J. Archaeol. Sci. 35, 2770–2777.
Garrison, T.G., Chapman, B., Houston, S., Román, E., Garrido López, J.L., 2011. Discovering ancient Maya settlements using airborne radar elevation data. J. Archaeol. Sci. 38, 1655–1662.
Garrison, T.G., Houston, S., Alcover Firpi, O., 2019. Recentering the rural: Lidar and articulated landscapes among the Maya. J. Anthropol. Archaeol. 53, 133–146.
GEO, Group on Earth Observation, 2017. Earth observations for cultural heritage documentation. http://www.earthobservations.org/activity.php?id=86/, Accessed date: 10 June 2019.
Gheyle, W., Trommelmans, R., Bourgeois, J., Goossens, R., Bourgeois, I., De Wulf, A., Willems, T., 2004. Evaluating CORONA: a case study in the Altai Republic (South Siberia). Antiquity 78, 391–403.
Gheyle, W., Stichelbaut, B., Saey, T., Note, N., Van den Berghe, H., Van Eetvelde, V., Van Meirvenne, M., Bourgeois, J., 2018. Scratching the surface of war. Airborne laser scans of the Great War conflict landscape in Flanders (Belgium). Appl. Geogr. 90, 55–68.
GHF, Global Heritage Fund, 2011. The global heritage network: threat monitoring and collaborative solutions for cultural heritage sites in the developing world. http://www.ghn.globalheritagefund.org/, Accessed date: 10 June 2019.
Ghoneim, E., Benedetti, M., El-Baz, F., 2012. An integrated remote sensing and GIS analysis of the Kufrah Paleoriver, Eastern Sahara. Geomorphology 139-140, 242–257.
Giardino, M.J., 2011. A history of NASA remote sensing contributions to archaeology. J. Archaeol. Sci. 38, 2003–2009.
Giardino, M.J., 2012. NASA remote sensing and archaeology. Remote Sensing and Digital Image Processing 16, 157–176.
Gibbs, M., Colley, S., 2012. Digital preservation, online access and historical archaeology 'grey literature' from New South Wales, Australia. Aust. Archaeol. 75, 95–103.
Goossens, R., De Wulf, A., Bourgeois, J., Gheyle, W., Willems, T., 2006. Satellite imagery and archaeology: the example of CORONA in the Altai Mountains. J. Archaeol. Sci. 33, 745–755.
Gould, R.A., 1987. Archaeological survey by air: a case from the Australian Desert. J. Field Archaeol. 14, 431–443.
Grammer, B., Draganits, E., Gretscher, M., Muss, U., 2017. LiDAR-guided archaeological survey of a Mediterranean landscape: lessons from the Ancient Greek Polis of Kolophon (Ionia, Western Anatolia). Archaeol. Prospect. 24, 311–333.
Gray, A., Farrismanning, P., 2003. Repeat-pass interferometry with airborne synthetic aperture radar. IEEE Trans. Geosci. Remote Sens. 31, 180–191.
Green, S., Bevan, A., Shapland, M., 2014. A comparative assessment of structure from motion methods for archaeological research. J. Archaeol. Sci. 46, 173–181.
Gumerman, G.J., Lyons, T.R., 1971. Archeological methodology and remote sensing. Science 172, 126–132.
Guo, H., 1997. Spaceborne multifrequency, polarametric and interferometric radar for detection of the targets on earth surface and subsurface. J. Remote. Sens. 1, 32–39 (in Chinese).
Guo, H., 2018. Steps to the digital silk road. Nature 554, 25–27.
Guo, H., Liu, H., Wang, X., Shao, Y., Sun, Y., 2000. Subsurface old drainage detection and paleoenvironment analysis using spaceborne radar images in Alxa Plateau. Sci. China Earth Sci. 43, 439–448.
Guo, Q., Li, W., Yu, H., Alvarez, O., 2010. Effects of topographic variability and Lidar sampling density on several DEM interpolation methods. Photogramm. Eng. Remote Sens. 76, 701–712.
Guo, L., Chehata, N., Mallet, C., Boukir, S., 2011. Relevance of airborne lidar and multispectral image data for urban scene classification using Random Forests. ISPRS J. Photogramm. Remote Sens. 66, 56–66.
Guo, H., Liu, Z., Jiang, H., Wang, C., Liu, J., Liang, D., 2017. Big Earth Data: a new challenge and opportunity for digital Earth's development. International Journal of Digital Earth 10, 1–12.
Guo, H., Liu, J., Qiu, Y., Menenti, M., Chen, F., Uhlir, P., Zhang, L., Van Genderen, J., Liang, D., Natarajan, I., Zhu, L., Liu, J.L., 2018. The digital belt and road program in support of regional sustainability. International Journal of Digital Earth 11, 657–669.
Guyot, A., Hubert-Moy, L., Lorho, T., 2018. Detecting Neolithic burial mounds from LiDAR-derived elevation data using a multi-scale approach and machine learning techniques. Remote Sens. 10, 225.
Hadjimitsis, D., Agapiou, A., Alexakis, D., Sarris, A., 2013a. Exploring natural and anthropogenic risk for cultural heritage in Cyprus using remote sensing and GIS. International Journal of Digital Earth 6, 115–142.
Hadjimitsis, D., Agapiou, A., Themistocleous, K., Alexakis, D., Sarris, A., 2013b. Remote sensing for archaeological applications: Management, documentation and monitoring. In: Hadjimitsis, D. (Ed.), Remote Sensing of Environment - Integrated Approaches. IntechOpen, pp. 57–95.
Hanson, W., Oltean, I., 2013. Archaeology from Historical Aerial and Satellite Archives. Springer, New York.
Hanssen, R., 2001. Radar Interferometry. Kluwer Academic Publishers, Dordrecht, The Netherlands.
Hare, T., Masson, M., Russell, B., 2014. High-density LiDAR mapping of the ancient city of Mayapán. Remote Sens. 6, 9064–9085.
Harmon, J.M., Leone, M.P., Prince, S.D., Snyder, M., 2006. LiDAR for archaeological landscape analysis: a case study of two eighteenth-century Maryland plantation sites. Am. Antiq. 71, 649–670.
Harrower, M., Comer, D., 2013. Introduction: the history and future of geospatial and

space technologies in archaeology. In: Comer, D., Harrower, M. (Eds.), Mapping Archaeological Landscapes from Space. Springer, New York, pp. 1–8.
Hesse, R., 2010. LiDAR-derived local relief models-a new tool for archaeological prospection. Archaeol. Prospect. 17, 67–72.
Hillier, J.K., Bunbury, J.M., Graham, A., 2007. Monuments on a migrating Nile. J. Archaeol. Sci. 34, 1011–1015.
HIST, International Centre on Space Technologies for Natural and Cultural Heritage, 2011. Introduction to HIST. http://www.unesco-hist.org/index.php?r=en/article/index&cid=163/, Accessed date: 10 June 2019.
Holcomb, D.W., 1992. Shuttle imaging radar and archaeological survey in China's Taklamakan Desert. J. Field Archaeol. 19, 129–138.
Holcomb, D.W., 1996. Radar archaeology: space age tools aid in uncovering the past. Earth Observation Magazine 5, 22–26.
Holcomb, D.W., 2007. Imaging radar in archaeological investigation: an image processing perspective. In: Wiseman, J., El-Baz, F. (Eds.), Remote Sensing in Archaeology. Springer, New York, pp. 11–45.
Holden, N., 2001. Digital airborne remote sensing: the principles of LIDAR and CASI. AARGNews 22, 23.
Hritz, C., 2013. A malarial-ridden swamp: using Google Earth Pro and Corona to access the southern Balikh valley, Syria. J. Archaeol. Sci. 40, 1975–1987.
Huang, H., Luo, F., Liu, J., Yang, Y., 2015. Dimensionality reduction of hyperspectral images based on sparse discriminant manifold embedding. ISPRS J. Photogramm. Remote Sens. 106, 42–54.
Huang, H., Chen, Y., Clinton, N., Wang, J., Wang, X., Liu, C., Gong, P., Yang, J., Bai, Y., Zheng, Y., Zhu, Z., 2017. Mapping major land cover dynamics in Beijing using all Landsat images in Google Earth Engine. Remote Sens. Environ. 202, 166–176.
Huisman, H., Heeres, G., Van Os, B., Derickx, W., Schoorl, J., 2016. Erosion and errors: testing the use of repeated LIDAR analyses and erosion modelling for the assessment and prediction of erosion of archaeological sites? Conservation and Management of Archaeological Sites 18, 205–216.
ICOMOS, International Council on Monuments and Sites, 2017. ICOMOS action plan: cultural heritage and localizing the UN sustainable development goals (SDGs). https://www.icomos.org/en/focus/un-sustainable-development-goals/8778-cultural-heritage-and-sustainable-development/, Accessed date: 10 June 2019.
Inomata, T., Pinzón, F., Ranchos, J.L., Haraguchi, T., Nasu, H., Fernandez-Diaz, J.C., Aoyama, K., Yonenobu, H., 2017. Archaeological application of airborne LiDAR with object-based vegetation classification and visualization techniques at the lowland Maya site of Ceibal, Guatemala. Remote Sens. 9, 563.
Inomata, T., Triadan, D., Pinzón, F., Burham, M., Ranchos, J.L., Aoyama, K., Haraguchi, T., 2018. Archaeological application of airborne LiDAR to examine social changes in the Ceibal region of the Maya lowlands. PLoS One 13, e0191619.
Intrieri, E., Gigli, G., Nocentini, M., Lombardi, L., Mugnai, F., Fidolini, F., Casagli, N., 2015. Sinkhole monitoring and early warning: an experimental and successful GB-InSAR application. Geomorphology 241, 304–314.
Jahjah, M., Ulivieri, C., 2010. Automatic archaeological feature extraction from satellite VHR images. Acta Astronautica 66, 1302–1310.
Jiang, A., Chen, F., Masini, N., Capozzoli, L., Romano, G., Sileo, M., Yang, R., Tang, P., Chen, P., Lasaponara, R., Liu, G., 2017. Archeological crop marks identified from Cosmo-SkyMed time series: the case of Han-Wei capital city, Luoyang, China. International Journal of Digital Earth 10, 846–860.
Johnson, K.M., Ouimet, W.B., 2014. Rediscovering the lost archaeological landscape of southern New England using airborne light detection and ranging (LiDAR). J. Archaeol. Sci. 43, 9–20.
José Luis, P.-G., Antonio Tomás, M.-C., Vicente, B.-C., Alejandro, J.-S., 2019. Photogrammetric studies of inaccessible sites in archaeology: case study of burial chambers in Qubbet el-Hawa (Aswan, Egypt). J. Archaeol. Sci. 102, 1–10.
Keay, S., Parcak, S., Strutt, K., 2014. High resolution space and ground-based remote sensing and implications for landscape archaeology: the case from Portus, Italy. J. Archaeol. Sci. 52, 277–292.
Kennedy, D., 1998. Declassified satellite photographs and archaeology in the Middle East: case studies from Turkey. Antiquity 72, 553–561.
Kim, K., Jezek, K., Liu, H., 2006. Orthorectified image mosaic of Antarctica from 1963 Argon satellite photography: image processing and glaciological applications. Int. J. Remote Sens. 28, 5357–5373.
Kim, W., Nie, Y., Zhu, J., Deng, B., Yu, L., Liu, F., Gao, H., 2013. Local orientation based detection of circular soil marks of ancient graves by GA. Journal of Remote Sensing 17, 671–678.
Krasinski, K.E., Wygal, B.T., Wells, J., Martin, R.L., Seager-Boss, F., 2016. Detecting late Holocene cultural landscape modifications using LiDAR imagery in the boreal forest, Susitna valley, Southcentral Alaska. J. Field Archaeol. 41, 255–270.
Kraus, K., Pfeifer, N., 1998. Determination of terrain models in wooded areas with airborne laser scanner data. ISPRS J. Photogramm. Remote Sens. 53, 193–203.
Křivánek, R., 2017. Comparison study to the use of geophysical methods at archaeological sites observed by various remote sensing techniques in the Czech Republic. Geosciences (Switzerland) 7, 81.
Kvamme, K.L., Ahler, S.A., 2007. Integrated remote sensing and excavation at Double Ditch State Historic Site, North Dakota. Am. Antiq. 72, 539–561.
Ladefoged, T.N., McCoy, M.D., Asner, G.P., Kirch, P.V., Puleston, C.O., Chadwick, O.A., Vitousek, P.M., 2011. Agricultural potential and actualized development in Hawai'i: an airborne LiDAR survey of the leeward Kohala field system (Hawai'i Island). J. Archaeol. Sci. 38, 3605–3619.
Lambers, K., 2018. Airborne and spaceborne remote sensing and digital image analysis in archaeology. In: Siart, C., Forbriger, M., Bubenzer, O. (Eds.), Digital Geoarchaeology. New Techniques for Interdisciplinary Human-Environmental Research. Springer, Heidelberg, pp. 109–122.
Lasaponara, R., Masini, N., 2007. Detection of archaeological crop marks by using satellite QuickBird multispectral imagery. J. Archaeol. Sci. 34, 214–221.
Lasaponara, R., Masini, N., 2011. Satellite remote sensing in archaeology: past, present and future perspectives. J. Archaeol. Sci. 38, 1995–2002.
Lasaponara, R., Masini, N., 2012a. Image enhancement, feature extraction and geospatial analysis in an archaeological perspective. Remote Sensing and Digital Image Processing 16, 17–47.
Lasaponara, R., Masini, N., 2012b. Pan-sharpening techniques to enhance archaeological marks: an overview. In: Lasaponara, R., Masini, N. (Eds.), Satellite Remote Sensing: A New Tool for Archaeology. Springer, Dordrecht, pp. 87–109.
Lasaponara, R., Masini, N., 2012c. Remote sensing in archaeology: from visual data interpretation to digital data manipulation. In: Lasaponara, R., Masini, N. (Eds.), Satellite Remote Sensing: A New Tool for Archaeology. Springer, Dordrecht, pp. 3–16.
Lasaponara, R., Masini, N., 2013. Satellite synthetic aperture radar in archaeology and cultural landscape: an overview. Archaeol. Prospect. 20, 71–78.
Lasaponara, R., Masini, N., 2014. Beyond modern landscape features: new insights in the archaeological area of Tiwanaku in Bolivia from satellite data. Int. J. Appl. Earth Obs. Geoinf. 26, 464–471.
Lasaponara, R., Masini, N., 2018. Space-based identification of archaeological illegal excavations and a new automatic method for looting feature extraction in desert areas. Surv. Geophys. 39, 1323–1346.
Lasaponara, R., Coluzzi, R., Gizzi, F.T., Masini, N., 2010. On the LiDAR contribution for the archaeological and geomorphological study of a deserted medieval village in Southern Italy. J. Geophys. Eng. 7, 155–163.
Lasaponara, R., Coluzzi, R., Masini, N., 2011. Flights into the past: full-waveform airborne laser scanning data for archaeological investigation. J. Archaeol. Sci. 38, 2061–2070.
Lasaponara, R., Danese, M., Masini, N., 2012. Satellite-based monitoring of archaeological looting in Peru. Remote Sensing and Digital Image Processing 16, 177–193.
Lasaponara, R., Leucci, G., Masini, N., Persico, R., Scardozzi, G., 2016. Towards an operative use of remote sensing for exploring the past using satellite data: the case study of Hierapolis (Turkey). Remote Sens. Environ. 174, 148–164.
Lasaponara, R., Masini, N., Pecci, A., Perciante, F., Pozzi Escot, D., Rizzo, E., Scavone, M., Sileo, M., 2017a. Qualitative evaluation of COSMO SkyMed in the detection of earthen archaeological remains: the case of Pachamacac (Peru). J. Cult. Herit. 23, 55–62.
Lasaponara, R., Murgante, B., Elfadaly, A., Qelichi, M.M., Shahraki, S.Z., Wafa, O., Attia, W., 2017b. Spatial open data for monitoring risks and preserving archaeological areas and landscape: case studies at Kom el Shoqafa, Egypt and Shush, Iran. Sustainability (Switzerland) 9, 572.
Lasaponara, R., Yang, R., Chen, F., Li, X., Masini, N., 2018. Corona satellite pictures for archaeological studies: a review and application to the lost Forbidden City of the Han–Wei Dynasties. Surv. Geophys. 39, 1303–1322.
Le Tourneau, F.M., 1998. Ancient irrigation network and remote sensing in the Samarkand area. Bulletin d'Association de Geographes Francais 1998, 224–234.
Le, T.S., Chang, C.P., Nguyen, X.T., Yhokha, A., 2016. TerraSAR-X data for high-precision land subsidence monitoring: a case study in the historical centre of Hanoi, Vietnam. Remote Sens. 8, 338.
Lee, J., Woodyatt, A., Berman, M., 1990. Enhancement of high spectral resolution remote-sensing data by a noise-adjusted principal components transform. IEEE Trans. Geosci. Remote Sens. 28, 295–304.
Lefebvre, A., 2017. Beijing between heritage and modernity: a change of the urban morphology observed by satellite for 50 years. CyberGeo 2017, 129–166.
Lefsky, M., Cohen, W., Parker, G., Harding, D., 2002. Lidar remote sensing for ecosystem studies. BioScience 52, 19–30.
Leisz, S., 2013. An overview of the application of remote sensing to archaeology during the twentieth century. In: Comer, D., Harrower, M. (Eds.), Mapping Archaeological Landscape from Space. Springer, New York, NY, pp. 11–19.
Lin, A.Y.M., Novo, A., Har-Noy, S., Ricklin, N.D., Stamatiou, K., 2011. Combining GeoEye-1 satellite remote sensing, UAV aerial imaging, and geophysical surveys in anomaly detection applied to archaeology. IEEE Journal of Selected Topics in Applied Earth Observations and Remote Sensing 4, 870–876.
Lin, H., Ma, P., Wang, X., 2017. Urban infrastructure health monitoring with spaceborne multi-temporal synthetic aperture radar interferometry. Acta Geodaeticaet Cartographica Sinica 46, 1421–1433.
Linck, R., Busche, T., Buckreuss, S., Fassbinder, J.W.E., Seren, S., 2013. Possibilities of archaeological prospection by high-resolution x-band satellite radar - a case study from Syria. Archaeol. Prospect. 20, 97–108.
Liritzis, Y., Miserlis, P., Rigopoulos, R., 1983. Aerial photography of some Greek coastal regions and its archaeological implications. Int. J. Naut. Archaeol. 12, 191–202.
Liss, B., Howland, M., Levy, T., 2017. Testing Google Earth Engine for the automatic identification and vectorization of archaeological features: a case study from Faynan, Jordan. J. Archaeol. Sci. Rep. 5, 299–304.
Liu, Y., Ma, P., Lin, H., Wang, W., Shi, G., 2019. Distributed scatterer InSAR reveals surface motion of the ancient Chaoshan residence cluster in the Lianjiang Plain, China. Remote Sens. 11, 166.
Löhrer, R., Bertrams, M., Eckmeier, E., Protze, J., Lehmkuhl, F., 2013. Mapping the distribution of weathered Pleistocene Wadi deposits in Southern Jordan using ASTER, SPOT-5 data and laboratory spectroscopic analysis. Catena 107, 57–70.
Lu, P., Yang, R., Chen, P., Guo, Y., Chen, F., Masini, N., Lasaponara, R., 2017. On the use of historical archive of aerial photographs for the discovery and interpretation of ancient hidden linear cultural relics in the alluvial plain of eastern Henan, China. J. Cult. Herit. 23, 20–27.
Lunden, B., 1985. Aerial thermography - a remote sensing technique applied to detection of buried archaeological remains at a site in Dalecarlia, Sweden. Geografiska Annaler, Series A 67, 161–166.
Luo, L., Wang, X., Guo, H., Liu, C., Liu, J., Li, L., Du, X., Qian, G., 2014a. Automated

extraction of the archaeological tops of Qanat shafts from VHR imagery in Google Earth. Remote Sens. 6, 11956–11976.
Luo, L., Wang, X., Liu, C., Guo, H., Du, X., 2014b. Integrated RS, GIS and GPS approaches to archaeological prospecting in the Hexi Corridor, NW China: a case study of the royal road to ancient Dunhuang. J. Archaeol. Sci. 50, 178–190.
Luo, L., Wang, X., Liu, J., Guo, H., Lasaponara, R., Ji, W., Liu, C., 2017a. Uncovering the ancient canal-based tuntian agricultural landscape at China's northwestern frontiers. J. Cult. Herit. 23, 79–88.
Luo, L., Wang, X., Liu, J., Guo, H., Zong, X., Ji, W., Cao, H., 2017b. VHR GeoEye-1 imagery reveals an ancient water landscape at the Longcheng site, northern Chaohu Lake Basin (China). International Journal of Digital Earth 10, 139–154.
Luo, L., Wang, X., Guo, H., Lasaponara, R., Shi, P., Bachagha, N., Li, L., Yao, Y., Masini, N., Chen, F., Ji, W., Cao, H., Li, C., Hu, N., 2018a. Google Earth as a powerful tool for archaeological and cultural heritage applications: a review. Remote Sens. 10, 1558.
Luo, L., Wang, X., Lasaponara, R., Xiang, B., Zhen, J., Zhu, L., Yang, R., Liu, D., Liu, C., 2018b. Auto-extraction of linear archaeological traces of Tuntian Irrigation Canals in Miran Site (China) from Gaofen-1 satellite imagery. Remote Sens. 10, 718.
Masini, N., Lasaponara, R., 2007. Investigating the spectral capability of QuickBird data to detect archaeological remains buried under vegetated and not vegetated areas. J. Cult. Herit. 8, 53–60.
Masini, N., Lasaponara, R., 2013. Airborne lidar in archaeology: overview and a case study. Lecture Notes in Computer Science LNCS 7972 (PART 2), 663–676.
Masini, N., Lasaponara, R., 2017. Sensing the past from space: approaches to site detection. In: Masini, N., Soldovieri, F. (Eds.), Sensing the Past. From Artifact to Historical Site. Springer International Publishing, pp. 23–60.
Masini, N., Gizzi, F., Biscione, M., Fundone, V., Sedile, M., Sileo, M., Pecci, A., Lacovara, B., Lasaponara, R., 2018. Medieval archaeology under the canopy with LiDAR. The (re)discovery of a medieval fortified settlement in Southern Italy. Remote Sens. 10, 1598.
McCauley, J., Schaber, G., Breed, C., Grolier, M., Haynes, C., Issawi, B., Elachi, C., Blom, R., 1982. Subsurface valleys and geoarchaeology of the eastern Sahara revealed by shuttle radar. Science 218, 1004–1020.
McCoy, M.D., 2017. Geospatial big data and archaeology: prospects and problems too great to ignore. J. Archaeol. Sci. 84, 74–94.
McCoy, M.D., Ladefoged, T.N., 2009. New developments in the use of spatial technology in archaeology. J. Archaeol. Res. 17, 263–295.
McCoy, M.D., Asner, G.P., Graves, M.W., 2011. Airborne LiDAR survey of irrigated agricultural landscapes: an application of the slope contrast method. J. Archaeol. Sci. 38, 2141–2154.
McLeester, M., Casana, J., Schurr, M.R., Hill, A.C., Wheeler III, J.H., 2018. Detecting prehistoric landscape features using thermal, multispectral, and historical imagery analysis at Midewin National Tallgrass Prairie, Illinois. J. Archaeol. Sci. Rep. 21, 450–459.
Meng, X., Currit, N., Zhao, K., 2010. Ground filtering algorithms for airborne LiDAR data: a review of critical issues. Remote Sens. 2, 833–860.
Menna, F., Agrafiotis, P., Georgopoulos, A., 2018. State of the art and applications in archaeological underwater 3D recording and mapping. J. Cult. Herit. 33, 231–248.
Menze, B.H., Ur, J.A., 2012. Mapping patterns of long-term settlement in Northern Mesopotamia at a large scale. Proc. Natl. Acad. Sci. U. S. A. 109, E778–E787.
Menze, B.H., Ur, J.A., 2014. Multitemporal fusion for the detection of static spatial patterns in multispectral satellite images - with application to archaeological survey. IEEE Journal of Selected Topics in Applied Earth Observations and Remote Sensing 7, 3513–3524.
Menze, B.H., Ur, J.A., Sherratt, A.G., 2006. Detection of ancient settlement mounds: archaeological survey based on the SRTM terrain model. Photogramm. Eng. Remote. Sens. 72, 321–327.
Mondino, E.B., Perotti, L., Piras, M., 2012. High resolution satellite images for archeological applications: the Karima case study (Nubia region, Sudan). European Journal of Remote Sensing 45, 243–259.
Moore, E., Freeman, A., 1996. The application of microwave scattering mechanism to the study of early Ankorean water management. In: Paper Read at 6th International Conference on European Association of Southeast Asian Archaeologists, Leiden, pp. 1–13.
Moore, E., Freeman, A., Hensley, S., 2007. Spaceborne and airborne radar at Angkor: introducing new technology to the ancient site. In: Wiseman, J., El-Baz, F. (Eds.), Remote Sensing in Archaeology. Springer, New York, pp. 185–216.
Mozas-Calvache, A.T., Pérez-García, J.L., Cardenal-Escarcena, F.J., Mata-Castro, E., Delgado-García, J., 2012. Method for photogrammetric surveying of archaeological sites with light aerial platforms. J. Archaeol. Sci. 39, 521–530.
Nie, Y., Yang, L., 2009. Applications and development of archaeological remote sensing technology in China. Journal of Remote Sensing 13, 940–962.
Nikolakopoulos, K.G., Soura, K., Koukouvelas, I.K., Argyropoulos, N.G., 2017. UAV vs classical aerial photogrammetry for archaeological studies. J. Archaeol. Sci. Rep. 14, 758–773.
Nita, M.D., Munteanu, C., Gutman, G., Abrudan, I.V., Radeloff, V.C., 2018. Widespread forest cutting in the aftermath of World War II captured by broad-scale historical Corona spy satellite photography. Remote Sens. Environ. 204, 322–332.
Noviello, M., Ciminale, M., De Pasquale, V., 2013. Combined application of pan-sharpening and enhancement methods to improve archaeological cropmark visibility and identification in QuickBird imagery: two case studies from Apulia, Southern Italy. J. Archaeol. Sci. 40, 3604–3613.
Ødegård, Ø., Hansen, R.E., Singh, H., Maarleveld, T.J., 2018. Archaeological use of synthetic aperture sonar on Deepwater wreck sites in Skagerrak. J. Archaeol. Sci. 89, 1–13.
Opitz, R., Herrmann, J., 2018. Recent trends and long-standing problems in archaeological remote sensing. Journal of Computer Applications in Archaeology 1, 19–41.
Opitz, R.S., Ryzewski, K., Cherry, J.F., Moloney, B., 2015. Using airborne LiDAR survey to explore historic-era archaeological landscapes of Montserrat in the Eastern Caribbean. J. Field Archaeol. 40, 523–541.
Orazio, T., Da Pelo, P., Marani, R., Guaragnella, C., 2015. Automated extraction of archaeological traces by a modified variance analysis. Remote Sens. 7, 3565.
O'Reilly, D., Evans, D., Shewan, L., 2017. Airborne LiDAR prospection at Lovea, an Iron Age moated settlement in central Cambodia. Antiquity 91, 947–965.
Orengo, H.A., Krahtopoulou, A., Garcia-Molsosa, A., Palaiochoritis, K., Stamati, A., 2015. Photogrammetric re-discovery of the hidden long-term landscapes of western Thessaly, central Greece. J. Archaeol. Sci. 64, 100–109.
Osmanoğlu, B., Dixon, T.H., Wdowinski, S., Cabral-Cano, E., Jiang, Y., 2011. Mexico City subsidence observed with persistent scatterer InSAR. Int. J. Appl. Earth Obs. Geoinf. 13, 1–12.
Papworth, H., Ford, A., Welham, K., Thackray, D., 2016. Assessing 3D metric data of digital surface models for extracting archaeological data from archive stereo-aerial photographs. J. Archaeol. Sci. 72, 85–104.
Parcak, S., 2007. Satellite remote sensing methods for monitoring archaeological tells in the Middle East. J. Field Archaeol. 32, 65–81.
Parcak, S., 2009. Satellite Remote Sensing for Archaeology. Routledge, Landon, pp. 1–286.
Parcak, S., Tuttle, C.A., 2016. Hiding in plain sight: the discovery of a new monumental structure at Petra, Jordan, using WorldView-1 and WorldView-2 satellite imagery. Bull. Am. Sch. Orient. Res. 375, 35–51.
Parcak, S., Gathings, D., Childs, C., Mumford, G., Cline, E., 2016. Satellite evidence of archaeological site looting in Egypt: 2002–2013. Antiquity 90, 188–205.
Parcharidis, Is, Lagios, E., Sakkas, V., Raucoules, D., Feurer, D., Le Mouelic, S., King, C., Carnec, C., Novali, F., Ferretti, A., Capes, R., Cooksley, G., 2006. Subsidence monitoring within the Athens Basin (Greece) using space radar interferometric techniques. Earth, Planets and Space 58, 505–513.
Parry, J.T., 1992. The investigative role of Landsat-TM in the examination of pre- and proto-historic water management sites in northeast Thailand. Geocarto International 7, 5–24.
Pascucci, C., Cavalli, R., Palombo, A., Pignatti, S., 2010. Suitability of CASI and ATM airborne remote sensing data for archaeological subsurface structure detection under different land cover: the Arpi case study (Italy). J. Geophys. Eng. 7, 183–189.
Patruno, J., Dore, N., Crespi, M., Pottier, E., 2013. Polarimetric multifrequency and multi-incidence SAR sensors analysis for archaeological purposes. Archaeol. Prospect. 20, 89–96.
Peak, K.D., 1978. In perspective: a photogrammetrist's view of the use of oblique photography. Aerial Archaeology 2, 24–27.
Perna, S., Wimmer, C., Moreira, J., Fornaro, G., 2008. X-band airborne differential interferometry: results of the OrbiSAR campaign over the Perugia area. IEEE Trans. Geosci. Remote Sens. 46, 489–503.
Philip, G., Donoghue, D., Beck, A., Galiatsatos, N., 2002. CORONA satellite photography: an archaeological application from the Middle East. Antiquity 76, 109–118.
Piga, C., Piroddi, L., Pompianu, E., Ranieri, G., Stocco, S., Trogu, A., 2014. Integrated geophysical and aerial sensing methods for archaeology: a case history in the Punic site of villamar (Sardinia, Italy). Remote Sens. 6, 10986–11012.
Plaza, A., Martinez, P., Plaza, J., Perez, R., 2005. Unsupervised feature selection using feature similarity. IEEE Trans. Geosci. Remote Sens. 43, 466–479.
Poirier, N., Hautefeuille, F., Calastrenc, C., 2013. Low altitude thermal survey by means of an automated unmanned aerial vehicle for the detection of archaeological buried structures. Archaeol. Prospect. 20, 303–307.
Pringle, H., 2010. Google Earth shows clandestine worlds. Science 329, 1008–1009.
Quintus, S., Clark, J.T., Day, S.S., Schwert, D.P., 2015. Investigating regional patterning in archaeological remains by pairing extensive survey with a lidar dataset: the case of the Manu'a group, American Samoa. J. Archaeol. Sci. Rep. 2, 677–687.
Rajani, M.B., Rajawat, A.S., 2011. Potential of satellite based sensors for studying distribution of archaeological sites along palaeo channels: Harappan sites a case study. J. Archaeol. Sci. 38, 2010–2016.
Rayne, L., Donoghue, D., 2018. A remote sensing approach for mapping the development of ancient water management in the Near East. Remote Sens. 10, 2042.
Reigber, A., Scheiber, R., 2003. Airborne differential SAR interferometry: first results at L-band. IEEE Trans. Geosci. Remote Sens. 41, 1516–1520.
Reimann, L., Vafeidis, A.T., Brown, S., Hinkel, J., Tol, R.S.J., 2018. Mediterranean UNESCO world heritage at risk from coastal flooding and erosion due to sea-level rise. Nat. Commun. 9, 4161.
Remondino, F., Barazzetti, L., Nex, F., Scaioni, M., Sarazzi, D., 2011. UAV photogrammetry for mapping and 3D modelling–current status and future perspectives. International archives of the photogrammetry. Remote Sensing and Spatial Information Sciences XXXVIII-1 (C22), 25–31.
Richards, J.D., 1997. Preservation and re-use of digital data: the role of the archaeology data service. Antiquity 71, 1057–1059.
Rigaud, P., Herse, M., 1986. Remote sensing by infrared photographs from a tethered balloon. Comptes Rendus - Academie des Sciences, Serie II 303, 1703–1708.
Risbøl, O., Gustavsen, L., 2018. LiDAR from drones employed for mapping archaeology - potential, benefits and challenges. Archaeol. Prospect. 25, 329–338.
Risbøl, O., Briese, C., Doneus, M., Nesbakken, A., 2015. Monitoring cultural heritage by comparing DEMs derived from historical aerial photographs and airborne laser scanning. J. Cult. Herit. 16, 202–209.
Rochelo, M.J., Davenport, C., Selch, D., 2015. Revealing pre-historic Native American Belle Glade earthworks in the Northern Everglades utilizing airborne LiDAR. J. Archaeol. Sci. Rep. 2, 624–643.
Rosenswig, R.M., López-Torrijos, R., Antonelli, C.E., Mendelsohn, R.R., 2013. Lidar mapping and surface survey of the Izapa state on the tropical piedmont of Chiapas, Mexico. J. Archaeol. Sci. 40, 1493–1507.

Rosenswig, R.M., López-Torrijos, R., Antonelli, C.E., 2015. Lidar data and the Izapa polity: new results and methodological issues from tropical Mesoamerica. Archaeol. Anthropol. Sci. 7, 487–504.
Rowlands, A., Sarris, A., 2007. Detection of exposed and subsurface archaeological remains using multi-sensor remote sensing. J. Archaeol. Sci. 34, 795–803.
Rutishauser, S., Erasmi, S., Rosenbauer, R., Buchbach, R., 2017. SARchaeology—detecting palaeochannels based on high resolution radar data and their impact of changes in the settlement pattern in Cilicia (Turkey). Geosciences (Switzerland) 7, 109.
Sadr, K., 2016. A comparison of accuracy and precision in remote sensing stone-walled structures with Google Earth, high resolution aerial photography and LiDAR; a case study from the south African Iron Age. Archaeol. Prospect. 23, 95–104.
Sarris, A., Papadopoulos, N., Agapiou, A., Salvi, M., Hadjimitsis, D., Parkinson, W., Yerkes, R., Gyucha, A., Duffy, P., 2013. Integration of geophysical surveys, ground hyperspectral measurements, aerial and satellite imagery for archaeological prospection of prehistoric sites: the case study of Vésztő-Mágor Tell, Hungary. J. Archaeol. Sci. 40, 1454–1470.
Savage, S.H., Levy, T.E., Jones, I.W., 2012. Prospects and problems in the use of hyperspectral imagery for archaeological remote sensing: a case study from the Faynan copper mining district, Jordan. J. Archaeol. Sci. 39, 407–420.
Schaepman, M.E., Ustin, S.L., Plaza, A.J., Painter, T.H., Verrelst, J., Liang, S., 2009. Earth system science related imaging spectroscopy—an assessment. Remote Sens. Environ. 113, S123–S137.
Scollar, I., Tabbagh, A., Hesse, A., Herzog, I., 1990. Archaeological Prospecting and Remote Sensing. Cambridge University Press, Cambridge.
Scudder, S.J., Foss, J.E., Collins, M.E., 1996. Soil science and archaeology. Adv. Agron. 57, 1–36.
Šedina, J., Housarová, E., Raeva, P., 2019. Using RPAS for the detection of archaeological objects using multispectral and thermal imaging. European Journal of Remote Sensing 52 (Suppl. 1), 182–191.
Sevara, C., Verhoeven, G., Doneus, M., Draganits, E., 2018. Surfaces from the visual past: recovering high-resolution terrain data from historic aerial imagery for multi-temporal landscape analysis. J. Archaeol. Method Theory 25, 611–642.
Shih, P.T.Y., Chen, Y.H., Chen, J.C., 2014. Historic shipwreck study in Dongsha Atoll with bathymetric LiDAR. Archaeol. Prospect. 21, 139–146.
Siart, C., Eitel, B., Panagiotopoulos, D., 2008. Investigation of past archaeological landscapes using remote sensing and GIS: a multi-method case study from Mount Ida, Crete. J. Archaeol. Sci. 35, 2918–2926.
Singh, K.K., Vogler, J.B., Shoemaker, D.A., Meentemeyer, R.K., 2012. LiDAR-Landsat data fusion for large-area assessment of urban land cover: balancing spatial resolution, data volume and mapping accuracy. ISPRS J. Photogramm. Remote Sens. 74, 110–121.
Sithole, G., Vosselman, G., 2004. Experimental comparison of filter algorithms for bare-earth extraction from airborne laser scanning point clouds. ISPRS J. Photogramm. Remote Sens. 59, 85–101.
Sivitskis, A.J., Harrower, M.J., David-Cuny, H., Dumitru, I.A., Nathan, S., Wiig, F., Viete, D.R., Lewis, K.W., Taylor, A.K., Dollarhide, E.N., Zaitchik, B., Al-Jabri, S., Livi, K.J.T., Braun, A., 2018. Hyperspectral satellite imagery detection of ancient raw material sources: soft-stone vessel production at Aqir al-Shamoos (Oman). Archaeol. Prospect. 25, 363–374.
Smith, M.J., 1989. A photogrammetric system for archaeological mapping using oblique non-metric photography. Photogramm. Rec. 13, 95–105.
Sonnemann, T.F., Comer, D.C., Patsolic, J.L., Megarry, W.P., Malatesta, E.H., Hofman, C.L., 2017. Semi-automatic detection of indigenous settlement features on Hispaniola through remote sensing data. Geosciences (Switzerland) 7, 127.
Sowter, A., Bin Che Amat, M., Cigna, F., Marsh, S., Athab, A., Alshammari, L., 2016. Mexico City land subsidence in 2014–2015 with Sentinel-1 IW TOPS: results using the intermittent SBAS (ISBAS) technique. Int. J. Appl. Earth Obs. Geoinf. 52, 230–242.
St Joseph, J., 1945. Air photography and archaeology. Geogr. J. 105, 47–59.
St Joseph, J., 1961. Aerial Reconnaissance in Wales. Antiquity 35, 263–275.
Stewart, C., 2017. Detection of archaeological residues in vegetated areas using satellite synthetic aperture radar. Remote Sens. 9, 118.
Stewart, C., Lasaponara, R., Schiavon, G., 2013. ALOS PALSAR analysis of the archaeological site of Pelusium. Archaeol. Prospect. 20, 109–116.
Stewart, C., Lasaponara, R., Schiavon, G., 2014. Multi-frequency, polarimetric SAR analysis for archaeological prospection. Int. J. Appl. Earth Obs. Geoinf. 28, 211–219.
Stewart, C., Oren, E.D., Cohen-Sasson, E., 2018. Satellite remote sensing analysis of the Qasrawet archaeological site in North Sinai. Remote Sens. 10, 1090.
Stichelbaut, B., 2005. The application of Great War aerial photography in battlefield archaeology: the example of Flanders. J. Confl. Archaeol. 1, 235–243.
Stichelbaut, B., 2006. The application of first world war aerial photography to archaeology. Antiquity 80, 161–172.
Stichelbaut, B., 2011. The first thirty kilometres of the western front 1914–1918: an aerial archaeological approach with historical remote sensing data. Archaeol. Prospect. 18, 57–66.
Stone, E.C., 2008. Patterns of looting in southern Iraq. Antiquity 82, 125–138.
Stott, D., Kristiansena, S., Lichtenberger, A., Rajac, R., 2018. Mapping an ancient city with a century of remotely sensed data. Proc. Natl. Acad. Sci. U. S. A. 115, E5450–E5458.
Štular, B., Kokalj, T., Oštir, K., Nuninger, L., 2012. Visualization of lidar-derived relief models for detection of archaeological features. J. Archaeol. Sci. 39, 3354–3360.
Szeliski, R., 2010. Structure from motion. In: Szeliski, R. (Ed.), Computer Vision. Texts in Computer Science. Springer, London.
Tan, K., Wan, Y., Yang, Y., Duan, Q., 2005. Study of hyperspectral remote sensing for archaeology. Journal of Infrared and Millimeter Waves 24, 437–440.
Tang, P., Chen, F., Zhu, X., Zhou, W., 2016. Monitoring cultural heritage sites with advanced multi-temporal InSAR technique: the case study of the summer palace. Remote Sens. 8, 432.
Tapete, D., 2018. Remote sensing and geosciences for archaeology. Geosciences (Switzerland) 8, 41.
Tapete, D., Cigna, F., 2017a. InSAR data for geohazard assessment in UNESCO world heritage sites: state-of-the-art and perspectives in the Copernicus era. Int. J. Appl. Earth Obs. Geoinf. 63, 24–32.
Tapete, D., Cigna, F., 2017b. Trends and perspectives of space-borne SAR remote sensing for archaeological landscape and cultural heritage applications. J. Archaeol. Sci. Rep. 14, 716–726.
Tapete, D., Cigna, F., 2018. Appraisal of opportunities and perspectives for the systematic condition assessment of heritage sites with Copernicus Sentinel-2 high-resolution multispectral imagery. Remote Sens. 10, 561.
Tapete, D., Fanti, R., Cecchi, R., Petrangeli, P., Casagli, N., 2012. Satellite radar interferometry for monitoring and early-stage warning of structural instability in archaeological sites. J. Geophys. Eng. 9, S10–S25.
Tapete, D., Cigna, F., Masini, N., Lasaponara, R., 2013. Prospection and monitoring of the archaeological heritage of Nasca, Peru, with ENVISAT ASAR. Archaeol. Prospect. 20, 133–147.
Tapete, D., Cigna, F., Donoghue, D.N.M., 2016. 'Looting marks' in space-borne SAR imagery: measuring rates of archaeological looting in Apamea (Syria) with TerraSAR-X staring spotlight. Remote Sens. Environ. 178, 42–58.
Tapete, D., Banks, V., Jones, L., Kirkham, M., Garton, D., 2017. Contextualising archaeological models with geological, airborne and terrestrial LiDAR data: the Ice Age landscape in Farndon Fields, Nottinghamshire, UK. J. Archaeol. Sci. 81, 31–48.
Thomas, H., 1945. Recent developments in air photography. Nature 156, 409–411.
Thomas, H., 2018. Some like it hot: the impact of next generation FLIR systems thermal cameras on archaeological thermography. Archaeol. Prospect. 25, 81–87.
Torres-Martínez, J., Seddaiu, M., Rodríguez-Gonzálvez, P., Hernández-López, D., González-Aguilera, D., 2016. A multi-data source and multi-sensor approach for the 3D reconstruction and web visualization of a complex archaeological site: the case study of "Tolmo De Minateda". Remote Sens. 8, 550.
Tosi, L., Lio, C., Teatini, P., Strozzi, T., 2018. Land subsidence in coastal environments: knowledge advance in the Venice Coastland by TerraSAR-X PSI. Remote Sens. 10, 1191.
Traviglia, A., Cottica, D., 2011. Remote sensing applications and archaeological research in the Northern Lagoon of Venice: the case of the lost settlement of Constanciacus. J. Archaeol. Sci. 38, 2040–2050.
Trier, Ø.D., Piløø, L.H., 2012. Automatic detection of pit structures in airborne laser scanning data: automatic detection of pits in ALS data. Archaeol. Prospect. 19, 103–121.
Trier, Ø.D., Cowley, D.C., Waldeland, A.U., 2018. Using deep neural networks on airborne laser scanning data: results from a case study of semi-automatic mapping of archaeological topography on Arran, Scotland. Archaeol. Prospect. 1–11. https://doi.org/10.1002/arp.1731. (early view, online).
Ullman, S., 1979. The interpretation of structure from motion. Proc. R. Soc. Lond. B203, 405–426.
UN, United Nations, 2015. Transforming our World: The 2030 Agenda for Sustainable Development. A/RES/70/1. Division for Sustainable Development Goals, New York, NY, USA.
Ur, J., 2003. CORONA satellite photography and ancient road networks: a northern Mesopotamian case study. Antiquity 77, 102–115.
Vaz, A.S., Gonçalves, J.F., Pereira, P., Santarém, F., Vicente, J.R., Honrado, J.P., 2019. Earth observation and social media: evaluating the spatiotemporal contribution of non-native trees to cultural ecosystem services. Remote Sens. Environ. 230, 111193.
Veraverbeke, S., Dennison, P., Gitas, I., Hulley, G., Kalashnikova, O., Katagis, T., Kuai, L., Meng, R., Roberts, D., Stavros, N., 2018. Hyperspectral remote sensing of fire: state-of-the-art and future perspectives. Remote Sens. Environ. 216, 105–121.
Verhoeven, G., 2008. Imaging the invisible using modified digital still cameras for straightforward and low-cost archaeological near-infrared photography. J. Archaeol. Sci. 35, 3087–3100.
Verhoeven, G., 2012. Near-infrared aerial crop mark archaeology: from its historical use to current digital implementations. J. Archaeol. Method Theory 19, 132–160.
Verhoeven, G., 2017. Are we there yet? A review and assessment of archaeological passive airborne optical imaging approaches in the light of landscape archaeology. Geosciences (Switzerland) 7, 86.
Verhoeven, G., 2018. Satellite hyperspectral and multispectral imaging. In: Varela, S.L.L. (Ed.), The Encyclopedia of Archaeological Sciences. JohnWiley & Sons, Inc, NewYork.
Verhoeven, G., Schmitt, K., 2010. An attempt to push back frontiers – digital near-ultraviolet aerial archaeology. J. Archaeol. Sci. 37, 833–845.
Verhoeven, G., Sevara, C., 2016. Trying to break new ground in aerial archaeology. Remote Sens. 8, 918.
Verhoeven, G., Vermeulen, F., 2016. Engaging with the canopy-multi-dimensional vegetation mark visualisation using archived aerial images. Remote Sens. 8, 752.
Verhoeven, G., Doneus, M., Briese, C., Vermeulen, F., 2012. Mapping by matching: a computer vision-based approach to fast and accurate georeferencing of archaeological aerial photographs. J. Archaeol. Sci. 39, 2060–2070.
Vierling, K.T., Vierling, L.A., Gould, W.A., Martinuzzi, S., Clawges, R.M., 2008. Lidar: shedding new light on habitat characterization and modeling. Front. Ecol. Environ. 6, 90–98.
Vlachidis, A., Binding, C., Tudhope, D., May, K., 2010. Excavating grey literature: a case study on the rich indexing of archaeological documents via natural language-processing techniques and knowledge-based resources. ASLIB Proc. 62, 466–475.
Von Schwerin, J., Richards-Rissetto, H., Remondino, F., Agugiaro, G., Girardi, G., 2013. The mayaarch3d project: a 3D webgis for analyzing ancient architecture and landscapes. Literary and Linguistic Computing 28, 736–753.

Von Schwerin, J., Richards-Rissetto, H., Remondino, F., 2016a. Lidar survey over ancient Maya City. GIM Int. 30, 16–19.
Von Schwerin, J., Richards-Rissetto, H., Remondino, F., Spera, M.G., Auer, M., Billen, N., Loos, L., Stelson, L., Reindel, M., 2016b. Airborne LiDAR acquisition, post-processing and accuracy-checking for a 3D WebGIS of Copan, Honduras. J. Archaeol. Sci. Rep. 5, 85–104.
Waagen, J., 2019. New technology and archaeological practice. Improving the primary archaeological recording process in excavation by means of UAS photogrammetry. J. Archaeol. Sci. 101, 11–20.
Wagner, W., 2010. Radiometric calibration of small-footprint full-waveform airborne laser scanner measurements: basic physical concepts. ISPRS J. Photogramm. Remote Sens. 65, 505–513.
Wang, J., Chang, C., 2006. Independent component analysis-based dimensionality reduction with applications in hyperspectral image analysis. IEEE Trans. Geosci. Remote Sens. 44, 1586–1600.
Wang, X., Guo, H., 2015. Space archaeology: disciplinary attribute, research object, method and tasks. Bull. Chin. Acad. Sci. 30, 360–367 (in Chinese).
Wang, C.K., Philpot, W.D., 2007. Using airborne bathymetric lidar to detect bottom type variation in shallow waters. Remote Sens. Environ. 106, 123–135.
Wang, X., Guo, H., Chang, Y., Zha, L., 2004. On paleodrainage evolution in mid-late Epipleistocene based on radar remote sensing in northeastern Ejin Banner, Inner Mongolia. J. Geogr. Sci. 14, 235–241.
Wang, Y., Li, G., Ding, J., Guo, Z., Tang, S., Wang, C., Huang, Q., Liu, R., Chen, J.M., 2016. A combined GLAS and MODIS estimation of the global distribution of mean forest canopy height. Remote Sens. Environ. 174, 24–43.
Wang, S., Hu, Q., Wang, F., Ai, M., Zhong, R., 2017a. A microtopographic feature analysis-based LiDAR data processing approach for the identification of Chu tombs. Remote Sens. 9, 880.
Wang, X., Lasaponara, R., Tariq, S., Khatteli, H., Luo, L., Liu, J., Masini, N., Ishwaran, N., Chen, F., 2017b. Conservation and utilization of cultural heritage along the belt and road: challenges and solutions. Bull. Chin. Acad. Sci. 32, 42–51.
Watanabe, N., Nakamura, S., Liu, B., Wang, N., 2017. Utilization of structure from motion for processing CORONA satellite images: application to mapping and interpretation of archaeological features in Liangzhu Culture, China. Archaeological Research in Asia 11, 38–50.
Wei, G., Shalei, S., Bo, Z., Shuo, S., Faquan, L., Xuewu, C., 2012. Multi-wavelength canopy LiDAR for remote sensing of vegetation: design and system performance. ISPRS J. Photogramm. Remote Sens. 69, 1–9.
Weishampel, J.F., Hightower, J.N., Chase, A.F., Chase, D.Z., Patrick, R.A., 2011. Detection and morphologic analysis of potential below-canopy cave openings in the karst landscape around the Maya polity of Caracol using airborne LiDAR. Journal of Cave and Karst Studies 73, 187–196.
Weishampel, J.F., Hightower, J.N., Chase, A.F., Chase, D.Z., 2012. Use of airborne LiDAR to delineate canopy degradation and encroachment along the Guatemala-Belize border. Tropical Conservation Science 5, 12–24.
White, D., 2013. LIDAR, point clouds, and their archaeological applications. In: Comer, D., Harrower, M. (Eds.), Mapping Archaeological Landscapes from Space. Springer, New York, pp. 175–186.
Wilkinson, K.N., Beck, A.R., Philip, G., 2006. Satellite imagery as a resource in the prospection for archaeological sites in central Syria. Geoarchaeology 21, 735–750.
Winterbottom, S.J., Dawson, T., 2005. Airborne multi-spectral prospection for buried archaeology in mobile sand dominated systems. Archaeol. Prospect. 12, 205–219.
Wiseman, J., El-Baz, F., 2007. Remote Sensing in Archaeology. Springer, New York.
Witcher, R., 1999. GIS and landscapes of perception. In: Gillings, M., Mattingly, D., Van Dalen, J. (Eds.), Geographical Information Systems and Landscape Archaeology. Oxbow Books, Oxford, UK, pp. 13–22.
Witharana, C., Ouimet, W.B., Johnson, K.M., 2018. Using LiDAR and GEOBIA for automated extraction of eighteenth–late nineteenth century relict charcoal hearths in southern New England. GIScience and Remote Sensing 55, 183–204.
Woodhouse, I., Nichol, C., Sinclair, P., Jack, J., Morsdorf, F., Malthus, T., Patenaude, G., 2011. A multispectral canopy LiDAR demonstrator project. IEEE Geosci. Remote Sens. Lett. 8, 839–843.
Xiao, W., Mills, J., Guidi, G., Rodríguez-Gonzálvez, P., Gonizzi Barsanti, S., González-Aguilera, D., 2018. Geoinformatics for the conservation and promotion of cultural heritage in support of the UN sustainable development goals. ISPRS J. Photogramm. Remote Sens. 142, 389–406.
Yan, W.Y., Shaker, A., El-Ashmawy, N., 2015. Urban land cover classification using airborne LiDAR data: a review. Remote Sens. Environ. 158, 295–310.
Zhu, M., Wan, X., Fei, B., Qiao, Z., Ge, C., Minati, F., Vecchioli, F., Li, J., Costantini, M., 2018. Detection of building and infrastructure instabilities by automatic spatio-temporal analysis of satellite SAR interferometry measurements. Remote Sens. 10, 1816.
Zong, X., Wang, X., Luo, L., 2018. The integration of VHR satellite imagery, GPR survey and boring for archaeological prospection at the Longcheng Site in Anhui Province, China. Archaeometry 60, 1088–1105.